Université
de Montréal

New Stimuli-Responsive Block Random Copolymers and Their Aggregation

par

Mohammad T. Savoji

Département de Chimie

Faculté des arts et des sciences

Thèse présentée à la Faculté des études supérieures et postdoctorales
en vue de l'obtention du grade de
Ph.D. en chimie

Août, 2013

Résumé

Les polymères sensibles à des stimuli ont été largement étudiés ces dernières années notamment en vue d'applications biomédicales. Ceux-ci ont la capacité de changer leurs propriétés de solubilité face à des variations de pH ou de température. Le but de cette thèse concerne la synthèse et l'étude de nouveaux diblocs composés de deux copolymères aléatoires. Les polymères ont été obtenus par polymérisation radicalaire contrôlée du type RAFT (reversible addition-fragmentation chain-transfer). Les polymères à bloc sont formés de monomères de méthacrylates et/ou d'acrylamides dont les polymères sont reconnus comme thermosensibles et sensible au pH.

Premièrement, les copolymères à bloc aléatoires du type A_nB_m-b-A_pB_q ont été synthétisés à partir de N-n-propylacrylamide (nPA) et de N-ethylacrylamide (EA), respectivement A et B, par polymérisation RAFT. La cinétique de copolymérisation des poly(nPA$_x$-co-EA$_{1-x}$)-$block$-poly(nPA$_y$-co-EA$_{1-y}$) et leur composition ont été étudiées afin de caractériser et évaluer les propriétés physico-chimiques des copolymères à bloc aléatoires avec un faible indice de polydispersité . Leurs caractères thermosensibles ont été étudiés en solution aqueuse par spectroscopie UV-Vis, turbidimétrie et analyse de la diffusion dynamique de la lumière (DLS). Les points de trouble (CP) observés des blocs individuels et des copolymères formés démontrent des phases de transitions bien définies lors de la chauffe.

Un grand nombre de macromolécules naturels démontrent des réponses aux stimuli externes tels que le pH et la température. Aussi, un troisième monomère, 2-diethylaminoethyl methacrylate (DEAEMA), a été ajouté à la synthèse pour former des copolymères à bloc , sous la forme A_nB_m-b-A_pC_q , et qui offre une double réponse (pH et température), modulable en solution. Ce type de polymère, aux multiples stimuli, de la forme poly(nPA$_x$-co-DEAEMA$_{1-x}$)-$block$-poly(nPA$_y$-co-EA$_{1-y}$), a lui aussi été synthétisé par polymérisation RAFT. Les résultats indiquent des copolymères à bloc aléatoires aux

propriétés physico-chimiques différentes des premiers diblocs, notamment leur solubilité face aux variations de pH et de température.

Enfin, le changement d'hydrophobie des copolymères a été étudié en faisant varier la longueur des séquences des blocs. Il est reconnu que la longueur relative des blocs affecte les mécanismes d'agrégation d'un copolymère amphiphile. Ainsi avec différents stimuli de pH et/ou de température, les expériences effectuées sur des copolymères à blocaléatoires de différentes longueurs montrent des comportements d'agrégation intéressants, évoluant sous différentes formes micellaires, d'agrégats et de vésicules.

Mots clés : copolymères à blocaléatoires, thermo- et pH-sensible, polymérisation RAFT, copolymères à réponse variable, micelles et vésicules.

Abstract

Stimuli-responsive polymers and their use in biomedical applications have been widely investigated in recent years. These polymers change their physical properties such as water-solubility, when subjected to certain stimuli, for example change in temperature or pH. The main purpose of this work is to study new diblock copolymers consisting of two random copolymers, i.e., diblock random copolymers. Polymers with well-defined structures and tunable properties have been made using reversible addition−fragmentation chain-transfer (RAFT) polymerization, one of the controlled radical polymerization techniques. The blocks are made of acrylamide- and/or methacrylate-based monomers, which commonly show thermo-responsiveness and hence, double stimuli-responsive behavior is shown.

First, a diblock random copolymer in the form of A_nB_m-b-A_pB_q was synthesized with N-n-propylacrylamide (nPA) and N-ethylacrylamide (EA) as A and B using RAFT polymerization. Kinetic study of the copolymerization process confirmed the controlled character of the copolymerization. The diblock random copolymers with the compositions of poly(nPA$_x$-co-EA$_{1-x}$)-$block$-poly(nPA$_y$-co-EA$_{1-y}$) and low polydispersity were obtained. With UV-visible spectroscopy and dynamic light scattering (DLS) we investigate their thermoresponsive characteristics in aqueous solutions. Individual blocks showed tunable cloud points, and the diblock copolymer exhibited a well-separated two-step phase transition upon heating.

Macromolecules in nature can often respond to a combination of external stimuli, most commonly temperature and pH, rather than a single stimulus. Therefore, a second type of diblock random copolymer in the form of A_nB_m-b-A_pC_q was synthesized by combining a pH- and temperature-responsive block with another, only temperature-responsive block, producing responsiveness to multiple stimuli. This polymer with the composition of poly(nPA$_x$-co-DEAEMA$_{1-x}$)-$block$-poly(nPA$_y$-co-EA$_{1-y}$) where DEAEMA stands for 2-diethylaminoethyl methacrylate with well-defined structure and tunable properties has also been made using sequential RAFT polymerization. The resulting diblock random

copolymer changes its physico-chemical properties, such as water-solubility, in a quite controlled manner when subjected to the changes in temperature or pH.

What happens when blocks of different lengths change their relative hydrophilicity? It is known that the relative length of the blocks in amphiphilic diblock copolymers affects the aggregation mechanism. We compared three diblock copolymers with different block and chain lengths in aqueous solution when they change their relative hydrophilicity due to the change in the external stimuli. The variation of the length and chemical composition of the blocks allows the tuning of the responsiveness of the block copolymers toward both pH and temperature and determines the formation of either micelles or vesicles during the aggregation.

To: Sareh, Kosar and Tasnim
And my parents

Acknowledgements

First and foremost, I would like to thank my advisor, Prof. Julian. X. Zhu for giving me a chance to join his group, for his guidance through my study and research, for his constant encouragement and unending enthusiasm to explore new fields. Without his guidance as a great mentor, this work would not have been possible

I would also like to thank all my committee members, Prof. Françoise Winnik, Prof. C. Géraldine Bazuin and Prof. Guojun Liu for taking their valuable time and providing great input into this work.

Then I extend my appreciation to my fellow colleagues in the research laboratory, all the post-docs and graduate students, who helped me and shared their experiences and knowledge during my Ph.D. project.

I am also very thankful to Sylvain Essiembre, Pierre Menard-Tremblay and Patricia Moraille for their generous technical support and for providing me with trainings on the instruments.

Organizations that facilitated the completion of this work through their financial support are of course thanked: natural sciences and engineering research council of Canada (NSERC), the fonds de recherche du Québec - nature et technologies (FRQNT), the groupe de recherche en sciences et technologies biomédicales (GRSTB) and the centre for self-assembled chemical structures (CSACS).

My sincere gratitude goes to my parents and all my family. It would be impossible for me to finish the Ph.D study without their endless support, encouragement, love and patience. I thank my father for teaching me good values such as hard work and appreciation for the gift of life and my mother without whom I would not be the person that I am today.

Finally, I owe a big thank you to Sareh and my lovely daughters, Kosar and Tasnim. Their love and support have made my life better in so many ways. I owe the completion of this work to their enthusiasm and fresh perspective when things looked down.

Table of contents

List of Tables

List of Figures

List of acronyms, abbreviations and symbols

λ	wavelength
μ_i	mole fraction of ith monomer
η	viscosity
AFM	atomic force microscopy
AIBN	2,2-azobisisobutyronitrile
AM	acrylamide
AN	acrylonitrile
ATRP	atom transfer radical polymerization
BMA	butylmethacrylate
BPA	3-(Benzylsulfanylthiocarbonylsulfanyl)propionic acid
BPO	benzoyl peroxide
CP	cloud point
CTA	chain transfer agent
DEAEMA	2-diethylaminoethyl methacrylate
D_h	hydrodynamic diameter
DLS	dynamic light scattering
DMA	*N,N*-dimethylacrylamide
DMF	*N,N*-dimethylformamide
DMP	2-dodecylsulfanylthiocarbonylsulfanyl-2-methyl propionic acid
DMSO	dimethyl sulfoxide
dn/dc	refractive index increments
DSC	differential scanning calorimetry
DTP	degenerative chain transfer polymerization
EA	*N*-ethylacrylamide
ELPs	elastin-like polymers
EMA	ethyl methyl acrylamide
Et	ethyl
HDPE	high-density polyethylene

HEMA	2-hydroxyethyl methacrylate
iPr	isopropyl
k_a	activation rate constant
k_d	deactivation rate constant
k_i	initiation rate constant
k_p	propagation rate constant
LCST	lower critical solution temperature
LLDPE	linear low-density polyethylene
MA	methyl acrylate
M_{CTA}	molar mass of the chain transfer agent
Me	methyl
MA	methyl acrylate
MEMA	2-(*N*-morpholino)ethyl methacrylate
MMA	methyl methacrylate
M_n	number-average molar mass
M_w	weight-average molar mass
MWNTs	multiwalled carbon nanotubes
N_{agg}	aggregation number
NIPAM	*N*-isopropylacrylamide
NMP	nitroxide-mediated polymerization
NMR	nuclear magnetic resonance
nPA	*N*-propylacrylamide
nPr	n-propyl
NVC	*N*-vinylcarbazole
NVP	*N*vinylpyrrolidone
P2VP	Poly(2-vinylpyridine)
PAA	poly (acrylic acid)
PDEAEMA	poly(2-diethylaminoethyl methacrylate)
PDEAEMA	poly(2-diethylaminoethyl methacrylate)
PDI	polydispersity index

PDMA	poly(*N,N*-dimethylacrylamide)
PDMAEMA	poly(2-dimethylaminoethyl methacrylate)
PE	polyethylene
PEMA	poly(*N,N*-ethylmethylacrylamide)
PEO	poly(ethylene oxide)
PGA	poly(L-glutamic acid)
Ph	phenyl
PHEGMA	poly(hexa(ethylene glycol) methacrylate)
PHEGMA	poly(hexa(ethylene glycol) methacrylate)
PLL	poly(L-lysine)
PMMA	poly(methyl methacrylate)
PnPA	poly(*N*-n-propylacrylamide)
PP	polypropylene
PS	polystyrene
PtBA	poly(*N*-tert-butylacrylamide)
PVC	poly(vinyl chloride)
$R(\theta)$	Rayleigh ratio
RAFT	reversible addition fragmentation chain transfer
R_g	radius of gyration
R_h	hydrodynamic radius
SEM	scanning electron microscopy
SEC	size-exclusion chromatography
SFRP	stable free radical polymerization
SLS	static light scattering
St	styrene
tBA	*N*-tert-butylacrylamide
TEM	transmission electron microscopy
TEMPO	2,2,6,6-tetramethylpiperidinyloxy
THF	tetrahydrofuran
THP	tetrahydropyran

UCST	upper critical solution temperature
UE	electrophoretic mobility
VAc	vinyl acetate
VBC	vinylbenzyl chloride
Z	zeta potential

Chapter 1

Introduction

1.1 Stimuli-responsive or smart materials

Smart materials respond to environmental stimuli by producing a particular effect, such as changing their properties, structure or composition. For example, photochromic glasses are photo-responsive materials that reversibly change their color with changes in light intensity.

Polymers responding to environmental changes have attracted great interest in polymer technology. These smart polymers have one or more properties that change in a controlled manner by external stimuli. Several reports have been published on the synthesis and application of polymers responding to stimuli that could be chemical, such as pH[1, 2] and ionic strength,[3] biochemical, such as enzyme[4] and glucose,[5] or physical, such as temperature[6] and magnetic field.[7] In general, a significant change in properties can be induced by a small stimulus in stimuli-responsive polymers. For instance, a complete phase separation can take place by a little change in the temperature near the cloud point of a thermo-responsive solution.

The solution properties which can be changed in response to the external stimuli include individual chain dimensions/size, secondary structure, solubility (which is studied in this work), or the degree of intermolecular association.[8] The physical reasons for those responses are mostly formation or destruction of hydrogen bonding, hydrophobic effects, and electrostatic interactions, wheras chemical reasons mainly include simple reaction of the functional groups in the polymer chain, such as acid–base reactions.[8]

Smart polymers give promise to a large number of applications depending on the stimulus to which they respond in fields such as biomedicine, optics, electronics, diagnostics, and pharmaceutical and cosmetic formulations.[8, 9]

In this work, our focus is on thermo- and pH-responsive (co)polymers. Therefore, the responsiveness to these stimuli will be discussed in the next sections.

1.1.1 Thermoresponsive polymers

Thermoresponsive polymers are the most studied class of environmentally sensitive polymers. The first reported example of such polymers was poly(*N*-isopropylacrylamide) (PNIPAM) in 1968.[10] They exhibit a phase transition (typically in aqueous solution) at certain critical temperature according to their composition. If the polymer solution exhibits one phase below a certain temperature and phase separates above it, the temperature is called lower critical solution temperature (LCST). On the other hand, systems that appear monophasic above a specific temperature and biphasic below it, are characterized by an upper critical solution temperature (UCST). The systems described in this work show LCST-like behavior which is the focus of the following sections.

Lower critical solution temperature (LCST). Polymers showing LCST behavior in aqueous solutions are soluble in water below a certain critical temperature, because hydrogen bonding between the hydrophilic segments of the polymer chain and water molecules is dominant. The LCST was first explained for the aqueous solution of PNIPAM.[10] Partial displacement of water from the polymer coil occurs due to the increase in temperature, resulting in the weakening of hydrogen bonds. This increases the hydrophobic interactions in the polymer chain. As a result, the polymers collapse, aggregate and phase separate, because the intra- and intermolecular hydrogen bonds between the hydrophobic parts of polymer molecules are favored compared with the bonds to water molecules. Thermoresponsive polymer chains form the expanded coil conformation in solution, while they collapse to form compact globuli at the phase separation temperature.[11]

In other words, below the LCST, the enthalpy of formation of the hydrogen bonds between the polymer and the water molecules is responsible for the polymer dissolution.

When raising the temperature above the LCST, the solvent expands much more rapidly than the polymer, whose segments are covalently linked. Hence, mixing requires contraction of the solvent for compatibility of the polymer, resulting in a loss of entropy. Therefore, above the LCST, the separation is actually entropically favorable and polymer precipitates (Figure 1.1).

T > LCST

T < LCST

Hydrophilic; one phase   Hydrophobic; two phase
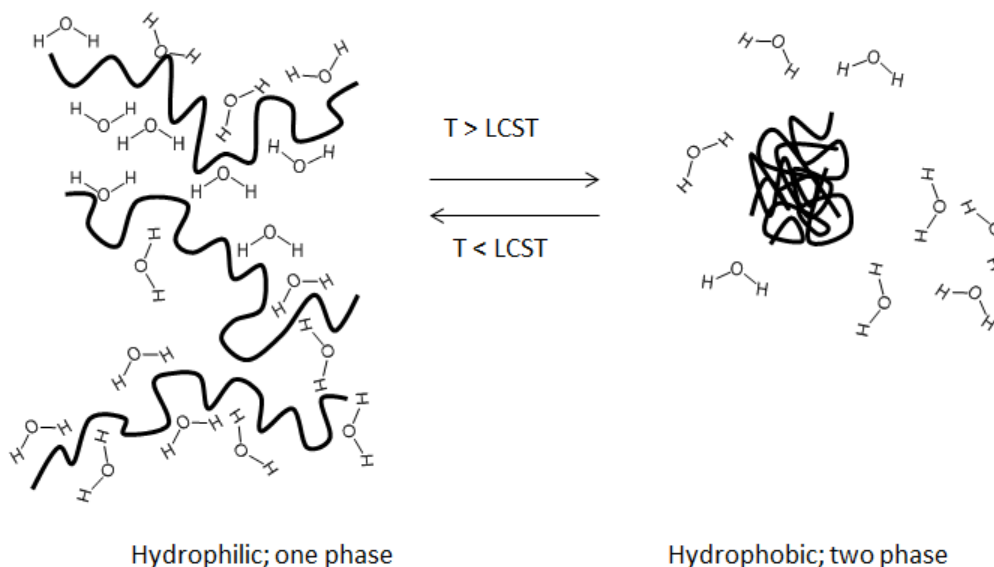
Figure 1.1 Phase separation of a thermo-responsive polymer which shows LCST in water.

The phase separation temperature depends on the polymer concentration. Therefore, the solubility phase diagram of the thermoresponsive polymers shows a composition dependent temperature over a wide range of concentrations as shown in Figure 1.2 for PNIPAM. LCST is the minimum point in this diagram,[10] while other phase separation temperatures have been assigned by different names such as cloud point or demixing temperature.[12] For simplicity, we will use the term LCST in the text.
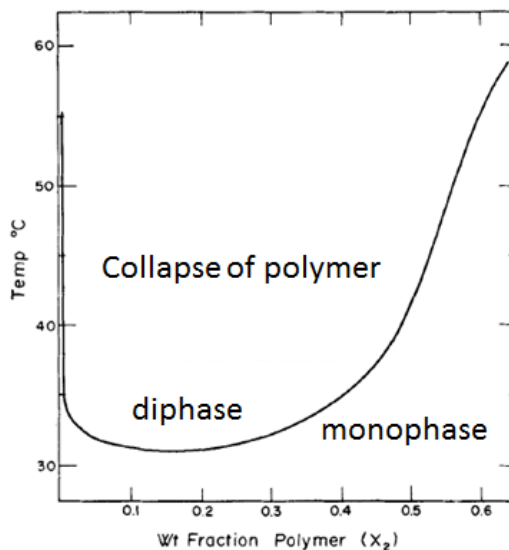
Figure 1.2 PNIPAM solubility phase diagram in water. Reproduced from Ref. 10, ©
1968 Taylor & Francis Group.

Monomers for thermoresponsive polymers. Most of the synthetic polymers with
temperature-dependent phase transition behavior belong to certain types of polymers;
poly(acrylamide)s, which will be the focus of this work, poly(methacrylamide)s,[13]
polyethers,[14] poly(N-vinylamide)s,[15] poly(oxazoline)s,[16] and poly(phosphazene)s,[17] whose
structures are shown in Figure 1.3.

R=H, Poly(acrylamide)s
R=CH₃ Poly(methacrylamide)s

Poly(ether)s

Poly(N-vinylamide)s
m=1-3

Poly(oxazoline)s

Poly(phosphazene)s
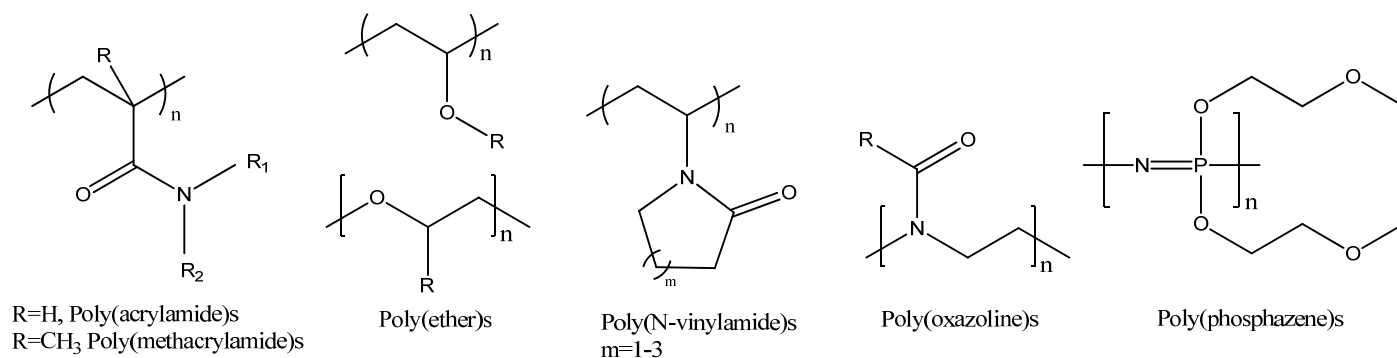
Figure 1.3 Common types of thermoresponsive polymers.

Aseyev *et al.*[11] have comprehensively reviewed different types of thermoresponsive
(co)polymers and have described various synthetic methods as well as aqueous solutions
properties of these polymers.

Modification of LCST. The LCST of thermoresponsive polymers can be tuned by copolymerization with hydrophilic or hydrophobic monomers as reported by our group[18, 19] and others.[20, 21] For example, desired thermosensitivity could be achieved by copolymerization of *N*-alkylacrylamides with cholic acid derivatives.[18] In another work, various alkylacrylamides were copolymerized to obtain the desired LCST.[19] In both cases, the thermosensitivity of the copolymers depends on their chemical composition.

In addition, in a series of works by our lab, multi-step LCSTs were shown for diblock and even triblock copolymers.[22, 23] In this case, the block copolymers show separate LCSTs for blocks with different compositions. For example, a three-step transition was observed for the ABC triblock copolymer from poly(*N*-n-propylacrylamide) (PnPA), PNIPAM, and poly(*N*, *N*-ethylmethylacrylamide) (PEMA), poly(nPA$_{124}$-*b*-NIPAM$_{80}$-*b*-EMA$_{44}$) at long detection wavelength in UV-vis spectra (Figure 1.4). Each transmittance step in Figure 1.4 comes from a certain block. For instance, the first transition at around 25 °C belongs to the most hydrophobic block, PnPA, and the last one at around 58 °C comes from the most hydrophilic block, PEMA. At short wavelengths (such as 250 nm), only one transition was observed due to the strong wavelength dependence of scattering ($\sim \lambda^{-4}$), which means that shorter wavelengths (blue) are scattered more strongly than longer (red) ones.[24]
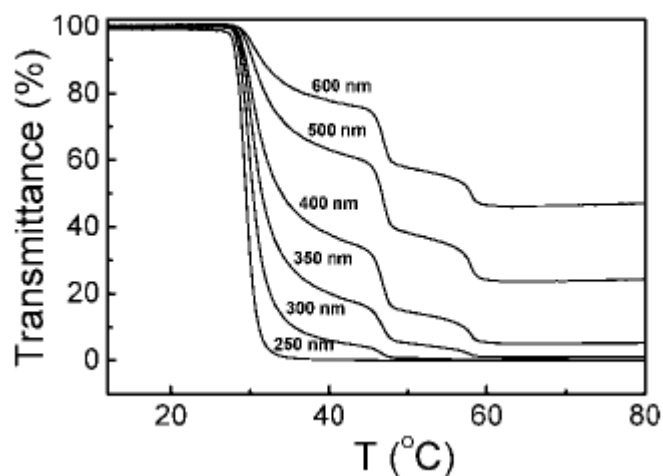
Figure 1.4 Transmittance of a 1.0 mg/mL aqueous solution of PnPA$_{124}$-*b*-PNIPAM$_{80}$-*b*-PEMA$_{44}$ as a function of temperature with heating rate of 0.1 °C/min observed at different wavelengths. Reprinted from Ref. 22, © 2009 American Chemical Society.

1.1.2 pH-responsive polymers

In pH-responsive polymers, a certain physical property, such as solubility, can be manipulated by the changes in external pH, and this response should be reversible. Regarding biomedical applications, since the pH in most tumors is significantly lower (~ 6.5) than the pH of the blood (7.4) at 37 $^{\circ}$C,[25] pH-responsive polymers can be designed for various potential applications, such as controlled drug delivery, industrial coatings, oil exploration, viscosity modifiers, colloidal stabilization, water remediation, etc.[1, 2]

Monomers for pH-responsive polymers. Polyelectrolyte is a general name for polymers containing ionizable groups either in the backbone or as pendent groups. Since ionization occurs as a result of pH change, polyelectrolytes are pH-sensitive and can be divided into two main classes: polyacids and polybases. The solubility of weak polyelectrolytes depends on the degree of ionization, which varies by changing the pH. Increasing the pH of acidic polyelectrolyte solutions, such as poly(acrylic acid) (PAA), results in deprotonation (ionization) of the carboxylic pendent groups. As a result, the solubility of the polymer chains increases because of negative charges. Inversely, the carboxylic groups protonate by decreasing the pH (below the pK$_a$) rendering the polymer hydrophobic and less water-soluble. On the other hand, polybases, such as poly(2-diethylaminoethyl methacrylate) (PDEAEMA), ionize and become positively charged at low pHs (below their pK$_a$) due to the protonation of amine groups. Polymer chains become less water-soluble by increasing the pH and neutralization of the amine groups.

Figure 1.5 shows the ionization processes of PAA and PDEAEMA as examples of polyacids and polybases, respectively.
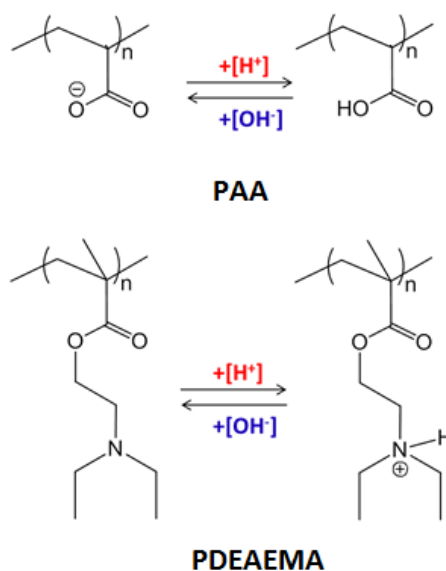
Figure 1.5 Ionization processes of two representative pH-responsive polymers, PAA and PDEAEMA.

The diblock copolymer of polystyrene and poly(acrylic acid), PS-*b*-PAA, is one of the earliest and most extensively studied pH-responsive PAA-based polymeric system.[1] At low pH, the polymer is water-insoluble, and with increasing pH, the ionization of PAA renders it negatively charged. As a result, the polymers self-assemble in solution and form aggregates of different morphologies, depending on the PAA block length, pH, and salt concentration. Among these morphologies, vesicles are of great interest owing to their potential applications as encapsulating agents, particularly in the fields of biomedicine and drug delivery.[26] PS-*b*-PAA diblock copolymer vesicles were thermodynamically stable in dioxane–THF–H$_2$O or DMF–THF–H$_2$O solutions. The vesicle sizes can be reversibly changed by manipulating the solvent composition, especially water content.[27]

Poly(2-diethylaminoethyl methacrylate), PDEAEMA is one of the polymers used in this work, so it is separately explained in this section. PDEAEMA is more hydrophobic than poly(2-diethylaminoethyl methacrylate), PDMAEMA. Hence it is water-insoluble at ambient temperature at neutral or basic pH and shows only pH-responsive, not thermo-responsive behavior.[1] Also the copolymerization of DMAEMA and DEAEMA has been demonstrated [28] and in such case, the aggregation number depends on pH. Decreasing the pH results in increasing positive charge in PDMAEMA-*b*-PDEAEMA micelles. This gives

micelles with swelled corona, accompanied by the reduction in the aggregation number due to electrostatic repulsion. Increasing ionic strength has the opposite effect on the aggregation number because of the screening of electrostatic repulsion between the chains. At high ionic strengths, the PDMAEMA-*b*-PDEAEMA corona shrinks, which results in an increase in aggregation number. Block copolymerization of PDEAEMA with hydrophilic poly(hexa(ethylene glycol) methacrylate), PHEGMA, yields double hydrophilic diblock copolymers.[29] The degree of ionization of PDEAEMA determines the hydrophilicity of the block copolymer. Unimers were observed at low pH due to the protonated hydrophilic tertiary amine units. However, deprotonation of the amine groups at higher solution pH makes PDEAEMA more hydrophobic, which induces the formation of micelles with PDEAEMA core and PHEGMA corona. Copolymerization of PDEAEMA with many other monomers is also reported, such as poly(ethylene oxide) (PEO),[30] PS,[31] poly(2-vinylpyridine) (P2VP).[32] PDEAEMA has also found application for example in bio-nanotechnology, where it has been grafted on the surfaces of multiwalled carbon nanotubes (MWNTs) to produce magnetic nanotubes after the assembly with negatively charged magnetic particles (Figure 1.6).[33] The magnetic nanotubes were used to assemble onto the red blood cells, resulting in the separation of the cells in a magnetic field.
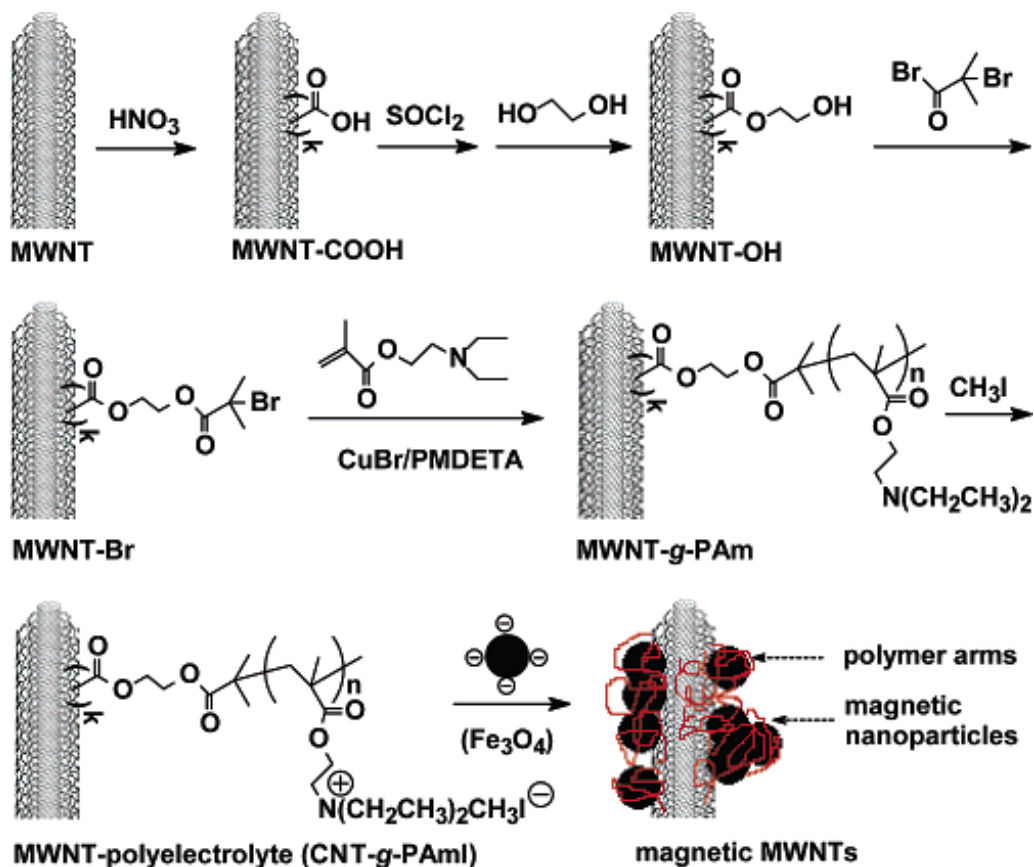
Figure 1.6 Synthetic route for magnetic MWNTs through ATRP and electrostatic assembly with Fe_3O_4. Reprinted from Ref. 33, © 2006 American Chemical Society.

The positively charged nature of PDEAEMA backbone in a comb-type copolymer with poly(L-lysine) (PLL) side chains allows binding DNA via electrostatic interaction. This system could be used as a pH-sensitive DNA carrier.[34]

1.1.3 Multi-stimuli responsive (co)polymers

Multi-stimuli responsive (co)polymers can be prepared either using a dually responsive monomer to make, for example, a pH- and thermo-responsive homopolymer or by copolymerizing one stimuli-responsive monomer with another one. As an example of the first system, PDMAEMA is a double stimuli-responsive polymer, with LCST values between 32-52 °C, depending on the solution pH. An example of the second system would be a diblock copolymer, where the blocks are amphiphilic and show responsiveness to different stimuli. This type of double-stimuli responsive polymers include copolymers of different monomers, each responsive to a certain stimulus.

Amphiphilic diblock copolymers. Amphiphilic block copolymers contain both hydrophobic and hydrophilic segments and can be made by joining two blocks of individual polymers. Hence, they have affinity for two different types of environments and can self-assemble in solution to form aggregates of varying shapes and sizes. Moreover, stimuli-responsive amphiphilic copolymers have been extensively studied and they are briefly explained in the next paragraphs.

Thermoresponsive amphiphilic copolymers can be made in two ways:

(1) Block copolymerization of a hydrophobic polymer with a thermoresponsive monomer. An example of such system is PNIPAM-*b*-PS.[35] This polymer is amphiphilic below the LCST of PNIPAM, while above the LCST both blocks are hydrophobic and insoluble in water.

(2) Block copolymerization of properly selected monomers to give blocks bearing different LCSTs in a double thermosensitive diblock copolymer. Typical behavior of this type of copolymer is shown in Figure 1.7 supposing that LCST1 < LCST2.

T < LCST1   LCST1 < T < LCST2   LCST2 < T

Heating
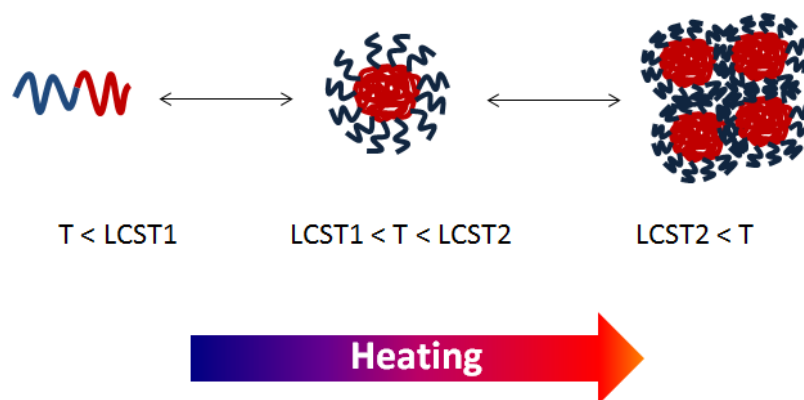
Figure 1.7 Schematic behavior of a double thermosensitive diblock copolymer by increasing temperature.

At temperatures below the LCSTs of both blocks, the diblock copolymer is completely water-soluble. Increasing the solution temperature above the first LCST makes one block insoluble while another block is still soluble in water. This makes the system amphiphilic.

Further increase in temperature above the second LCST results in completely insoluble material. This behavior has been reported by several research groups.[36, 37, 38]

Several reports have described the synthesis of dually responsive block copolymers using responsiveness to pH and temperature.[39, 40, 41, 42] PAA-*b*-PNIPAM is an example of a diblock copolymer composed of a pH- and thermoresponsive homopolymers.[43]

P2VP-*b*-PDMAEMA is sensitive to temperature, ionic strength, and pH. Micelles consist of hydrophobic P2VP core surrounded by protonated PDMAEMA corona at pH 6, and their size decreases when the ionic strength of the solution is increased by the addition of NaCl. At higher pH, hydrophobic P2VP remains in the core of the micelles surrounded by uncharged PDMAEMA corona. These micelles are not sensitive to ionic strength, but they precipitate by increasing the temperature above the LCST of PDMAEMA (ca. 40 °C).[44]

By introducing redox-sensitive bonds into the structure of pH- and thermo-responsive polymer, Klaikherd *et al.*[45] synthesized a triple stimuli-sensitive block copolymer consisting of acid-sensitive tetrahydropyran (THP)-protected 2-hydroxyethyl methacrylate (HEMA) and temperature-sensitive PNIPAM with an intervening disulfide bond as the redox-sensitive site (Figure 1.8).
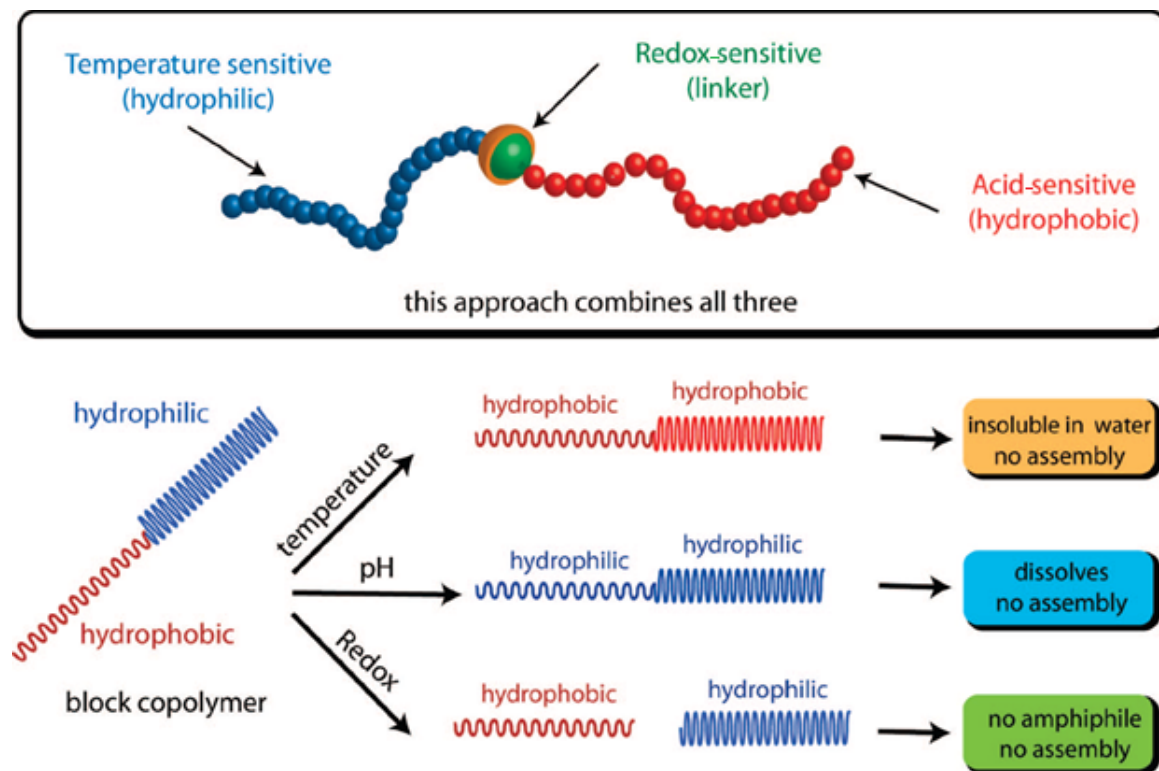
Figure 1.8 Schematic representation of amphiphilic block copolymer which can respond to three stimuli: pH, temperature, and redox agent. Reprinted from Ref. 45, © 2009 American Chemical Society.

1.2 Polymer synthesis methods

Synthetic polymers are classified according to the preparation method. If the reaction mechanism involves free-radicals or ion groups, and the monomers are added to the chain one at a time only, the polymer is a chain-growth polymer. On the other hand, if the reaction mechanism proceeds through functional groups of the monomers with the possibility of combination of monomer chains with one another directly, the polymer is called a step-growth polymer. Chain-growth polymers are usually made of unsaturated monomers having a double bond between carbon atoms, while step-growth polymers are produced from monomers bearing two or more functional groups, which can react together to form covalent links between repeating units such as ester or amide links.

Since only chain-growth polymers are synthesized in this work, the focus here will be on different types of chain polymerization.

1.2.1 Free radical, coordination and ionic polymerization

There are three significant stages taking place in chain polymerization: initiation (birth), propagation (growth), and termination (death).

Free radical polymerization is the most common type of chain-growth polymerization reaction.[46] The polymerization in this method is initiated by a free radical, which is a species containing an unpaired electron. The polymer chain is made by the addition of this free radical to an unsaturated monomer to catch one electron. Then, another free radical will be produced and its reaction continues to grow the polymer chain. We can consider the double bond as a potential site for opening to two single bonds.

Coordination polymerization is another type of chain polymerization, in which initiation takes place on a catalytic surface, and the monomer adds to a growing macromolecule through an organometallic active center. Although this polymerization technique was first developed in the 1950s, the reaction mechanism is still poorly understood, especially in heterogeneous Ziegler-Natta catalysts based on titanium tetrachloride and aluminum alkyl co-catalyst.[47] This method produces linear and high molar mass polymers, including commercially important high-density polyethylene (HDPE), linear low-density polyethylene (LLDPE). Polymers with specific tacticity can be obtained by this method, such as isotactic polypropylene (i-PP).

The two above-mentioned methods produce a dead polymer chain, which is not capable of chain growth by the addition of another monomer (living polymerization).

Ionic polymerization is initiated by an ionic species, which can be either anion or cation, and the polymerization is called anionic or cationic according to the initiation method. Anionic polymerization was first done by Szwarc[48] in 1956 as the first example of living polymerization. In ionic polymerization, the charge is transferred from ionic initiator to a monomer to make it reactive. This reactive monomer will react similarly with other monomers to form a polymer. Ionic polymerizations produce well-defined polymers with precise and predetermined molar masses capable of chain extension after the polymerization is complete. However, it suffers from two main disadvantages:[49] (i) only a narrow range of monomers, excluding functionalized monomers, could be polymerized

with this method, and (ii) special precautions are required, such as high purity of chemicals and stringent measures to avoid air and moisture.

1.2.2 Controlled radical polymerization

Due to the difficulties and limitations of living polymerization methods, the investigation of structure-dependent properties of polymers was limited until the last two decades. Especially stimuli-responsive polymers, whose properties are quite structure-dependent, made very slow progress.[50] Feasible methods to make well-defined polymers began to emerge during the 1980s and progressed very rapidly in the 1990s.[51] Figure 1.9 demonstrates the advances in the research of stimuli-responsive polymers by the exponential increase in the number of publications after the emergence of controlled radical polymerization techniques.
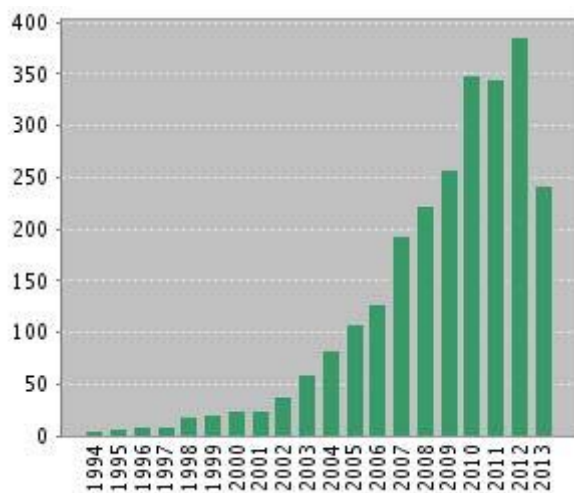
Figure 1.9 Publications per year on stimuli-responsive polymers based on a SciFinder search using the keyword of "stimuli-responsive polymers" (July 2013).

Some of the most recent polymerization methods are controlled radical polymerization, and they benefit from the advantages of both free radical polymerization and conventional ionic polymerization, i.e., they are easy to conduct for a wide range of vinylic monomers and can produce well-defined (block co)polymers.

Controlled radical polymerizations can be classified according to the nature of the X species in Figure 1.10. Three main classes of controlled radical polymerizations are nitroxide-mediated polymerization (NMP), atom transfer radical polymerization (ATRP), and reversible-fragmentation chain transfer (RAFT).

The general mechanism of controlled radical polymerization is shown in Figure 1.10. The rate constant for deactivation (k_{deact}) needs to be much higher than the activation rate constant (k_{act}) to keep termination reactions at a minimum. It means that the growing P_n chain is rapidly trapped in the deactivated state by species X, which is typically a stable radical (as in NMP), an organometallic species (as in ATRP), or a thiocarbonate (as in RAFT). The dormant species are activated again to reproduce the growing sites.
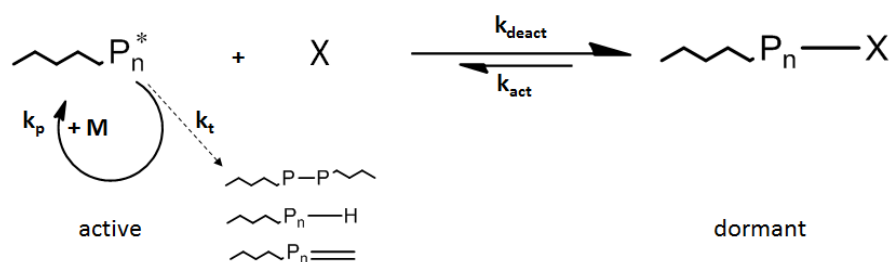
Figure 1.10 General mechanism of controlled radical polymerization.

Fast initiation and negligible termination reactions result in the continuous growth of polymer chains during the propagation. In this mechanism, the growing radicals mainly react with X, which is present at thousands of times higher concentration, rather than with themselves. This kind of polymerization is also called "living" radical polymerization, but it is not truly living, because coupling of the radicals, which leads to the termination of the polymerization, cannot be completely avoided.

The first two methods will be briefly introduced, and RAFT polymerization used in our work will be explained more in the next section.

Nitroxide-mediated polymerization (NMP) is also called stable free radical polymerization (SFRP),[52] and it is historically the first method applied to make various well-defined polymers, such as polyacrylates, using nitroxides and alkoxyamines as a radical trapping agent.[53] This method can polymerize vinyl monomers into moderately

uniform polymers with relatively low molecular weights. This method was first proofed experimentally in the work of Georges *et al.* in 1993.[49, 54]

Traditional NMP is initiated by a thermal initiator, such as 2,2-azobisisobutyronitrile (AIBN) or benzoyl peroxide (BPO), in combination with a relatively stable radical nitroxide, such as 2,2,6,6-tetramethylpiperidinyloxy (TEMPO), as a control agent.[54] NMP is based on reversible deactivation of the growing chain end by a nitroxide. Homolytic cleavage produces again the propagating radical and the nitroxide species (as the X in Figure 1.10).

The main parameter controlling the NMP is the molar ratio of the initial concentration of the nitroxide and the initial concentration of the initiator, $[\text{nitroxide}]_0/[\text{initiator}]_0$.[55] Actually, the only factor that affects the polymerization kinetics is the excess TEMPO remaining in the solution after the initiation.[56] To control this ratio, an alkoxyamine initiator was developed to provide a unimolecular initiation system. It decomposes to produce equal amounts of initiating radical and nitroxide. If either the initiating chain end or the nitroxide mediated chain end is properly functionalized, telechelic polymers can be obtained by the reaction of the terminal functional group (Figure 1.11).[57] By definition, telechelic polymers are macromolecules with functional groups at both ends, which can be used for further polymerization or other reactions.
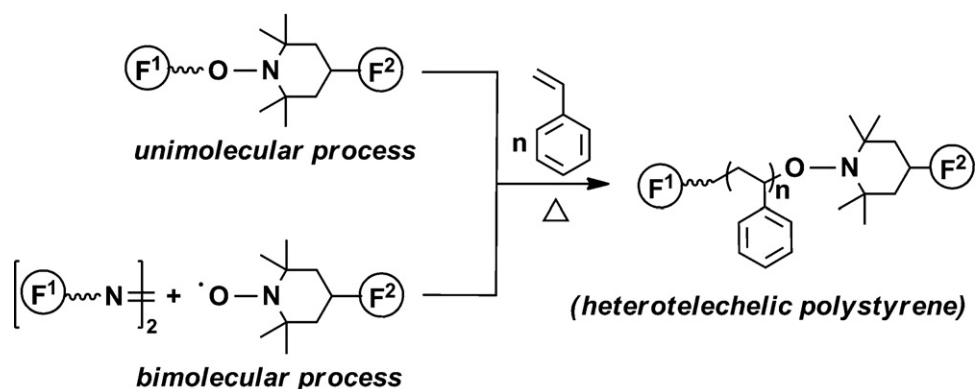
Figure 1.11 General strategies for the synthesis of telechelic polymers by NMP.
Reprinted from Ref. 57, © 2011 with permission from Elsevier.

Atom transfer radical polymerization (ATRP) is also called transition metal-catalyzed living radical polymerization.[51] This method was discovered by two research groups, Matyjaszewski and Sawamoto, at the same time in 1995.[58, 59] However, this method was not well developed until 2001.[51] The method utilizes a redox process of a transition metal complexes, most commonly those of Cu(I). The initiating system includes a halogenated compound as an initiator and a transition metal complex as a catalyst.[60] Percec *et al.*[61] used a non-transition metal salt, $Na_2S_2O_4$, to catalyze the polymerization of vinyl chloride initiated with iodoform.

Also ATRP is controlled by the equilibrium between active (P_n*) and dormant chain (P_nX) (Figure 1.10). The reaction proceeds with first-order kinetics[60] involving reversible homolytic cleavage of a carbon–halogen bond in the redox reaction between the metal complex (Mt^nLY) and alkyl halide (R–X) as the dormant species,[62] illustrated in Figure 1.12.
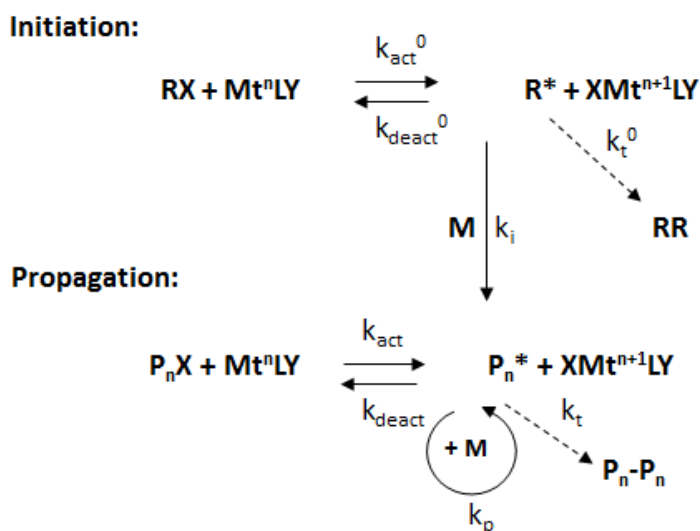
Figure 1.12 Schematic mechanism of ATRP.

As stated before, k_{deact} in this mechanism is much higher than k_{act}, and therefore, most of the chains are present in the dormant state (P_n–X).

There are several routes to make telechelic polymers by ATRP.[57] The most convenient method is to use a functionalized initiator (RX in Figure 1.12) with[63] or without[64]

protection. Another route involves the reaction of the terminal halide group by nucleophilic substitution to reach the desired functionality.[65]

1.2.3 Reversible addition-fragmentation chain transfer (RAFT) polymerization

RAFT polymerization, first discovered in 1998,[66] is one of the most recent and most efficient methods among the controlled radical polymerization techniques, because it tolerates various functionalities, such as amides, amines, acidic groups, as well as vinyl acetate and its derivatives. A large variety of monomers and solvents, even water, can be used in RAFT polymerization.[67] It can also be used in heterogeneous media, using techniques such as emulsion polymerization,[68] surfactant-free emulsion polymerization with macro-RAFT agents as stabilizers,[69] suspension polymerization,[70] and non-aqueous dispersion polymerization in organic solvents.[71]

Mechanism of RAFT polymerization. There are numerous reviews on the mechanism and kinetics of RAFT.[72, 73, 74] The RAFT mechanism proposed in Figure 1.13 is based on the addition–fragmentation equilibrium.[74]
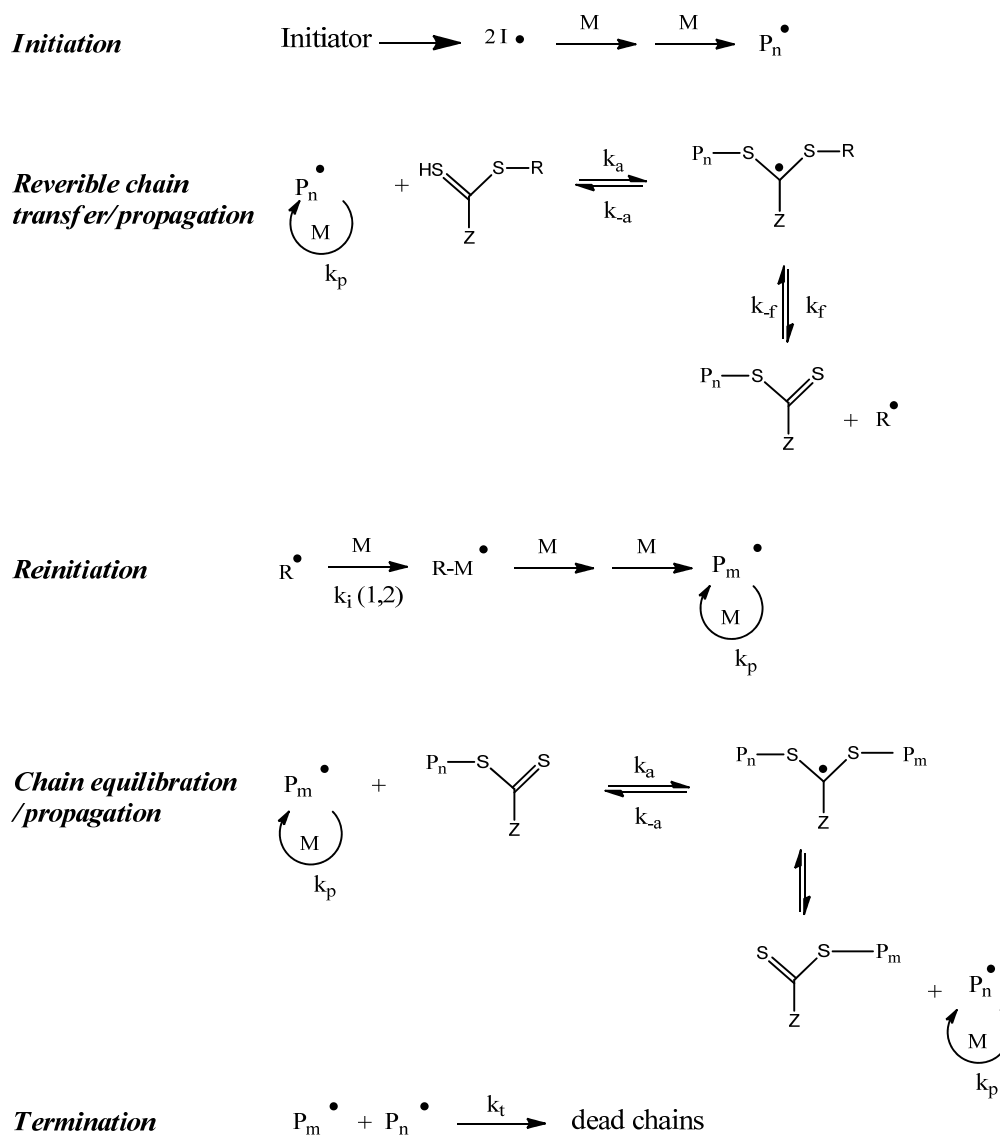
Figure 1.13 Mechanism of RAFT polymerization

As shown in Figure 1.13, the initiation process and radical termination mechanism are similar to conventional radical polymerization. In the early steps, propagating macroradicals ($P_n\bullet$) add to the carbon-sulfur double bond of a RAFT reagent [RSC(Z)=S] with an addition rate constant k_a. The intermediate radical yields again the reactants (k_{-a}) or it fragments into another initiating (macro)radical ($R\bullet$) and polymeric thiocarbonylthio compound [$P_nS(Z)C=S$] with a fragmentation rate constant k_f. The reaction of this radical ($R\bullet$) with monomer (M) leads to a new propagating radical ($P_m\bullet$), which participates again in the addition and fragmentation processes with the RAFT agent and establishes an

equilibrium with the previous propagating chain ($P_n\bullet$). This way, the equilibrium between dormant $[P_nSC(Z)–SP_m]\bullet$ and active species ($P_n\bullet$ and $P_m\bullet$) is established. The product of these reactions is a polymer chain with thiocarbonylthio end group, which can be isolated and used to continue the reaction, if needed.

Choice of RAFT agents. A variety of thiocarbonylthio RAFT agents (ZC(=S)SR) has been reported.[75, 76, 77] Both R and Z groups of a RAFT agent should be carefully selected to provide appropriate control over the polymerization.

Generally, the RAFT agent should have a reactive C=S bond for the fast addition and a loose S–R bond to accelerate the fragmentation. Reinitiation should also be faster than propagation to ensure the simultaneous growth of the chains. Therefore, the free radical leaving group R$\bullet$ should be more stable than $P_n\bullet$, it should be a good leaving group, and it should also mimic the propagating radical. Z influences the stability of the thiocarbonylthio radical intermediate and should be chosen according to the reactivity of the monomer. Hence, a certain RAFT reagent is effective for a particular polymerization.[72, 73, 74] Figure 1.14 shows the guidelines for selecting a suitable RAFT agent to polymerize certain monomers.
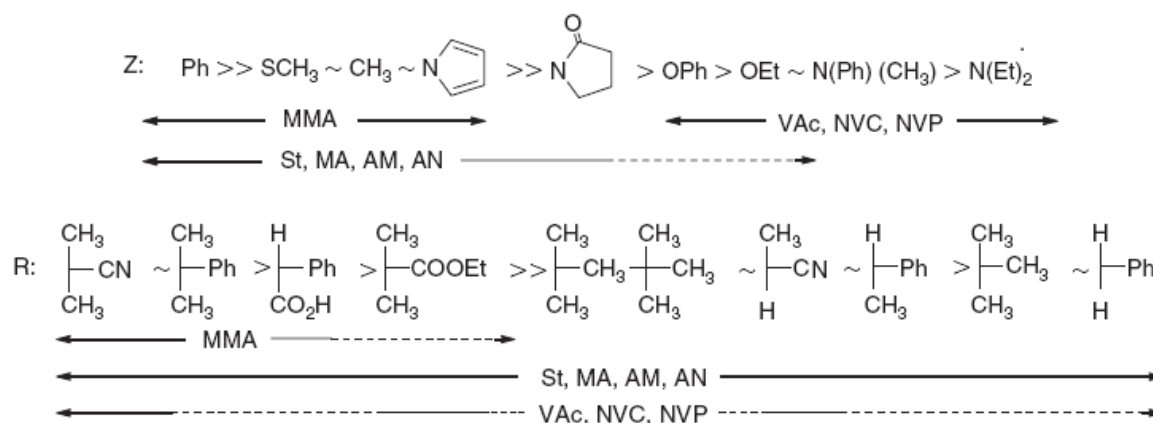
Figure 1.14 Guidelines for selecting a suitable RAFT agent to polymerize certain monomers. For Z, the addition rates decrease and fragmentation rates increase from left to right. For R, the fragmentation rates decrease from left to right. Dashed lines indicate partial control of the polymerization. Reprinted from Ref. 72 with permission of CSIRO publishing.

Initiators. Organic initiators, typically azo compounds with the decomposition temperature (T_{decom}) of 25-80 ^{o}C or peroxides (T_{decom} > 90 ^{o}C), are extensively used for RAFT polymerization. In general, the molar ratio [RAFT agent]:[initiator] should be >10:1 to have control over the molecular weight.[72] It should be noted that dead chains are produced from the generated radicals at the initiation stage. However, the majority of the chains will be initiated by R and terminated by the thiocarbonylthio group and hence, they are able to initiate RAFT polymerization with another monomer to produce block copolymers.

Telechelic polymers made by RAFT polymerization. The polymer chains prepared by RAFT polymerization have R and Z groups of the RAFT agent at their two ends.

To obtain functionalized polymer chains by RAFT polymerization, the functionality can be incorporated in the RAFT agent as R and/or Z, i. e., by using a functional RAFT agent. Various functional RAFT agents have been synthesized so far with a wide range of functional end groups, such as OH,[78] COOH,[79] CHO,[80] pyridyl,[81] N_3,[82] alkyne,[83] peptide[84] groups, etc.

Another possible route includes the transformation of the chain end CTA into a desired functional end group. Many researchers are interested in the processes for CTA end group removal or post-modification of the polymer chains. The main reactions for the end group modification include hydrolysis,[85] radical-induced reductions,[86] aminolysis[87] and metal-assisted reduction,[88] which are summarized in Figure 1.15 for dithiocarbonate-terminated polymers.
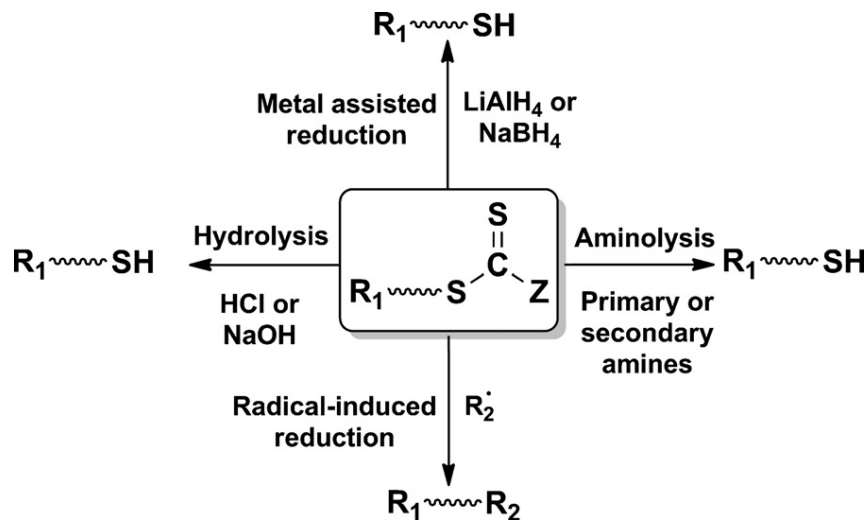
Figure 1.15 End group transformation reactions for dithiocarbonate-terminated RAFT polymers. Reprinted from Ref. 57, © 2011 with permission from Elsevier.

1.3 Poly(*N*-alkylacrylamide)s

Acrylamide is highly water-soluble vinyl monomer prepared by microbial hydrolysis of acrylonitrile using nitrile hydratase as a catalyst.[89] However, *N*-alkyl-substituted (meth)acrylamides, with the general structure shown in Figure 1.16, are made by reacting (meth)acryloyl chloride with the corresponding alkylamines.[90]
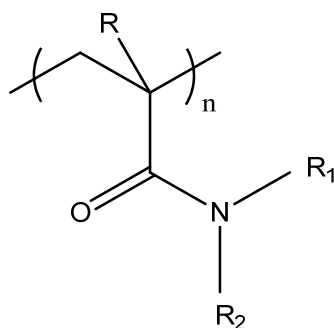
R=H, Poly(acrylamide)s
R=CH$_3$ Poly(methacrylamide)s
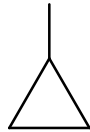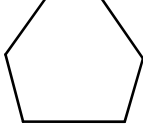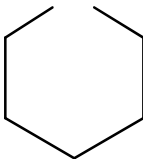
Figure 1.16 General structure of poly((meth)acrylamide)s

1.3.1 Thermoresponsive poly(*N*-alkylacrylamide)s

As mentioned previously, there are a huge number of thermo-responsive polymers. Among them, poly(*N*-alkylacrylamide)s are the most studied type, because they can provide a wide range of LCST values, and they are stable at both acidic and basic environments. The first and most widely studied neutral monomer for water-soluble thermoresponsive polymer is *N*-isopropylacrylamide (NIPAM).[9, 10, 11] The resulting polymer, PNIPAM shows the LCST of ~32 $^\circ$C in water, near the physiological temperature (37 $^\circ$C). On the basis of literature, PNIPAM itself has been studied as much as all other types of thermosensitive polymers together, and it is often used as a model polymer for phase transition studies.[91, 92]

Since the advent of PNIPAM in 1968,[10] many synthetic advances have appeared in making thermosensitive poly(*N*-alkylacrylamide)s. In contrast to numerous reports on PNIPAM, little work has been done on other thermo-responsive poly(*N*-alkylacrylamide)s. Some of the synthesized poly(*N*-alkylacrylamide) homopolymers with their LCSTs are listed in Table 1.1. They have different substituents on the nitrogen that affects their solution behavior. Smaller substituents such as H and methyl group (Me) in soluble PAA and poly(*N*,*N*-dimethylacrylamide) (PDMA) do not induce LCST in aqueous solutions below 100 °C, while the more sterically hindered groups, such as butyl in all its isomeric forms, make the polymer insoluble in water because of their hydrophobicity. Other polymers are between these two extremes: by increasing the hydrophobicity of the substituents, the hydrophilicity of the polymer decreases and the LCST decreases accordingly, down to the LCST of PnPA at ~23 $^\circ$C.

Table 1.1 LCST of aqueous solutions of selected poly(*N*-alkylacrylamide)s
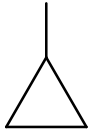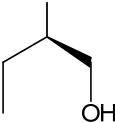
Full name	R_1	R_2	LCST (°C)	Method, ref
Poly(acrylamide)	H	H	soluble	[19]
Poly(*N, N*-dimethylacrylamide)	CH_3	CH_3	soluble	[19]
Poly(*N*-ethylacrylamide)	H	CH_3CH_2	73	DSC[93]
			74	Turbidimetry[94]
			82	DSC[19]
Poly(*N, N*-ethylmethylacrylamide)	CH_3	CH_3CH_2	70	UV[23]
Poly(*N*-cyclopropylacrylamide)	H	(cyclopropyl)	57	Turbidimetry[94]
Poly(*N*-acryloylpyrrolidine)	(pyrrolidine ring)		51	Turbidimetry[95]
Poly(*N*-isopropylacrylamide)	H	$CH(CH_3)_2$	32	Turbidimetry[92]
			36	UV[23]
Poly(*N, N*-diethylacrylamide)	CH_3CH_2	CH_3CH_2	29	UV[96]
			32	UV,[23] DSC[19]
			Syndiotactic is insoluble	[97]
Poly(*N*-n-propylacrylamide)	H	$CH_3CH_2CH_2$	22.5	SLS[98]
			25	UV[23]
Poly(*N*-acryloylpiperidine)	(piperidine ring)		4	UV[99]
Poly(*N*-tert-butylacrylamide)	H	$CH_3C(CH_3)_2$	insoluble	[19]

The values reported in Table 1.1 for a single polymer might vary in literature, because the LCST depends on factors such as determination method, molecular weight, and tacticity

of the polymer. Although poly(acrylamide)s are studied in this work, a list of their thermo-responsive analogous, poly(methacrylamide)s, is also shown in Table 1.2.

Table 1.2 LCST of aqueous solutions of selected poly(N-alkylmethacrylamide)s

Full name	R$_1$	R$_2$	LCST (^{o}C)	Method, ref
Poly(methacrylamide)	H	H	soluble	[94]
Poly(N-ethylmethacrylamide)	H	CH$_3$CH$_2$	67	Turbidimetry[94]
Poly(N-isopropylmethacrylamide)	H	CH(CH$_3$)$_2$	44	Turbidimetry[92]
Poly(N-cyclopropylmethacrylamide)	H		59	UV[100]
Poly(N-(L)-(1-hydroxymethyl)propylmethacrylamide)	H		30	Turbidimetry[101]
Poly(N-n-propylmethacrylamide)	H	CH$_3$CH$_2$CH$_2$	28	UV[100]

1.3.2 Synthesis

Before the discovery of controlled radical polymerization techniques, most of the synthetic poly(N-alkylacrylamide)s were prepared by free radical polymerization, because the slightly acidic amide proton of monosubstituted (N-alkylacrylamide)s inhibits anionic polymerization. As an exception, the polymerization of monomers by living anionic polymerization has been possible for disubstituted (N-alkylacrylamide)s[102] and for monosubstituted monomers with protected active hydrogen.[103] Isotactic PNIPAM obtained by this method showed much lower solubility in water than atactic PNIPAM synthesized by free radical polymerization.[50]

The discovery of living radical polymerization of (N-alkylacrylamide)s[104] had a revolutionary effect on the study of such systems. Since then, poly(N-alkylacrylamide)s have been synthesized by ATRP,[105] NMP,[106] and RAFT.[107] In addition to molecular weight and PDI, tacticity of the polymers can also be controlled by these methods.[108] Figure 1.17 shows the structure of a diblock copolymer made by RAFT polymerization from PNIPAM in which the difference between two blocks is in their tacticity of the PNIPAM.[108]

a = atactic

i = isotactic

a-poly(NIPAM)

(a-b-i)poly(NIPAM)
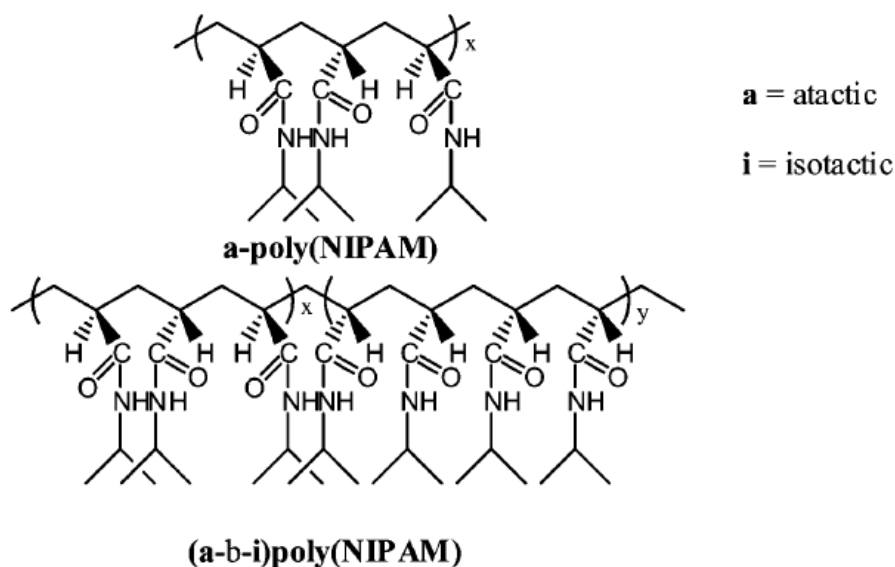
Figure 1.17 PNIPAM with desired tacticity made by RAFT polymerization. Reprinted from Ref. 108, © 2004 American Chemical Society.

The work done in our lab[23] is one of the most extensive studies on the RAFT polymerization of *N*-alkyl-substituted acrylamides. This study covers a wide range of mono- and disubstituted poly(*N*-alkylacrylamide)s from soluble poly(*N,N*-dimethylacrylamide) to insoluble poly(*N-n*-butylacrylamide) with the molar masses of ca. 10 kDa. Polymerizations were conducted at 70, 80, and 90 $^{\circ}$C using 2-dodecylsulfanylthiocarbonylsulfanyl-2-methyl propionic acid (DMP), dimethyl sulfoxide (DMSO), and AIBN as the RAFT agent, solvent and initiator, respectively. Well-defined polymers with narrow PDIs were obtained in reaction times of up to 180 min. However, longer reaction time (higher conversion) at elevated temperatures caused an increase in the PDI. Our study revealed that although the disubstituted (*N*-alkylacrylamide) monomers were better controlled than the monosubstituted counterparts under the same polymerization conditions, monosubstituted monomers resulted in successful chain extension to yield block copolymers. The reason for the better control of disubstituted monomers is the stronger electron-donating effect leading to higher reactivity and more stable intermediate radicals. On the other hand, their relative high chain transfer constants caused the better blocking ability of monosubstituted poly(*N*-alkylacrylamide) macro-CTAs.

1.3.3 Polymer architecture

Random copolymers. Although poly(*N*-alkylacrylamide)s produce a wide range of LCSTs (Table 1.1), there is a need for more tunable LCSTs for particular applications. Making random copolymers is a convenient way to have control over the LCST. For example, *N,N*-dimethylacrylamide (DMA) and *N*-tert-butylacrylamide (tBA) can be copolymerized to produce thermoresponsive copolymers with desired LCST[19] (Figure 1.18) even though their corresponding homopolymers, PDMA and PtBA, would be soluble and insoluble, respectively.
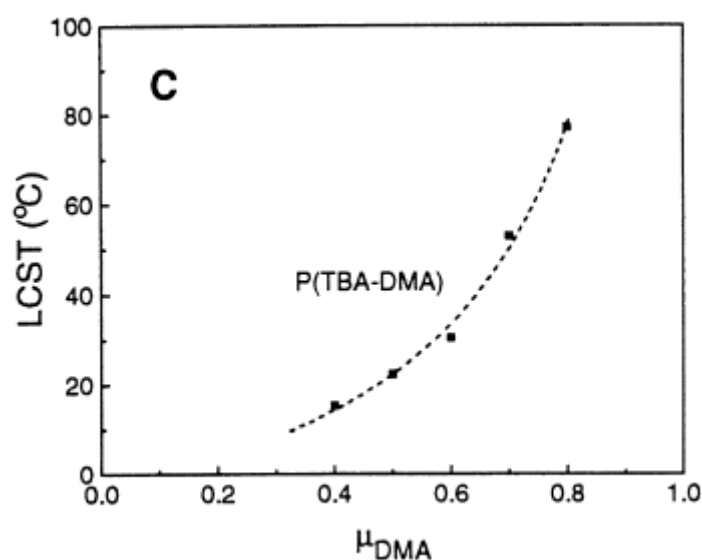
Figure 1.18 LCSTs of the random copolymers of DMA and tBA in water plotted as a function of the molar fraction of DMA. Reprinted from Ref. 19, © 1999 with permission from Elsevier.

Block copolymers. As mentioned above, living radical polymerization methods provide a facile way to synthesize block copolymers with controlled molecular weight and narrow PDI. Block copolymers consisting of poly(*N*-alkylacrylamide) attached to a more hydrophilic block such as acrylamide[109] or hydrophobic block such as PS[110] can produce amphiphilic polymers which form micelles in block-selective solvents.

Block copolymers of *N*-alkyl-substituted acrylamides are also possible. As indicated earlier, an extensive library of block copolymers of various poly(*N*-alkylacrylamide)s with different hydrophilicities in blocks has been made in our lab using RAFT polymerization.

Diblock copolymers are expected to show a two-step thermally induced self-assembly, as shown in Figure 1.7. A three-step temperature transition can be observed (Figure 1.4) for an ABC triblock copolymer with the composition $P(nPA_{124}\text{-}b\text{-}NIPAM_{80}\text{-}b\text{-}EMA_{44})$.[22]   A tetrablock copolymer $PnPA_{129}\text{-}b\text{-}PNIPAM_{52}\text{-}b\text{-}PEMA_{63}\text{-}b\text{-}PDMA_{184}$ was also prepared with low PDI (<1.25) and studied for its solution behavior.[23]

Other structures of polymers. Various architectures from poly(*N*-alkylacrylamide)s have been investigated so far. Kotsuchibashi *et al.*[111] made block copolymers consisting of random segments. Highly branched dendrimers with hollow cores and dense shells with NIPAM segments were made by You *et al.*[112] Lambeth *et al.*[113] prepared star block copolymers with the PNIPAM as the thermo-responsive interior block and PDMA as the water-soluble exterior block. Highly branched PNIPAM was made by Carter *et al.*[114] for use in protein purification. Tsuji *et al*[115] grafted PNIPAM and its copolymers with PAA on a St-VBC core to make "hairy particles" using living radical graft polymerization. Successful grafting was observed using scanning electron microscopy (SEM).

1.4 Applications

Developments in controlled polymerization techniques allow for the synthesis of polymers with well-defined architectures, reproducible molecular weights, low polydispersities, and end-group fidelity. These properties applied to stimuli-responsive polymers have opened the door to a wide range of promising applications in various fields. The majority of possible applications for these materials are in biomedicine, which are briefly explained in the following paragraphs, and the reader is referred to the numerous reviews in this field. Stuart *et al.*[116] reviewed different architectures derived from stimuli-responsive polymers in two-dimensional (films) and three-dimensional (assemblies) systems and how these systems can be used in selected applications. As shown in Figure 1.19, two-dimensional films may include polymer brushes, multilayered films made of different polymers (LBL), hybrid systems that combine polymers and particles, thin films of polymer networks, and membranes that are thin films with channels/pores. On the other hand, micelles, nanogels, capsules and vesicles, core–shell particles, hybrid particle-in-

particle structures, and their assemblies in solutions and at interfaces in emulsions and foams are examples of three-dimensional assemblies.
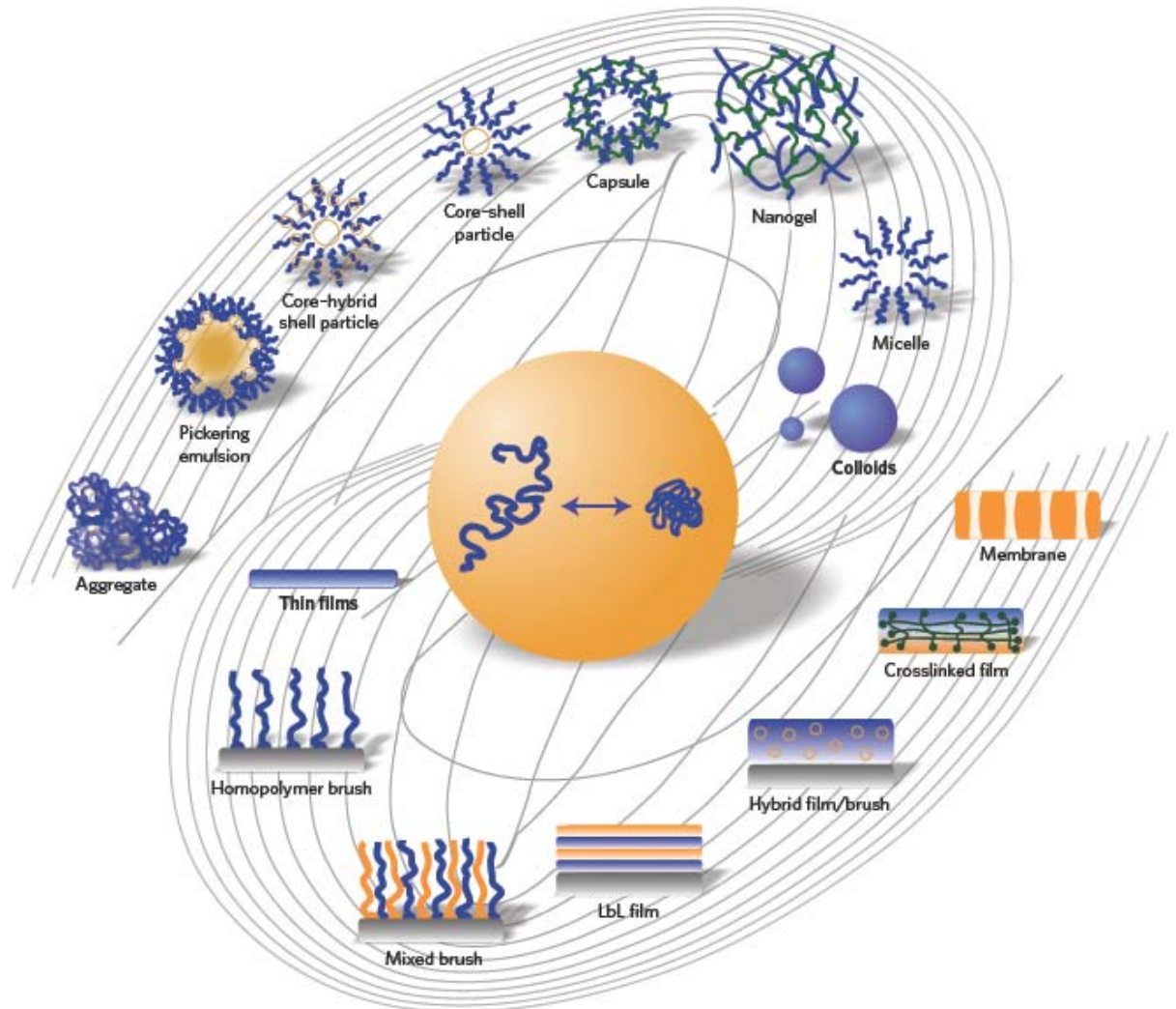
Figure 1.19 Various structures obtained from stimuli-responsive polymer materials in the form of films and assemblies. Reprinted by permission from Macmillan Publishers Ltd: Ref 116, © 2010.

1.4.1 Biomedical applications

Stimuli-responsive polymer both in the form of solution assemblies and surface-grafted polymers (Figure 1.20) have been investigated for various biomedical applications including drug delivery, medical diagnostics and imaging, tissue engineering, biosensors, and bioseparations.[117] These "smart" materials can be designed to respond to biological

stimuli (e.g. pH, reduction–oxidation, enzymes, glucose) and/or externally applied triggers (e.g. temperature, light, solvent quality).
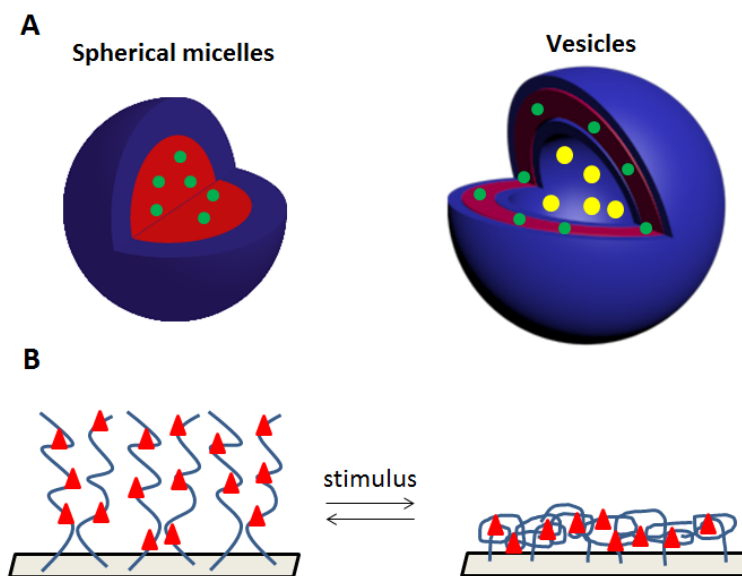
Figure 1.20 Stimuli-responsive (co)polymers. (A) Solution assemblies, micelles and vesicles. Hydrophobic and hydrophilic parts are represented by red and blue, respectively. Hydrophobic and hydrophilic encapsulated agents are shown in green and yellow, respectively. (B) surface-grafted (co)polymers. Functional groups (red triangles) are exposed in the extended form and hidden in the collapsed form of the polymer.

Figure 1.20A shows a typical example of solution self-assemblies encapsulating therapeutics, such as small molecules or proteins, for protection during the injection or circulation in the body. Using such carriers helps to improve circulation times and increase the amount of active drug released to the targeted site. Figure 1.20B represents a typical brush polymer grafted on the surface that can swell or shrink by applying a stimulus. For example, Ebara *et al.*[118] described thermoresponsive brushes made from poly(NIPAM-*co*-CIPAM), where CIPAM is 2-carboxyisopropylacrylamide and functionalized with the arginine-glycine-aspartic acid (RGD) sites to promote cell attachment. Above the LCST of PNIPAM, human umbilical vein endothelial cells were immobilized on the surface owing to the collapse of PNIPAM and accessibility of RGD integrin. Below the LCST of

PNIPAM hydrated brush chains shielded the RGD sites from the cells and the cell–surface interactions were disrupted resulting in facile cell release.

A variety of pH can be found in different types of tissues in the body. The meaningful difference between the pH of tumor tissues (pH~6.5-7.2),[119] normal tissues (pH~7.4), and the digestive tract (pH 1–8.2) allows for altering the polymer structure for *in vivo* applications. However, precise temperature control *in vivo* is difficult, and thermoresponsive polymers have attracted research interest mainly for applications *in vitro*.[117]

1.5 Scope and the structure of the present work

Amphiphilic block copolymers have attracted much research interest in many fields of science and technology. However, all the reported stimuli-responsive diblock copolymers were composed of blocks consisting of a single monomer when the present research began. Therefore, they benefit from a change in their solution properties under fixed pH or temperature value. Hence, tuning such responsiveness may not be easy given the limited choice of the monomers, even though multiblock copolymers may exhibit multiple responses to external stimuli.

The main objective of this work was to develop diblock random copolymers with the ability of showing both tunable and stepwise stimuli-responsive behavior in water as a new type of polymer structure. To reach this goal, two major modification methods were applied together on the same polymer in view of obtaining a tunable stimuli–responsive polymeric material. The first modification method is making block copolymers to develop multi-responsive copolymers, and the second one is to introduce random copolymers which are capable of tuning the cloud point by adjusting the comonomer ratio. Hence, diblock copolymers were developed for the first time which can respond in a controlled manner to the pre-determined solution pH and/or external temperature. It was achieved by using random copolymers as the blocks that allow the tuning of the cloud point by adjusting the monomer composition in the blocks. Stepwise responsiveness was also observed due to the block nature of the copolymer.

The studied stimuli in this work were pH and temperature, the most common ones in nature. The thermo- and pH-responsive diblock random copolymer was so designed that show so-called "schizophrenic" behavior. These systems form micelles capable of inverting their shell and core in aqueous solutions without adding any organic solvent, in response to an external stimulus that alters the relative hydrophilicity of the blocks. The temperature-dependent inversion of core and shell blocks in the micellar aggregates of such dually behaving block copolymers has been reported in aqueous solutions based on lower and upper critical solution temperatures (LCST and UCST) of the blocks, but sometimes observing a clear UCST is difficult as the transition may be broad. To the best of our knowledge, there has been no report on such invertible systems with dual thermo-responsiveness exploiting the LCST-like behavior of both blocks. Hence, for the first time an invertible system was made in quite a controlled manner, where both tunable blocks in a diblock copolymer show separate cloud points in water.

The synthetic approach developed in our group for making RAFT (co)polymerization, one of the most effective controlled radical polymerization methods, was employed to synthesize the copolymers from acrylamide-based (nPA and EA) and methacrylate-based (DEAEMA) comonomers. Several analytical techniques were optimized in this study to understand the solution behavior of diblock random copolymers.

This thesis consists of five chapters including this introduction and a conclusion. All the work presented and the reports were made by the author of this thesis with the help of his supervisor, Prof. Julian Zhu. Transmission electron microscopy (TEM) experiments were done by Dr. Satu Strandman. She also helped with the correction of the manuscripts as well as valuable discussions during the work.

Chapter 2 introduces a novel diblock copolymer made of two random copolymers, each being thermoresponsive. The block nature of the polymer allows for a double step phase transition corresponding to both blocks. In addition, each transition takes place at the desired temperature tuned by the random nature of the corresponding block. This chapter has been published as a paper (Savoji, M. T.; Strandman, S.; Zhu, X. X., Block random copolymers of *N*-alkyl-substituted acrylamides with double thermosensitivity. *Macromolecules* **2012,** *45* (4), 2001-2006).

Chapter 3 describes how diblock random copolymers can be made responsive to multiple stimuli, i.e. pH and temperature. This was achieved by introducing a weakly basic monomer, DEAEMA, to one of the blocks to render it pH-responsive. By doing so, in addition to double responsiveness at desired pH and temperature, invertible structures were obtained by a change in the external stimuli. This chapter has been published as a paper in *Langmuir* on 2013 (Savoji, M. T.; Strandman, S.; Zhu, X. X., Switchable vesicles Formed by diblock random copolymers with tunable pH- and thermo-responsiveness. *Langmuir* **2013,** *29* (23), 6823-6832).

Given the complexity of the invertible structures obtained in Chapter 2, a more detailed study was conducted in Chapter 4 to better understand the effect of the structure of the diblock random copolymer on the solution behavior of such systems. Switchable micelles and vesicles were observed and characterized in this chapter. This chapter has been submitted for publication in *Soft Matter*. (Savoji, M. T.; Strandman, S.; Zhu, X. X., Invertible vesicles and micelles formed by dually-responsive diblock random copolymers in aqueous solutions)

Finally, in Chapter 5, a conclusion giving an overal summary of the previous chapters and suggestions for future work are presented.

1.6 References

1.   Dai, S.; Ravi, P.; Tam, K. C. pH-Responsive polymers: synthesis, properties and applications. *Soft Matter* **2008,** *4* (3), 435-449.

2.   Schmaljohann, D. Thermo- and pH-responsive polymers in drug delivery. *Adv. Drug Delivery Rev.* **2006,** *58* (15), 1655-1670.

3.   Huang, J.; Hu, X.; Zhang, W.; Zhang, Y.; Li, G. pH and ionic strength responsive photonic polymers fabricated by using colloidal crystal templating. *Colloid Polym. Sci.* **2008,** *286* (1), 113-118.

4.   Guo, D.-S.; Zhang, T.-X.; Wang, Y.-X.; Liu, Y. Enzyme-responsive supramolecular polymers by complexation of bis(p-sulfonatocalixarenes) with suberyl dicholine-based pseudorotaxane. *Chem. Commun.* **2013,** *49* (60), 6779-6781.

5.   Yao, Y.; Wang, X.; Tan, T.; Yang, J. A facile strategy for polymers to achieve glucose-responsive behavior at neutral pH. *Soft Matter* **2011,** *7* (18), 7948-7951.

6.   Weber, C.; Hoogenboom, R.; Schubert, U. S. Temperature responsive bio-compatible polymers based on poly(ethylene oxide) and poly(2-oxazoline)s. *Prog. Polym. Sci.* **2012,** *37* (5), 686-714.

7.   Filipcsei, G.; Csetneki, I.; Szilagyi, A.; Zrinyi, M. Magnetic field-responsive smart polymer composites. *Adv. Polym. Sci.* **2007,** *206*, 137-189.

8.   Roy, D.; Cambre, J. N.; Sumerlin, B. S. Future perspectives and recent advances in stimuli-responsive materials. *Prog. Polym. Sci.* **2010,** *35* (1–2), 278-301.

9.   Smith, A. E.; Xu, X.; McCormick, C. L. Stimuli-responsive amphiphilic (co)polymers via RAFT polymerization. *Prog. Polym. Sci.* **2010,** *35* (1–2), 45-93.

10.   Heskins, M.; Guillet, J. E. Solution Properties of Poly(*N*-isopropylacrylamide). *J. Macromol. Sci., Chem.* **1968,** *2* (8), 1441-1455.

11.   Aseyev, V.; Tenhu, H.; Winnik, F. Non-ionic Thermoresponsive Polymers in Water. In *Self Organized Nanostructures of Amphiphilic Block Copolymers II*, Müller, A. H. E.; Borisov, O., Eds.; Springer Berlin Heidelberg, 2011; Vol. 242, pp 29-89.

12.   Koningsveld, R.; Stockmayer, W. H.; Nies, E. *Polymer Phase Diagrams*; Oxford University Press: Oxford 2001.

13.   Shi, Y.; van den Dungen, E. T. A.; Klumperman, B.; van Nostrum, C. F.; Hennink, W. E. Reversible Addition–Fragmentation Chain Transfer Synthesis of a Micelle-Forming, Structure Reversible Thermosensitive Diblock Copolymer Based on the N-(2-Hydroxy propyl) Methacrylamide Backbone. *ACS Macro Lett.* **2013,** *2* (5), 403-408.

14.   Cai, Y.; Aubrecht, K. B.; Grubbs, R. B. Thermally Induced Changes in Amphiphilicity Drive Reversible Restructuring of Assemblies of ABC Triblock Copolymers with Statistical Polyether Blocks. *J. Am. Chem. Soc.* **2010,** *133* (4), 1058-1065.

15.   Yamamoto, K.; Serizawa, T.; Akashi, M. Synthesis and Thermosensitive Properties of Poly[(*N*-vinylamide)-co-(vinyl acetate)]s and Their Hydrogels. *Macromol. Chem. Phys.* **2003,** *204* (7), 1027-1033.

16.   Hoogenboom, R.; Thijs, H. M. L.; Jochems, M. J. H. C.; van Lankvelt, B. M.; Fijten, M. W. M.; Schubert, U. S. Tuning the LCST of poly(2-oxazoline)s by varying composition and molecular weight: alternatives to poly(*N*-isopropylacrylamide)? *Chem. Commun.* **2008,** *0* (44), 5758-5760.

17.   Silva Nykanen, V. P.; Nykanen, A.; Puska, M. A.; Silva, G. G.; Ruokolainen, J. Dual-responsive and super absorbing thermally cross-linked hydrogel based on methacrylate substituted polyphosphazene. *Soft Matter* **2011,** *7* (9), 4414-4424.

18.   Avoce, D.; Liu, H. Y.; Zhu, X. X. *N*-Alkylacrylamide copolymers with (meth)acrylamide derivatives of cholic acid: synthesis and thermosensitivity. *Polymer* **2003,** *44* (4), 1081-1087.

19.   Liu, H. Y.; Zhu, X. X. Lower critical solution temperatures of *N*-substituted acrylamide copolymers in aqueous solutions. *Polymer* **1999,** *40* (25), 6985-6990.

20.   Chen, G.; Hoffman, A. S. Temperature-induced phase transition behaviors of random vs. graft copolymers of *N*-isopropylacrylamide and acrylic acid. *Macromol. Rapid Commun.* **1995,** *16* (3), 175-182.

21.   Jones, M. S. Effect of pH on the lower critical solution temperatures of random copolymers of *N*-isopropylacrylamide and acrylic acid. *Eur. Polym. J.* **1999,** *35* (5), 795-801.

22.   Cao, Y.; Zhao, N.; Wu, K.; Zhu, X. X. Solution properties of a thermosensitive triblock copolymer of *N*-alkyl substituted acrylamides. *Langmuir* **2009,** *25* (3), 1699-704.

23.   Cao, Y.; Zhu, X. X.; Luo, J.; Liu, H. Effects of Substitution Groups on the RAFT Polymerization of *N*-Alkylacrylamides in the Preparation of Thermosensitive Block Copolymers. *Macromolecules* **2007,** *40* (18), 6481-6488.

24.   Kerker, M. in *The scattering of light, and other electromagnetic*; Academic Press, New York, 1969; p 339.

25.   Vaupel, P.; Kallinowski, F.; Okunieff, P. Blood Flow, Oxygen and Nutrient Supply, and Metabolic Microenvironment of Human Tumors: A Review. *Cancer Res.* **1989,** *49* (23), 6449-6465.

26. Vriezema, D. M.; Comellas Aragonès, M.; Elemans, J. A. A. W.; Cornelissen, J. J. L. M.; Rowan, A. E.; Nolte, R. J. M. Self-Assembled Nanoreactors. *Chem. Rev.* **2005,** *105* (4), 1445-1490.

27. Luo, L.; Eisenberg, A. Thermodynamic Size Control of Block Copolymer Vesicles in Solution. *Langmuir* **2001,** *17* (22), 6804-6811.

28. Lee, A. S.; Bütün, V.; Vamvakaki, M.; Armes, S. P.; Pople, J. A.; Gast, A. P. Structure of pH-Dependent Block Copolymer Micelles: Charge and Ionic Strength Dependence. *Macromolecules* **2002,** *35* (22), 8540-8551.

29. Vamvakaki, M.; Palioura, D.; Spyros, A.; Armes, S. P.; Anastasiadis, S. H. Dynamic Light Scattering vs 1H NMR Investigation of pH-Responsive Diblock Copolymers in Water. *Macromolecules* **2006,** *39* (15), 5106-5112.

30. He, E.; Ravi, P.; Tam, K. C. Synthesis and Self-Assembly Behavior of Four-Arm Poly(ethylene oxide)-*b*-poly(2-(diethylamino)ethyl methacrylate) Star Block Copolymer in Salt Solutions. *Langmuir* **2007,** *23* (5), 2382-2388.

31. Sharifi-Sanjani, N.; Mahdavian, A. R.; Bataille, P. Emulsion polymerization of styrene and DEAEMA with a core–shell structure. *J. Appl. Polym. Sci.* **2000,** *78* (11), 1977-1985.

32. Dupin, D.; Rosselgong, J.; Armes, S. P.; Routh, A. F. Swelling Kinetics for a pH-Induced Latex-to-Microgel Transition. *Langmuir* **2007,** *23* (7), 4035-4041.

33. Gao, C.; Li, W.; Morimoto, H.; Nagaoka, Y.; Maekawa, T. Magnetic Carbon Nanotubes: Synthesis by Electrostatic Self-Assembly Approach and Application in Biomanipulations. *J. Phys. Chem. B* **2006,** *110* (14), 7213-7220.

34. Asayama, S.; Maruyama, A.; Cho, C.-S.; Akaike, T. Design of Comb-Type Polyamine Copolymers for a Novel pH-Sensitive DNA Carrier. *Bioconjugate Chem.* **1997,** *8* (6), 833-838.

35. Zhang, L.; Daniels, E. S.; Dimonie, V. L.; Klein, A. Synthesis and characterization of PNIPAM/PS core/shell particles. *J. Appl. Polym. Sci.* **2010,** *118* (5), 2502-2511.

36.   Weiss, J.; Böttcher, C.; Laschewsky, A. Self-assembly of double thermoresponsive block copolymers end-capped with complementary trimethylsilyl groups. *Soft Matter* **2011,** *7* (2), 483.

37.   Jochum, F. D.; Roth, P. J.; Kessler, D.; Theato, P. Double Thermoresponsive Block Copolymers Featuring a Biotin End Group. *Biomacromolecules* **2010,** *11* (9), 2432-2439.

38.   Lee, H.-N.; Bai, Z.; Newell, N.; Lodge, T. P. Micelle/Inverse Micelle Self-Assembly of a PEO−PNIPAm Block Copolymer in Ionic Liquids with Double Thermoresponsivity. *Macromolecules* **2010,** *43* (22), 9522-9528.

39.   Hsu, S.-P.; Chu, I. M.; Yang, J.-D. Thermo- and pH-Responsive Polymersomes of Poly(α,β-*N*-substituted-DL-aspartamide)s. *J. Appl. Polym. Sci.* **2012,** *125* (1), 133-144.

40.   Bai, Y.; Zhang, Z.; Zhang, A.; Chen, L.; He, C.; Zhuang, X.; Chen, X. Novel thermo- and pH-responsive hydroxypropyl cellulose- and poly (l-glutamic acid)-based microgels for oral insulin controlled release. *Carbohydr. Polym.* **2012,** *89* (4), 1207-1214.

41.   Jiang, X.; Lu, G.; Feng, C.; Li, Y.; Huang, X. Poly(acrylic acid)-graft-poly(*N*-vinylcaprolactam): a novel pH and thermo dual-stimuli responsive system. *Polym. Chem.* **2013,** *4* (13), 3876-3884.

42.   Abdullah Al, N.; Lee, K. S.; Mosaiab, T.; Park, S. Y. pH and thermo-responsive poly(*N*-isopropylacrylamide) copolymer grafted to poly(ethylene glycol). *J. Appl. Polym. Sci.* **2013,** *130* (1), 168-174.

43.   Chen, P.; Chen, J.; Cao, Y. Self-Assembly Behavior of Thermo- and Ph-Responsive Diblock Copolymer of Poly(*N*-isopropylacrylamide)- Block-Poly(acrylic acid) Synthesized Via Reversible Addition-Fragmentation Chain Transfer Polymerization. *J. Macromol. Sci., Pure Appl. Chem.* **2013,** *50* (5), 478-486.

44.   Gohy, J.-F.; Antoun, S.; Jérôme, R. pH-Dependent Micellization of Poly(2-vinylpyridine)-block-poly((dimethylamino)ethyl methacrylate) Diblock Copolymers. *Macromolecules* **2001,** *34* (21), 7435-7440.

45.   Klaikherd, A.; Nagamani, C.; Thayumanavan, S. Multi-Stimuli Sensitive Amphiphilic Block Copolymer Assemblies. *J. Am. Chem. Soc.* **2009,** *131* (13), 4830-4838.

46.   Ebewele, R. O. *Polymer science and technology*; CRC Press LLC2000.

47.   Bahadur, P.; Sastry, N. V. *Principles of Polymer Science*; Second ed.; Alpha Science Int'l Ltd.2005. p 33-34.

48.   Szwarc, M. 'Living' Polymers. *Nature* **1956,** *178*, 1168-1169.

49.   Nicolas, J.; Guillaneuf, Y.; Lefay, C.; Bertin, D.; Gigmes, D.; Charleux, B. Nitroxide-mediated polymerization. *Prog. Polym. Sci.* **2013,** *38* (1), 63-235.

50.   Aoshima, S.; Kanaoka, S. Synthesis of Stimuli-Responsive Polymers by Living Polymerization: Poly(*N*-Isopropylacrylamide) and Poly(Vinyl Ether)s. In *Wax Crystal Control · Nanocomposites · Stimuli-Responsive Polymers*; Springer Berlin Heidelberg, 2008; Vol. 210, pp 169-208.

51.   Ouchi, M.; Terashima, T.; Sawamoto, M. Transition Metal-Catalyzed Living Radical Polymerization: Toward Perfection in Catalysis and Precision Polymer Synthesis. *Chem. Rev.* **2009,** *109* (11), 4963-5050.

52.   Debuigne, A.; Chan-Seng, D.; Li, L.; Hamer, G. K.; Georges, M. K. Synthesis and Evaluation of Sterically Hindered 1,1-Diadamantyl Nitroxide as a Low-Temperature Mediator for the Stable Free Radical Polymerization Process. *Macromolecules* **2007,** *40* (17), 6224-6232.

53.   Solomon, D.; Rizzardo, E.; P, C. Polymerization Process and Polymers Produced Thereby US Patent 4,581,429, 1986.

54.   Georges, M. K.; Veregin, R. P. N.; Kazmaier, P. M.; Hamer, G. K. Narrow molecular weight resins by a free-radical polymerization process. *Macromolecules* **1993,** *26* (11), 2987-2988.

55.   Odell, P. G.; Veregin, R. P. N.; Michalak, L. M.; Brousmiche, D.; Georges, M. K. Rate Enhancement of Living Free-Radical Polymerizations by an Organic Acid Salt. *Macromolecules* **1995,** *28* (24), 8453-8455.

56.   Dollin, M.; Szkurhan, A. R.; Georges, M. K. Rapid additive-free TEMPO-mediated stable free radical polymerizations of styrene. *J. Polym. Sci., Part A: Polym. Chem.* **2007,** *45* (23), 5487-5493.

57.   Tasdelen, M. A.; Kahveci, M. U.; Yagci, Y. Telechelic polymers by living and controlled/living polymerization methods. *Prog. Polym. Sci.* **2011,** *36* (4), 455-567.

58.   Wang, J.-S.; Matyjaszewski, K. Controlled/"Living" Radical Polymerization. Halogen Atom Transfer Radical Polymerization Promoted by a Cu(I)/Cu(II) Redox Process. *Macromolecules* **1995,** *28* (23), 7901-7910.

59.   Kato, M.; Kamigaito, M.; Sawamoto, M.; Higashimura, T. Polymerization of Methyl Methacrylate with the Carbon Tetrachloride/Dichlorotris-(triphenylphosphine)ruthenium(II)/Methylaluminum Bis(2,6-di-tert-butylphenoxide) Initiating System: Possibility of Living Radical Polymerization. *Macromolecules* **1995,** *28* (5), 1721-1723.

60.   Ayres, N. Atom Transfer Radical Polymerization: A Robust and Versatile Route for Polymer Synthesis. *Polym. Rev.* **2011,** *51* (2), 138-162.

61.   Percec, V.; Popov, A. V.; Ramirez-Castillo, E.; Coelho, J. F. J.; Hinojosa-Falcon, L. A. Non-transition metal-catalyzed living radical polymerization of vinyl chloride initiated with iodoform in water at 25 °C. *J. Polym. Sci., Part A: Polym. Chem.* **2004,** *42* (24), 6267-6282.

62.   Lin, C. Y.; Coote, M. L.; Gennaro, A.; Matyjaszewski, K. Ab Initio Evaluation of the Thermodynamic and Electrochemical Properties of Alkyl Halides and Radicals and Their Mechanistic Implications for Atom Transfer Radical Polymerization. *J. Am. Chem. Soc.* **2008,** *130* (38), 12762-12774.

63.   Broyer, R. M.; Quaker, G. M.; Maynard, H. D. Designed Amino Acid ATRP Initiators for the Synthesis of Biohybrid Materials. *J. Am. Chem. Soc.* **2007,** *130* (3), 1041-1047.

64.   Urbani, C. N.; Bell, C. A.; Whittaker, M. R.; Monteiro, M. J. Convergent Synthesis of Second Generation AB-Type Miktoarm Dendrimers Using "Click" Chemistry Catalyzed by Copper Wire. *Macromolecules* **2008,** *41* (4), 1057-1060.

65.   Zhang, W.; Müller, A. H. E. A "Click Chemistry" Approach to Linear and Star-Shaped Telechelic POSS-Containing Hybrid Polymers. *Macromolecules* **2010,** *43* (7), 3148-3152.

66.   Chiefari, J.; Chong, Y. K.; Ercole, F.; Krstina, J.; Jeffery, J.; Le, T. P. T.; Mayadunne, R. T. A.; Meijs, G. F.; Moad, C. L.; Moad, G.; Rizzardo, E.; Thang, S. H. Living Free-Radical Polymerization by Reversible Addition−Fragmentation Chain Transfer: The RAFT Process. *Macromolecules* **1998,** *31* (16), 5559-5562.

67.   McCormick, C. L.; Lowe, A. B. Aqueous RAFT Polymerization: Recent Developments in Synthesis of Functional Water-Soluble (Co)polymers with Controlled Structures†. *Acc. Chem. Res.* **2004,** *37* (5), 312-325.

68.   Zhang, W.; Charleux, B.; Cassagnau, P. Viscoelastic Properties of Water Suspensions of Polymer Nanofibers Synthesized via RAFT-Mediated Emulsion Polymerization. *Macromolecules* **2012,** *45* (12), 5273-5280.

69.   Rieger, J.; Stoffelbach, F. o.; Bui, C.; Alaimo, D.; Jérôme, C.; Charleux, B. Amphiphilic Poly(ethylene oxide) Macromolecular RAFT Agent as a Stabilizer and Control Agent in ab Initio Batch Emulsion Polymerization. *Macromolecules* **2008,** *41* (12), 4065-4068.

70.   Nguyen, T. L. U.; Eagles, K.; Davis, T. P.; Barner-Kowollik, C.; Stenzel, M. H. Investigation of the influence of the architectures of poly(vinyl pyrrolidone) polymers made via the reversible addition–fragmentation chain transfer/macromolecular design via the interchange of xanthates mechanism on the stabilization of suspension polymerizations. *J. Polym. Sci., Part A: Polym. Chem.* **2006,** *44* (15), 4372-4383.

71.   He, W.-D.; Sun, X.-L.; Wan, W.-M.; Pan, C.-Y. Multiple Morphologies of PAA-*b*-PSt Assemblies throughout RAFT Dispersion Polymerization of Styrene with PAA Macro-CTA. *Macromolecules* **2011,** *44* (9), 3358-3365.

72.   Moad, G.; Rizzardo, E.; Thang, S. H. Living Radical Polymerization by the RAFT Process – A Second Update. *Aust. J. Chem.* **2009,** *62* (11), 1402-1472.

73.   Klumperman, B.; McLeary, J. B.; van den Dungen, E. T. A.; Pound, G. NMR Spectroscopy in the Optimization and Evaluation of RAFT Agents. *Macromolecular Symposia* **2007,** *248* (1), 141-149.

74.   Moad, G.; Rizzardo, E.; Thang, S. H. Living Radical Polymerization by the RAFT Process—A First Update. *Aust. J. Chem.* **2006,** *59* (10), 669-692.

75.   Pietsch, C.; Fijten, M. W. M.; Lambermont-Thijs, H. M. L.; Hoogenboom, R.; Schubert, U. S. Unexpected reactivity for the RAFT copolymerization of oligo(ethylene glycol) methacrylates. *J. Polym. Sci., Part A: Polym. Chem.* **2009,** *47* (11), 2811-2820.

76.   Drache, M.; Schmidt-Naake, G. RAFT Polymerization - Investigation of the Initialization Period and Determination of the Transfer Coefficients. *Macromolecular Symposia* **2007,** *259* (1), 397-405.

77.   Chernikova, E. V.; Tarasenko, A. V.; Garina, E. S.; Golubev, V. B. Controlled radical polymerization of styrene mediated by dithiobenzoates as reversible addition-fragmentation chain-transfer agents. *Polym. Sci. Ser. A* **2006,** *48* (10), 1046-1057.

78.   Tao, L.; Xu, J.; Gell, D.; Davis, T. P. Synthesis, Characterization, and Bioactivity of Mid-Functional PolyHPMA−Lysozyme Bioconjugates. *Macromolecules* **2010,** *43* (8), 3721-3727.

79.   Chen, X.; Ayres, N. Synthesis of Novel Polymer/Urea Peptoid Conjugates Using RAFT Polymerization. *Macromolecules* **2010,** *43* (3), 1341-1348.

80.   Jackson, A. W.; Fulton, D. A. Dynamic Covalent Diblock Copolymers Prepared from RAFT Generated Aldehyde and Alkoxyamine End-Functionalized Polymers. *Macromolecules* **2009,** *43* (2), 1069-1075.

81.   Heredia, K. L.; Nguyen, T. H.; Chang, C.-W.; Bulmus, V.; Davis, T. P.; Maynard, H. D. Reversible siRNA-polymer conjugates by RAFT polymerization. *Chem. Commun.* **2008,** *0* (28), 3245-3247.

82.   Boyer, C.; Liu, J.; Bulmus, V.; Davis, T. P.; Barner-Kowollik, C.; Stenzel, M. H. Direct Synthesis of Well-Defined Heterotelechelic Polymers for Bioconjugations. *Macromolecules* **2008,** *41* (15), 5641-5650.

83.   Konkolewicz, D.; Gray-Weale, A.; Perrier, S. b. Hyperbranched Polymers by Thiol−Yne Chemistry: From Small Molecules to Functional Polymers. *J. Am. Chem. Soc.* **2009,** *131* (50), 18075-18077.

84.   Hentschel, J.; Bleek, K.; Ernst, O.; Lutz, J.-F.; Borner, H. G. Easy Access to Bioactive Peptide−Polymer Conjugates via RAFT. *Macromolecules* **2008,** *41* (4), 1073-1075.

85.   Thomas, D. B.; Convertine, A. J.; Hester, R. D.; Lowe, A. B.; McCormick, C. L. Hydrolytic Susceptibility of Dithioester Chain Transfer Agents and Implications in Aqueous RAFT Polymerizations†. *Macromolecules* **2004,** *37* (5), 1735-1741.

86.   Moad, G.; Chong, Y. K.; Postma, A.; Rizzardo, E.; Thang, S. H. Advances in RAFT polymerization: the synthesis of polymers with defined end-groups. *Polymer* **2005,** *46* (19), 8458-8468.

87.   Qiu, X.-P.; Winnik, F. M. Facile and Efficient One-Pot Transformation of RAFT Polymer End Groups via a Mild Aminolysis/Michael Addition Sequence. *Macromol. Rapid Commun.* **2006,** *27* (19), 1648-1653.

88.   Sumerlin, B. S.; Lowe, A. B.; Stroud, P. A.; Zhang, P.; Urban, M. W.; McCormick, C. L. Modification of Gold Surfaces with Water-Soluble (Co)polymers Prepared via Aqueous Reversible Addition−Fragmentation Chain Transfer (RAFT) Polymerization†. *Langmuir* **2003,** *19* (14), 5559-5562.

89.   Zheng, R.-C.; Zheng, Y.-G.; Shen, Y.-C.; Flickinger, M. C. Acrylamide, Microbial Production by Nitrile Hydratase. In *Encyclopedia of Industrial Biotechnology*; John Wiley & Sons, Inc., 2009.

90.   Shea, K. J.; Stoddard, G. J.; Shavelle, D. M.; Wakui, F.; Choate, R. M. Synthesis and characterization of highly crosslinked poly(acrylamides) and poly(methacrylamides). A new class of macroporous polyamides. *Macromolecules* **1990,** *23* (21), 4497-4507.

91.   Wu, C.; Wang, X. Globule-to-Coil Transition of a Single Homopolymer Chain in Solution. *Phys. Rev. Lett.* **1998,** *80* (18), 4092-4094.

92.   Fujishige, S.; Kubota, K.; Ando, I. Phase transition of aqueous solutions of poly (*N*-isopropylacrylamide) and poly (*N*-isopropylmethacrylamide). *J. Phys. Chem.* **1989,** *93* (8), 3311-3313.

93.   Cai, W.; Gupta, R. B. Poly (*N*-ethylacrylamide) hydrogels for lignin separation. *Ind. Eng. Chem. Res.* **2001,** *40* (15), 3406-3412.

94.   Taylor, L. D.; Cerankowski, L. D. Preparation of films exhibiting a balanced temperature dependence to permeation by aqueous solutions—a study of lower consolute behavior. *J. Polym. Sci.: Polym. Chem. Ed.* **1975,** *13* (11), 2551-2570.

95.   Mertoglu, M.; Garnier, S.; Laschewsky, A.; Skrabania, K.; Storsberg, J. Stimuli responsive amphiphilic block copolymers for aqueous media synthesised via reversible addition fragmentation chain transfer polymerisation (RAFT). *Polymer* **2005,** *46* (18), 7726-7740.

96.   Liu, S.; Liu, M. Synthesis and characterization of temperature-and pH-sensitive poly (N, N-diethylacrylamide-co-methacrylic acid). *J. Appl. Polym. Sci.* **2003,** *90* (13), 3563-3568.

97.   Kobayashi, M.; Okuyama, S.; Ishizone, T.; Nakahama, S. Stereospecific Anionic Polymerization of *N,N*-Dialkylacrylamides. *Macromolecules* **1999,** *32* (20), 6466-6477.

98.   Ito, D.; Kubota, K. Solution Properties and Thermal Behavior of Poly(*N*-n-propylacrylamide) in Water. *Macromolecules* **1997,** *30* (25), 7828-7834.

99.   Hoshino, K.; Taniguchi, M.; Kitao, T.; Morohashi, S.; Sasakura, T. Preparation of a new thermo-responsive adsorbent with maltose as a ligand and its application to affinity precipitation. *Biotechnol. Bioeng.* **1998,** *60* (5), 568-579.

100.   Ito, S. Phase Transition of Aqueous Solution of Poly (*N*-alkylacrylamide) Derivatives; Effects of Side Chain Structure. *Kobunshi Ronbunshu* **1989,** *46* (7), 437-443.

101.   Aoki, T.; Muramatsu, M.; Torii, T.; Sanui, K.; Ogata, N. Thermosensitive Phase Transition of an Optically Active Polymer in Aqueous Milieu. *Macromolecules* **2001,** *34* (10), 3118-3119.

102.   Kobayashi, M.; Ishizone, T.; Nakahama, S. Synthesis of highly isotactic poly (N, N-diethylacrylamide) by anionic polymerization with grignard reagents and diethylzinc. *J. Polym. Sci., Part A: Polym. Chem.* **2000,** *38* (S1), 4677-4685.

103. Ito, M.; Ishizone, T. Living anionic polymerization of *N*-methoxymethyl-*N*-isopropylacrylamide: Synthesis of well-defined poly(*N*-isopropylacrylamide) having various stereoregularity. *J. Polym. Sci., Part A: Polym. Chem.* **2006,** *44* (16), 4832-4845.

104. Ganachaud, F.; Monteiro, M. J.; Gilbert, R. G.; Dourges, M.-A.; Thang, S. H.; Rizzardo, E. Molecular Weight Characterization of Poly(*N*-isopropylacrylamide) Prepared by Living Free-Radical Polymerization. *Macromolecules* **2000,** *33* (18), 6738-6745.

105. Nath, N.; Chilkoti, A. Creating "Smart" Surfaces Using Stimuli Responsive Polymers. *Adv. Mater.* **2002,** *14* (17), 1243-1247.

106. Schierholz, K.; Givehchi, M.; Fabre, P.; Nallet, F.; Papon, E.; Guerret, O.; Gnanou, Y. Acrylamide-Based Amphiphilic Block Copolymers via Nitroxide-Mediated Radical Polymerization. *Macromolecules* **2003,** *36* (16), 5995-5999.

107. Bauri, K.; Roy, S.; Arora, S.; Dey, R.; Goswami, A.; Madras, G.; De, P. Thermal degradation kinetics of thermoresponsive poly(*N*-isopropylacrylamide-co-*N,N*-dimethylacrylamide) copolymers prepared via RAFT polymerization. *J Therm Anal Calorim* **2013,** *111* (1), 753-761.

108. Ray, B.; Isobe, Y.; Matsumoto, K.; Habaue, S.; Okamoto, Y.; Kamigaito, M.; Sawamoto, M. RAFT Polymerization of *N*-Isopropylacrylamide in the Absence and Presence of Y(OTf)3: Simultaneous Control of Molecular Weight and Tacticity. *Macromolecules* **2004,** *37* (5), 1702-1710.

109. Wever, D. A. Z.; Raffa, P.; Picchioni, F.; Broekhuis, A. A. Acrylamide Homopolymers and Acrylamide–*N*-Isopropylacrylamide Block Copolymers by Atomic Transfer Radical Polymerization in Water. *Macromolecules* **2012,** *45* (10), 4040-4045.

110. Zheng, C.; He, W.-D.; Liu, W.-J.; Li, J.; Li, J.-F. Novel One-Step Route for Preparing Amphiphilic Block Copolymers of Styrene and *N*-Isopropylacrylamide in a Microemulsion. *Macromol. Rapid Commun.* **2006,** *27* (15), 1229-1232.

111. Kotsuchibashi, Y.; Ebara, M.; Idota, N.; Narain, R.; Aoyagi, T. A 'smart' approach towards the formation of multifunctional nano-assemblies by simple mixing of block copolymers having a common temperature sensitive segment. *Polym. Chem.* **2012,** *3* (5), 1150.

112.   You, Y. Z.; Hong, C. Y.; Pan, C. Y.; Wang, P. H. Synthesis of a Dendritic Core–Shell Nanostructure with a Temperature-Sensitive Shell. *Adv. Mater.* **2004,** *16* (21), 1953-1957.

113.   Lambeth, R. H.; Ramakrishnan, S.; Mueller, R.; Poziemski, J. P.; Miguel, G. S.; Markoski, L. J.; Zukoski, C. F.; Moore, J. S. Synthesis and Aggregation Behavior of Thermally Responsive Star Polymers. *Langmuir* **2006,** *22* (14), 6352-6360.

114.   Carter, S.; Rimmer, S.; Rutkaite, R.; Swanson, L.; Fairclough, J. P. A.; Sturdy, A.; Webb, M. Highly Branched Poly(*N*-isopropylacrylamide) for Use in Protein Purification. *Biomacromolecules* **2006,** *7* (4), 1124-1130.

115.   Tsuji, S.; Kawaguchi, H. Temperature-Sensitive Hairy Particles Prepared by Living Radical Graft Polymerization. *Langmuir* **2004,** *20* (6), 2449-2455.

116.   Stuart, M. A. C.; Huck, W. T. S.; Genzer, J.; Muller, M.; Ober, C.; Stamm, M.; Sukhorukov, G. B.; Szleifer, I.; Tsukruk, V. V.; Urban, M.; Winnik, F.; Zauscher, S.; Luzinov, I.; Minko, S. Emerging applications of stimuli-responsive polymer materials. *Nat. Mater.* **2010,** *9* (2), 101-113.

117.   Kelley, E. G.; Albert, J. N. L.; Sullivan, M. O.; Epps, I. I. I. T. H. Stimuli-responsive copolymer solution and surface assemblies for biomedical applications. *Chem. Soc. Rev.* **2013,** *42* (17), 7057-7071.

118.   Ebara, M.; Yamato, M.; Aoyagi, T.; Kikuchi, A.; Sakai, K.; Okano, T. Temperature-Responsive Cell Culture Surfaces Enable "On−Off" Affinity Control between Cell Integrins and RGDS Ligands. *Biomacromolecules* **2004,** *5* (2), 505-510.

119.   Colson, Y. L.; Grinstaff, M. W. Biologically Responsive Polymeric Nanoparticles for Drug Delivery. *Adv. Mater.* **2012,** *24* (28), 3878-3886.

Chapter 2

Block random copolymers of *N*-alkyl-substituted acrylamides with double thermosensitivity*

Abstract

Block copolymers consisting of two segments of random copolymers of *N*-alkylacrylamides have been synthesized by a sequential reversible addition−fragmentation chain transfer (RAFT) polymerization. The copolymers in the form of A_nB_m-*b*-A_pB_q have been made of two blocks of *N*-n-propylacrylamide (nPA) and *N*-ethylacrylamide (EA) of different compositions to obtain polymers with stepwise thermosensitivity. The control of the RAFT polymerization was confirmed by studying the kinetics of the copolymerization process. The block random copolymer, poly(nPA_x-*co*-EA_{1-x})-*block*-poly(nPA_y-*co*-EA_{1-y}), is well-defined and has a low polydispersity. The cloud points of the random copolymers can be tuned by varying the chemical composition of the copolymers. The diblock copolymer exhibited a two-step phase transition upon heating to 41.5 and 53.0 °C, corresponding to the cloud points of the individual blocks. Dynamic light scattering experiments also showed the stepwise aggregation properties of the copolymer in aqueous solutions.

2.1   Introduction

Thermoresponsive polymers have been widely investigated for their potential in biomedical applications.[1−4] Many polymers based on *N*-alkyl-substituted acrylamides, the most well-known of which being poly(*N*-isopropylacrylamide), exhibit a lower critical

---

solution temperature (LCST) in water.[5] The thermoresponsiveness of these polymers depends on the relative hydrophobicity or hydrophilicity of the *N*-alkylacrylamide monomers.[5,6] It also depends on the molar mass, concentration, and additives in the polymer solution. Increased hydrophobicity of the substitution groups leads to a lower phase transition temperature of the polymers obtained.[7-10] The cloud points (CPs) of the polymers can be tuned by varying the chemical composition of the random copolymers based on *N*-alkylsubstituted (meth)acrylamides.[11-13] Diblock copolymers with dual thermoresponsive behavior have been synthesized by the incorporation of blocks with different cloud points.[4,14-19] We have made various di- and triblock copolymers of *N*-alkylacrylamides and showed that they exhibited multiple CPs in aqueous solutions,[20,21] corresponding to different stages of their aggregation.[22,23] The phase transitions are usually accompanied by changes in the micellar size or shape and solution properties. However, the choice of the substitution groups on such monomers limits the range of the phase transition temperatures. To tailor the properties of the materials, it would be ideal to have blocks available with a thermosensitivity at any desired temperature. This may be achieved by varying the chemical composition of a random copolymer.[12] Therefore, our approach is to make a block copolymer of two random copolymer sequeneces with different thermosensitivities. We chose to use the reversible addition fragmentation chain transfer (RAFT) polymerization method[24,25] to grow two block of random copolymers of *N*-n-propylacrylamide (nPA) and *N*-ethylacrylamide (EA) with compositions adjusted for the desired transition temperatures. We report here the design, synthesis, and characterization of a diblock thermoresponsive copolymer with two distinct transition temperatures corresponding to the two random copolymers synthesized by sequential RAFT copolymerization.

2.2   Experimental section

2.2.1   Materials

2,2′-Azobis(isobutyronitrile) (AIBN) from Eastman Kodak was recrystallized from methanol and stored in dark bottles in a refrigerator. Acryloyl chloride, ethylamine, and n-propylamine were purchased from Aldrich and were used without further purification. *N*-n-

Propylacrylamide (nPA) and *N*-ethylacrylamide (EA) were prepared by reacting acryloyl chloride with the corresponding alkylamines following a reported procedure.[26] 2-Dodecylsulfanylthiocarbonylsulfanyl-2-methylpropionic acid (DMP) was used as a highly efficient chain transfer reagent (CTA) and prepared according to the procedure reported by Lai *et al.*[27] Water was purified using a Millipore Milli-Q system. Anhydrous and oxygen-free dioxane was obtained by passage through columns packed with activated alumina and supported copper catalyst (Glass Contour, Irvine, CA).

2.2.2   Polymer synthesis

The monomers nPA and EA were added at a predetermined ratio along with trithiocarbonate DMP as the CTA and AIBN as the initiator in a 100 mL Schlenk tube equipped with a magnetic stirrer bar. A fixed volume of anhydrous dioxane was then transferred to the Schlenk tube. The ratio of [monomers]:[DMP]:[AIBN] was fixed at 200:1:0.1, and the total monomer concentration was 0.3 g/mL. The mixture was degassed by three freeze−pump−thaw cycles prior to immersing it in a preheated oil bath. The reaction temperature was set to 70 °C, and the reaction was conducted for 90 min before terminating it by exposing the reaction mixture to air and immersing it in an ice bath. The product was then precipitated in diethyl ether, filtered, and dried in vacuum oven at 60 °C to yield poly(nPA$_x$-*co*-EA$_{1-x}$)-CTA as a yellowish powder. The resulting random copolymer was then used as the DMP-ended macro-CTA in the second step to make a diblock copolymer using the reactant ratio [monomer]:[macro-CTA]:[AIBN] of 400:1:0.1. The procedure for diblock copolymerization was the same as for random copolymerization, except that DMP has been replaced by macro-CTA (Scheme 2.1). In the kinetic studies, aliquots of the reaction mixture were withdrawn during the course of the copolymerization and analyzed by size exclusion chromatography (SEC) and nuclear magnetic resonance (NMR) spectroscopy.
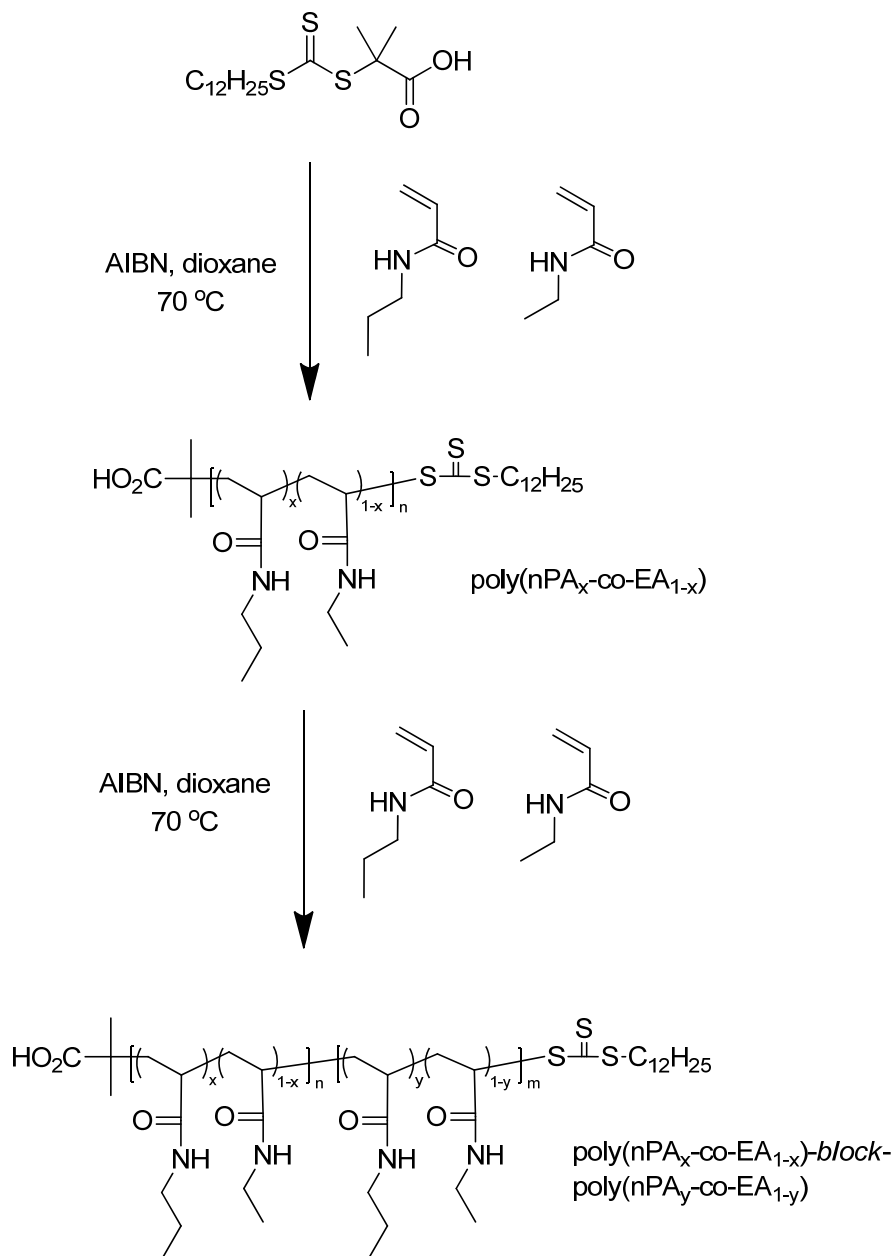
Scheme 2.1 RAFT copolymerization of nPA and EA for the preparation of poly(nPA$_x$-co-EA$_{1-x}$) and further chain extension leading to a diblock random copolymer poly(nPA$_x$-*co*-EA$_{1-x}$)-*block*-poly(nPA$_y$-*co*-EA$_{1-y}$)

2.2.3   Polymer characterization

Molar masses and polydispersity indices (PDI) of the polymers were obtained by SEC on a Waters 1525 system equipped with three Waters Styragel columns and a refractive index detector (Waters 2410) at 35 °C. *N,N*-Dimethylformamide (DMF) was employed as

the mobile phase at a flow rate of 1 mL/min, and the system was calibrated by poly(methyl methacrylate) standards. In kinetic studies, the volatile species were removed in a vacuum oven at 60 °C from the samples taken at different time intervals during the course of the reaction.

The NMR spectra of the monomers and polymers in deuterated chloroform ($CDCl_3$) were determined on a Bruker AV-400 spectrometer operating at 400 MHz for protons. The chemical shifts are given in reference to the solvent peak at 7.26 ppm. The theoretical molar masses were calculated from the conversions given by ^{1}H NMR according to

$$\bar{M}_{n,th} = M_{CTA} + \frac{[monomer]}{[CTA]} \times M_{monomer} \times conversion \qquad (2.1)$$

where M_{CTA} is the molar mass of the chain transfer agent and [monomer] and [CTA] are the initial monomer and CTA concentrations, respectively. $M_{monomer}$ is the weighted molar mass of the comonomers and calculated from the molar ratios of comonomers in the product obtained by ^{1}H NMR. The molar masses of the polymers were not determined by ^{1}H NMR because of the overlap of the methyl group signals from EA and from DMP end group at 0.99 ppm. For a block copolymer, [CTA] in eq 1 is replaced by the concentration of macro-CTA.

The CPs of the polymers were determined from the optical transmittance measured on a Cary 300 Bio UV−vis spectrophotometer equipped with a temperature-controlled sample holder. Samples were prepared by the dissolution of copolymers in distilled water in an ice−water bath, after which the solutions were homogenized by ultrasonication. The absorbance was measured at different wavelengths for the aqueous solution of polymers 1.0 mg/mL by continuous heating at rate of 0.1 °C/min over various temperature ranges or stepwise heating at 1 °C intervals with 20 min equilibration at each temperature, which was also the heating procedure used in the light scattering experiments where continuous heating was not possible. Here, the CP is defined as a temperature at which the differential of transmittance change with respect to the temperature at a certain wavelength is maximal.[28] Another definition is the temperature corresponding to a 10% or 50% reduction in the initial transmittance.[20,25,29] For individual blocks, the temperature at which 50% transmittance was lost upon heating was considered as the CP. For block copolymers, the

CP is determined from the middle point between the onset and the offset of the transmittance curve as a function of temperature.

Dynamic light scattering (DLS) studies on the temperature-dependent aggregation behavior were carried out on a CGS-3 compact goniometer (ALV GmbH) equipped with an ALV-5000 multi tau digital real time correlator at chosen temperatures using a Science/Electronics temperature controller. The laser wavelength was 632 nm, and the scattering angle was fixed at 90°. All solutions were made with the concentration of 2.0 mg/mL and filtered through 0.22 μm Millipore filters to remove dust. The samples were heated at 1 °C intervals within 20 min equilibration time. The results were analyzed by CONTIN inverse Laplace transform algorithm. The decay rate distributions were transformed to an apparent diffusion coefficient and the apparent intensity-weighted hydrodynamic diameters of the polymers was obtained from the Stokes−Einstein equation.

2.3   Results and discussion

2.3.1   Kinetics of the RAFT copolymerization of *N*-alkyl-substituted acrylamides

N-n-Propylacrylamide and *N*-ethylacrylamide were copolymerized in dioxane at 70 °C using a monomer ratio of 70:30 (nPA:EA) and a reactant ratio of [monomers]:[CTA]:[initiator] of 200:1:0.1. The conversion was monitored by ^{1}H NMR spectroscopy of the samples withdrawn from the reaction mixture at regular time intervals and determined by comparing the integrated areas of the characteristic proton signals from the vinyl group of monomers in the region of 5.5−6.3 ppm with the integrated areas of the methyl signals of the polymer at 0.8−1.2 ppm (Figure 2.S1, Supporting Information). Of course, the contribution of residual methyl group signals is subtracted from the total integration in the region of 0.8−1.2 ppm (as explained in Figure 2.S2).

The composition of the copolymer remained constant throughout the duration of the polymerization process as verified by ^{1}H NMR (Figure 2.S2), which indicates the random nature of the copolymerization. The evolution of the molar mass with conversion is presented in Figure 2.1.
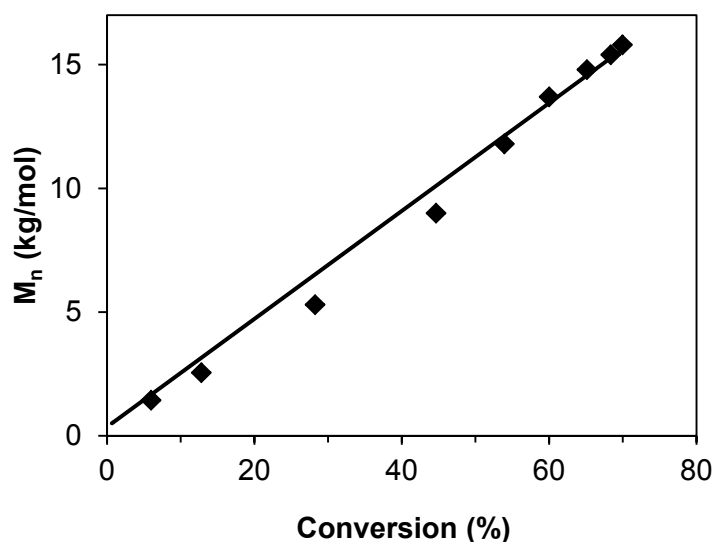
Figure 2.1 Number-average molar mass M_n as a function of conversion of the monomers for the RAFT copolymerization of nPA and EA at monomer ratio of 70:30 (nPA:EA). Solid line represents the theroretical molar masses calculated from Equation 2.1.

The increase in molar mass follows the theoretical line up to 70% conversion, which shows the controlled character of the copolymerization. An increase in polydispersity is observed at higher conversions (Figure 2.2A) and a negative deviation from linearity in the pseudo-first-order plot (Figure 2.2B) occurred after 120 min reaction time, both frequently reported for the RAFT polymerization of *N*-substituted acrylamides.[20,25,30–32] An inhibition period of ~15 min at the beginning of polymerization is attributed to the slow fragmentation of CTA.[33–36] The kinetic data indicate that the concentration of the radical species is constant during the reaction, and thus, the polymerization is controlled in this range of conversions. The SEC chromatograms of the samples withdrawn at different reaction times (Figure 2.S3) show that the higher polydispersities at high conversions arise from low-molar-mass tailing similar to our earlier observations[20] as well as those by other groups.[30,35,37]
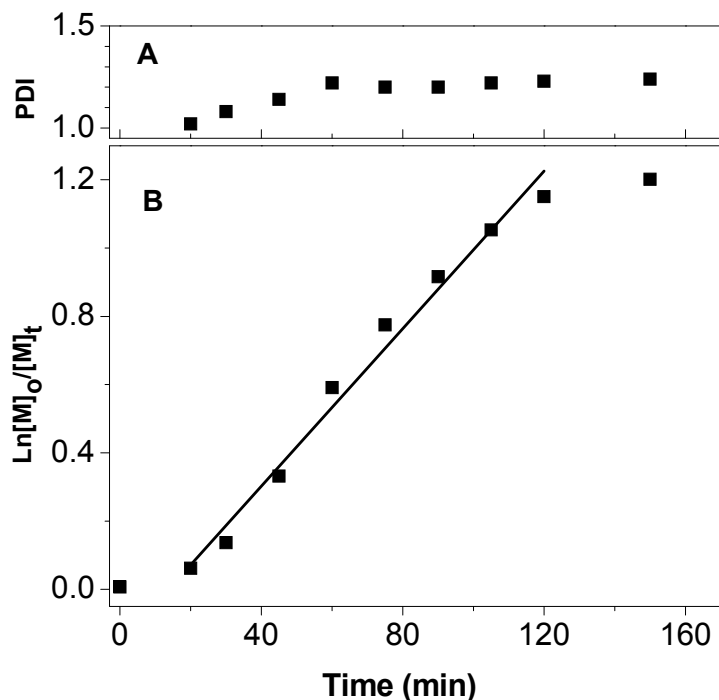
Figure 2.2 (A) Polydispersity index (PDI) and (B) semilogarithmic kinetic plot of the monomer conversion $\ln([M]_0/[M]_t)$ as a function of reaction time for the RAFT copolymerization of nPA and EA in dioxane at 70 °C with a monomer ratio [nPA]:[EA] of 70:30 and [monomers]:[CTA]:[initiator] ratio of 200:1:0.1. Solid line is a linear fit to part of the data to serve as a visual guide.

In our earlier discussion, we showed that the negative deviation of the kinetic plot may not arise from the initiator-derived radicals but is rather related to the number of other radicals, which can be corrected to some degree by lowering the polymerization temperature.[20] This was our motivation for the choice of current reaction temperature (70 °C). The reactivities of *N*-alkylacrylamides are also known to depend on their structure, the polymerizations of *N,N*-dialkyl-substituted acrylamides being faster and more controlled than those of their monosubstituted counterparts with less negative deviation in the kinetic behavior.[20] In comparison with our earlier kinetic data on the homopolymerization of nPA with the same [CTA]:[initiator] ratio at the same temperature,[20] the copolymerization of nPA and EA shows better linearity up to higher conversions. Other monomers (*N*-tert-butylacrylamide, tBA, and *N,N*-dimethylacrylamide, DMA) with different mole fractions were also copolymerized under the same conditions, and they showed the same kinetic

behavior as $P(nPA_{0.7}EA_{0.3})$ (data not shown). On the basis of the kinetic data, the reaction conditions are chosen to provide an active macro-CTA that can be employed in the subsequent block copolymerization.

2.3.2   CPs of the random copolymers

Various *N*-alkylsubstituted acrylamide homopolymers and corresponding random copolymers were synthesized and studied in our group.[12] Among them, *N*-n-propylacrylamide (nPA) and *N*-ethylacrylamide (EA) were selected for the current study. These monomers have different hydrophilicities and thus the corresponding copolymers have different CPs. A series of copolymers with different nPA:EA ratios were synthesized, and their thermoresponsiveness was tested in aqueous solutions. Table 2.1 shows the characteristics of the copolymers. The copolymer compositions are nearly identical to the feed ratios, supporting our earlier observations on the similar reactivity of *N*-alkylacrylamides[12] and suggesting that the copolymers are statistically random. Figure 2.3 shows the CPs of poly(nPA_x-*co*-EA_{1-x}) random copolymers as a function of the mole fraction of EA in the random copolymer. The CP increases with an increase in the mole fraction of the more hydrophilic monomer EA and follows eq 2-2 as a function of the comonomer composition:[12]

$$T = \frac{\mu_1 T_1 + k\mu_2 T_2}{\mu_1 + k\mu_2} \qquad (2.2)$$

where T, T_1, and T_2 are the CPs of the random copolymer, PEA, and PnPA, respectively. μ_1 and μ_2 are the mole fractions of EA and nPA (note that $\mu_1 = 1 - \mu_2$), respectively, and k is a weighting parameter which can be deduced from curve fitting to the experimental data. A *k* value of 1 would be obtained in the case of a linear relationship of T vs μ_1. In the current case, the plot has a concave shape, yielding a *k* value of 0.69. In comparison, a *k* value of 0.51 was observed for the copolymers of EA and a more hydrophobic monomer, *N*-tert-butylacrylamide (tBA).[12]
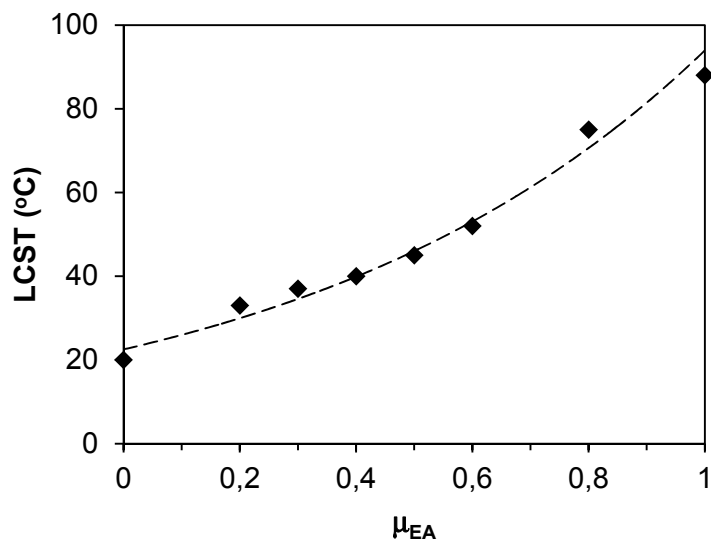
Figure 2.3 The CPs of poly(nPA$_x$-*co*-EA$_{1-x}$) aqueous solution as a function of the mole fraction of EA, μ_{EA}. The dashed line shows the curve fitting to Equation 2.2.

Table 2.1 The chemical compositions and CP of poly(nPA$_x$-*co*-EA$_{1-x}$) copolymers with different ratios of the comonomers

Polymer	M$_n$[1] (g/mol)	PDI[1]	nPA : EA ratio in final polymer[2]	CP (°C)[3]
PEA	19800	1.08	100 : 0	82
P(nPA$_{0.2}$EA$_{0.8}$)	15200	1.24	19.1 : 80.9	75
P(nPA$_{0.4}$EA$_{0.6}$)	19800	1.13	40.5 : 59.5	52
P(nPA$_{0.5}$EA$_{0.5}$)	12000	1.18	49.8 : 50.2	45
P(nPA$_{0.6}$EA$_{0.4}$)	20100	1.23	58.2 : 41.8	40
P(nPA$_{0.7}$EA$_{0.3}$)	13200	1.11	69.9 : 30.1	37
P(nPA$_{0.8}$EA$_{0.2}$)	16500	1.21	78.1 : 21.9	33
PnPA	12800	1.10	0 : 100	20

[1] Determined by SEC. [2] Determined by ^{1}H NMR. [3] Determined by UV-vis spectroscopy at $\lambda = 350$ nm.

Figure 2.3 shows a 15 °C difference between the CPs of P(nPA$_{0.4}$EA$_{0.6}$) and P(nPA$_{0.7}$EA$_{0.3}$), enough to distinguish the phase transitions in a block copolymer. Therefore, these monomer ratios were chosen to build the two blocks of the copolymer.

2.3.3 Preparation of a diblock random copolymer by RAFT polymerization

A random copolymer of nPA and EA with a comonomer ratio of 70:30, P(nPA$_{0.7}$EA$_{0.3}$), was synthesized to serve as a macro-CTA (macro-chain transfer agent) for the chain extension. The polymerization was stopped at 60% conversion to avoid the formation of dead chain ends. The polymer was purified by a precipitation in diethyl ether prior to the addition of the second block so that it was free of monomers as shown by ^{1}H NMR spectroscopy (Figure 2.S1, Supporting Information). The details of the macro-CTA copolymer are presented in Table 2.2.

Table 2.2 Conversions and the compositions of mono- and diblock random copolymers.

Polymer	nPA : EA ratio in the blocks (%)[1]	Conversion[1] (%)	M_n Theo.[2]	M_n SEC[3]	PDI[3]
P(nPA$_{0.7}$EA$_{0.3}$)	69.9 : 30.1	60	13500	13200	1.11
P(nPA$_{0.7}$EA$_{0.3}$)-*b*-P(nPA$_{0.4}$EA$_{0.6}$)	41.2 : 58.8	66	41000	45000	1.26

[1] Detemined by ^{1}H NMR. [2] Calculated from Equation 1. [3]Determined by SEC.

As mentioned above, the comonomer ratio for building the second block was chosen to yield two separable phase transitions in aqueous solution. The conditions of the block copolymerization of nPA and EA at a feed ratio of 60:40 were the same as in the first copolymerization, but the ratio of reactants [monomer]:[macro-CTA]:[AIBN] was set at 400:1:0.1 to provide a longer second block that would allow a better solubilization of the final block copolymer above the CP of the first block. It is known that some monomers tend to produce more deactivated macro-CTAs in a RAFT copolymerization than the others. Although this phenomenon is not fully understood, we have earlier shown that macro-CTAs of *N*-monosubstituted acrylamides such as nPA and iPA mostly remain

active, more than those of the disubstituted acrylamides.[20,21] The results of the block copolymerization are summarized in Table 2.2, and the SEC chromatograms of the macro-CTA and the resulting block copolymer are shown in Figure 2.4, indicating the livingness of block copolymerization.
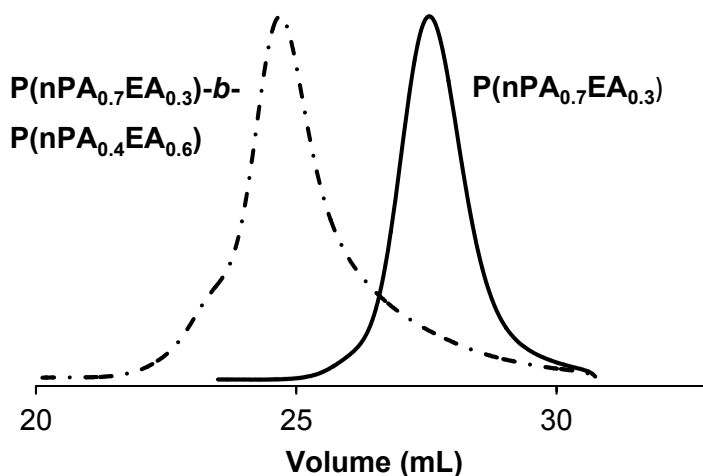
Figure 2.4 The SEC chromatograms of P(nPA$_{0.7}$EA$_{0.3}$) (macro-CTA) and
P(nPA$_{0.7}$EA$_{0.3}$)-*b*-P(nPA$_{0.4}$EA$_{0.6}$) (diblock copolymer).

The conversion of the second block was 66%, and the molar mass of the block random copolymer was well in accordance with the theoretical value calculated by eq 1. The polydispersity increased upon block copolymerization, indicating some loss of control over the RAFT polymerization process, commonly observed for macro-CTAs and associated with a small quantity of inactive species in the reaction.[38] The monomer composition of the P(nPA$_{0.4}$EA$_{0.6}$) block in Table 2.2 was calculated from the ^{1}H NMR spectra of macro-CTA and diblock copolymer (Figure 2.S4). On the basis of the molar masses given by SEC and the monomer compositions, the block ratio of the P(nPA$_{0.7}$EA$_{0.3}$)-*b*-P(nPA$_{0.4}$EA$_{0.6}$) diblock copolymer is 1:2.4.

2.3.4 Solution properties of copolymers and block random copolymer

To demonstrate the phase transitions of the individual blocks of P(nPA$_{0.7}$EA$_{0.3}$)-*b*-P(nPA$_{0.4}$EA$_{0.6}$) diblock random copolymer, the transmittance curves of aqueous solutions

of $P(nPA_{0.7}EA_{0.3})$ and $P(nPA_{0.4}EA_{0.6})$ at a concentration of 1.0 mg/mL upon heating are shown in Figure 2.5A, indicating CPs of 37 and 52 °C, respectively. The molar masses of the random copolymers were 13 200 and 19 800 g/mol, respectively (Table 1).
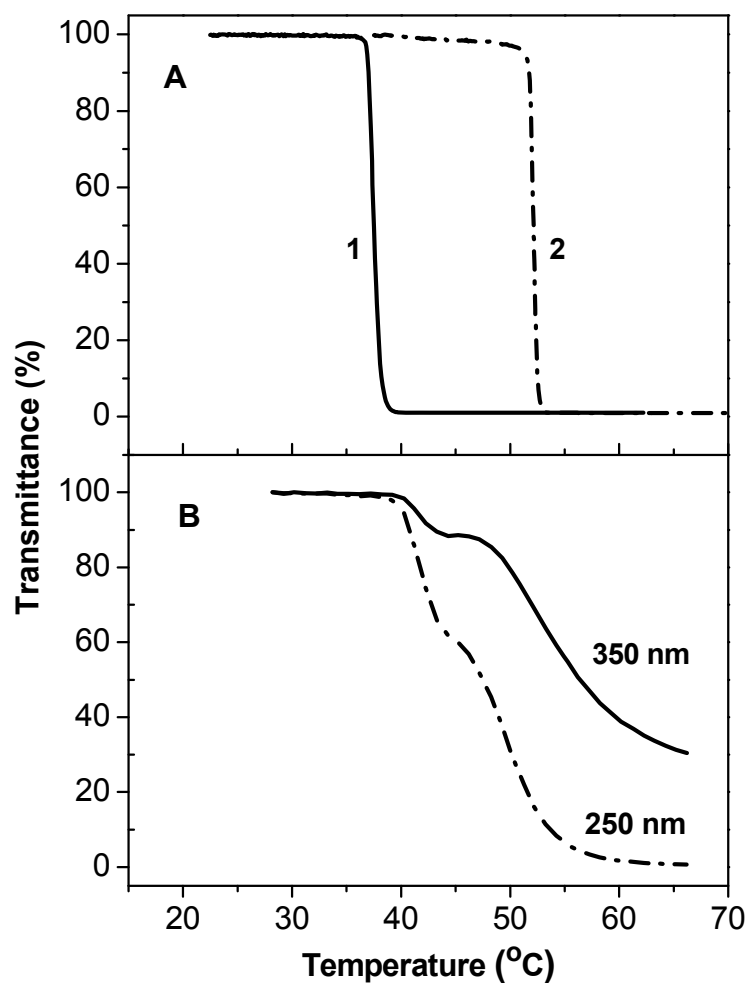
Figure 2.5 Temperature-dependent transmittance of 1.0 mg/mL aqueous solutions of (A) $P(nPA_{0.7}EA_{0.3})$ and $P(nPA_{0.4}EA_{0.6})$, observed at a wavelength of 350 nm, and (B) $P(nPA_{0.7}EA_{0.3})$-*b*-$P(nPA_{0.4}EA_{0.6})$ at two wavelengths, 350 and 250 nm. The samples were heated by 1 °C intervals followed by an equilibration for 20 minutes.

Figure 2.5B shows two clear shifts in the transmittance of $P(nPA_{0.7}EA_{0.3})$-*b*-$P(nPA_{0.4}EA_{0.6})$ solution with increasing temperature. When observed at 350 nm, the transmittance starts to decrease abruptly at 40 °C as the more hydrophobic $P(nPA_{0.7}EA_{0.3})$ block becomes insoluble upon heating, the middle point of the first transition being at 41.5

°C. When the temperature continues to rise, the second increase in the turbidity starts at 46 °C with a middle point of the transition at 53 °C, corresponding to the CP of P(nPA$_{0.4}$EA$_{0.6}$). The broadening of the phase transition temperatures may be influenced by the mutual and opposite effect of the two individual blocks: The more hydrophilic block drags the CP of the neighboring block to a higher temperature while the more hydrophobic one drags the other block to a lower CP. Fast continuous heating without equilibration led to lower apparent transition temperatures (Figure 2.S5), as it may not allow enough time for the reorganization of individual blocks during the aggregation. The temperature-dependent transmittance of the diblock random copolymer depends on the detection wavelength (Figure 2.S5). It is known that the scattering depends strongly on the wavelength of the light ($\sim\lambda^{-4}$).[39] This explains the higher transmittance at 350 nm than at 250 nm since the light of a shorter wavelength is more scattered than that of a longer wavelength.

The temperature dependence of apparent mean hydrodynamic diameter (D$_h$) of P(nPA$_{0.7}$EA$_{0.3}$)-*b*-P(nPA$_{0.4}$EA$_{0.6}$) in a 2.0 mg/mL solution is demonstrated in Figure 2.6, and the proposed mechanism for the aggregation process is shown in Scheme 2.2. At low temperatures, the solution consists of small micelles (D$_h \leq 22$ nm) possibly together with molecularly dissolved polymers, which compress upon heating prior to reaching the onset of the first CP. Such shrinking has been commonly observed for thermoresponsive polymers due to a coil-to-globule transition.[40–42] The micellization itself may stem from the hydrophobic C$_{12}$H$_{25}$ CTA end group of the block copolymer. The micelles start to aggregate when the temperature reaches the onset of the CP transition of the more hydrophobic P(nPA$_{0.7}$EA$_{0.3}$) block at 40 °C, and the mean diameter suddenly increases as the size distribution becomes bimodal due to the emergence of larger aggregates (D$_h \sim 88$ nm), similar to the observations by Laschewsky and co-workers on triblock copolymers.[43]
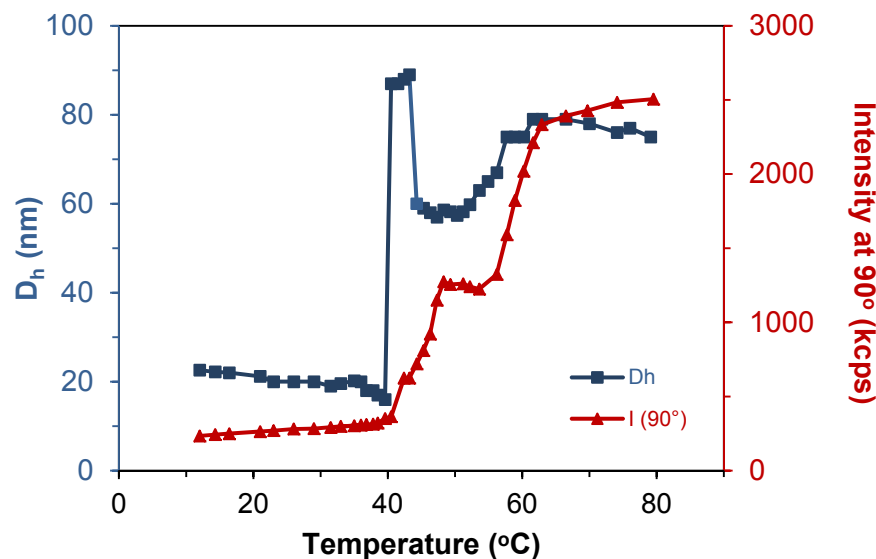
Figure 2.6 Temperature dependence of mean hydrodynamic diameter (D_h) and scattering intensity obtained by dynamic light scattering at 90° angle for a 2 mg/mL aqueous solution of $P(nPA_{0.7}EA_{0.3})$-b-$P(nPA_{0.4}EA_{0.6})$.

Further heating results in a collapse of the core at 44−48 °C upon the dehydration of the hydrophobic block, after which the aggregated species remain stable. We have earlier described similar aggregation behavior with an initial increase in D_h followed by a collapse for a poly(*N*-n-propylacrylamide) homopolymer as well as for its diblock and triblock copolymers.[22] At 53 °C, the more hydrophilic $P(nPA_{0.4}EA_{0.6})$ block reaches its CP and becomes more hydrophobic, leading to its contraction in water and further clustering of the micelles. Scattering intensity increases gradually during the aggregation/collapse and clustering processes, with a plateau in between. At 63 °C, the size distribution is monomodal and the mean hydrodynamic diameter of clusters is 79 nm, followed by a small contraction due to further dehydration of the outer block upon heating.
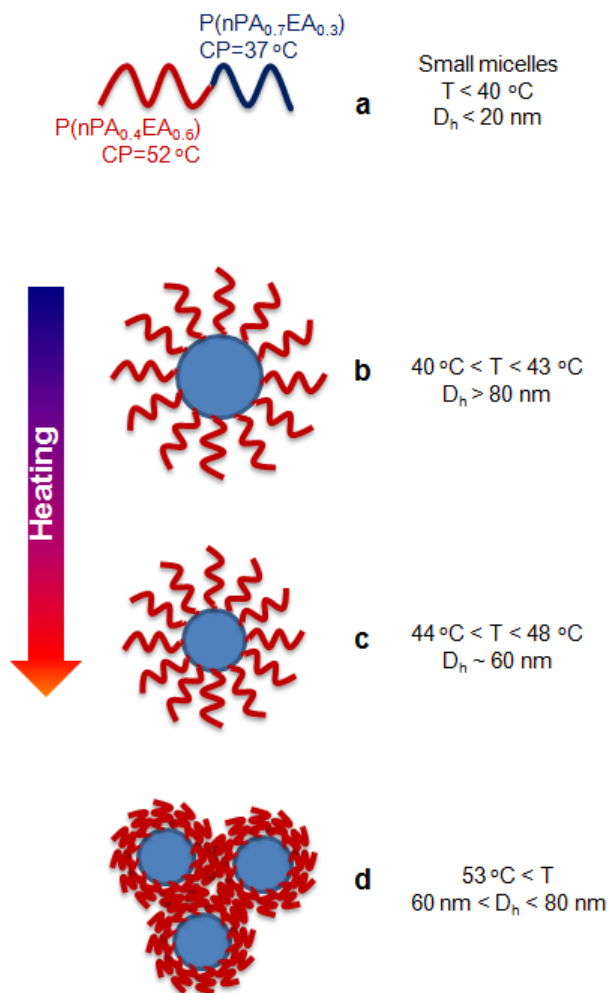
Scheme 2.2 Schematic illustration of the aggregation behavior of P(nPA$_{0.7}$EA$_{0.3}$)-*b*-P(nPA$_{0.4}$EA$_{0.6}$) in water upon heating. (a) Molecularly soluble polymers and small micelles below 40 $^{\circ}$C; (b) Dehydration of the P(nPA$_{0.7}$EA$_{0.3}$) core at 40 $^{\circ}$C; (c) Collapsed aggregates at 44-53 $^{\circ}$C; (d) Clusters above 53 $^{\circ}$C.

2.4 Conclusion

RAFT polymerization has been successfully used to make random copolymers of *N*-alkyl-substituted acrylamides with narrow molecular weight distributions. The kinetic study shows the controlled character of the RAFT copolymerization of the two monomers in the family of *N*-alkylacrylamides at conversions below 70%. The CP of the copolymers can be varied over a temperature range of 20−85 °C by adjusting the comonomer ratio, allowing

the design of block copolymers of two random copolymers with different phase transition temperatures. The stepwise aggregation of the block copolymer at different temperatures has been clearly shown. While raising the temperature above the CP of the first block leads to clustering and subsequent collapse of the core of the aggregates, heating above the CP of the second block induces further clustering and contraction of the shell through the dehydration of outer block. Further studies by dynamic and static light scattering together with microscopic methods may help to better understand the aggregation process. These block random copolymers expand the scope of thermoresponsive polymers and give promise to novel materials with tailored stimuli-responsive properties.

2.5 Acknowledgments

2.6 Supporting Information
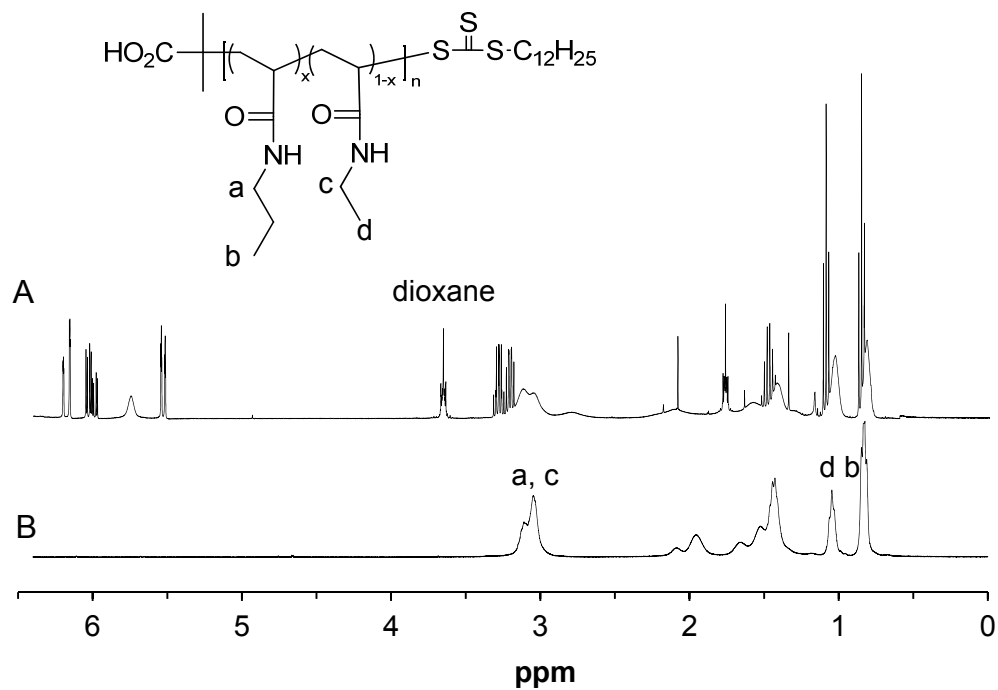
Figure 2.S1 ^{1}H NMR spectra of (A) the reaction mixture of the copolymerization of nPA and EA after 90 min reaction time, and (B) the corresponding copolymer P(nPA$_{0.7}$EA$_{0.3}$) after the purification. The signals from the pendant groups of the copolymer have been assigned.
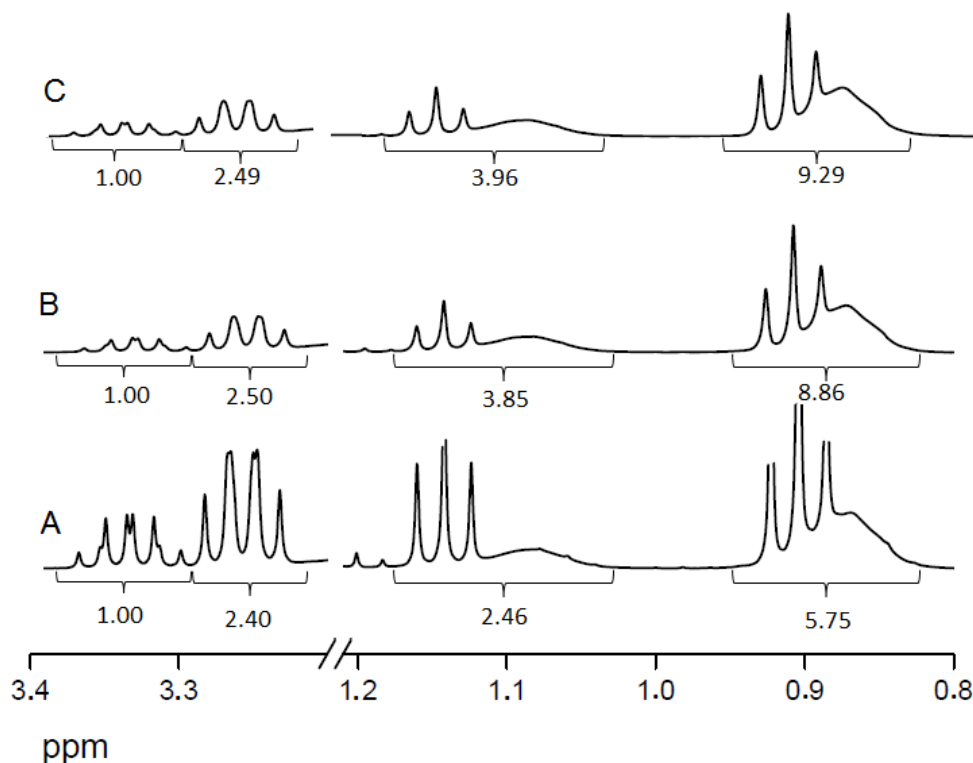
Figure 2.S2 ^{1}H NMR spectra of the reaction mixtures of the RAFT copolymerization with a monomer feed ratio of 70:30 (nPA:EA) at the reaction time of (A) 60 min, (B) 120 min, and (C) 150 min, with peak integration values shown at the bottom of the peaks. The compositions of the copolymers obtained is calculated to be (A) 69.1:30.1, (B) 68.4:31.6, and (C) 69.3:30.7, respectively, and correspond closely to the monomer composition in the feed. The composition of the copolymer (nPA : EA) based on the integrations of the CH_3 proton signals of the propyl (0.8-1.0 ppm) and ethyl groups (1.0-1.2 ppm) (assigned in Figure 2.S1) after subtracting the contribution of the signals from unreacted monomers as estimated from the CH_2 signal integrations of the monomers (3.2-3.3 ppm for nPA and 3.3-3.4 ppm for EA).
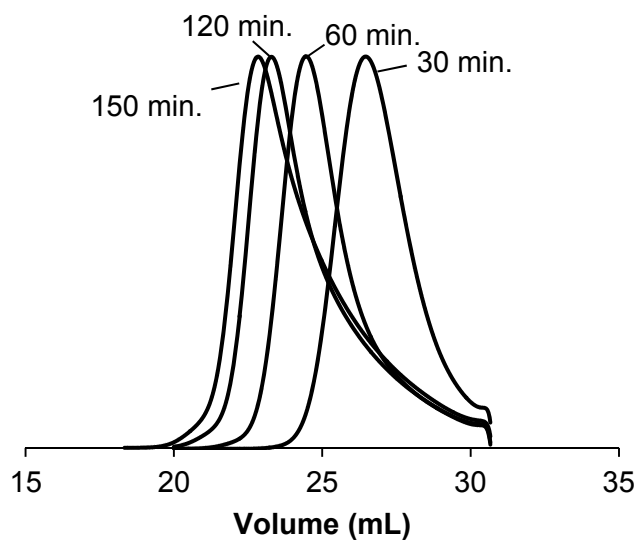
Figure 2.S3 SEC traces of poly(nPA$_{0.7}$-*co*-EA$_{0.3}$) obtained by RAFT copolymerization at different reaction times.
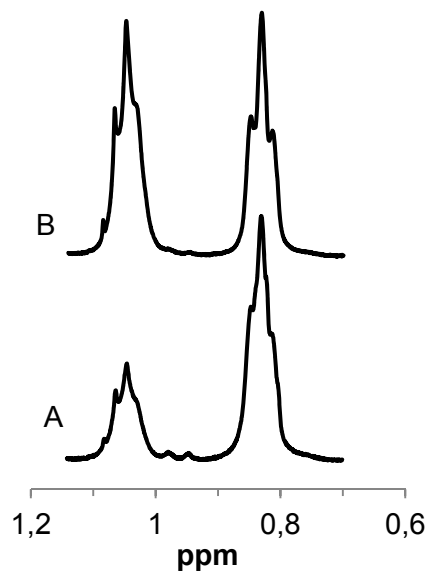
Figure 2.S4 ^{1}H NMR signals of EA methyl peak at 1.05 ppm and nPA methyl peak at 0.82 ppm in CDCl$_3$ for (A) P(nPA$_{0.7}$EA$_{0.3}$) (macro-CTA) and (B) P(nPA$_{0.7}$EA$_{0.3}$)-*b*-P(nPA$_{0.4}$EA$_{0.6}$) (diblock copolymer).
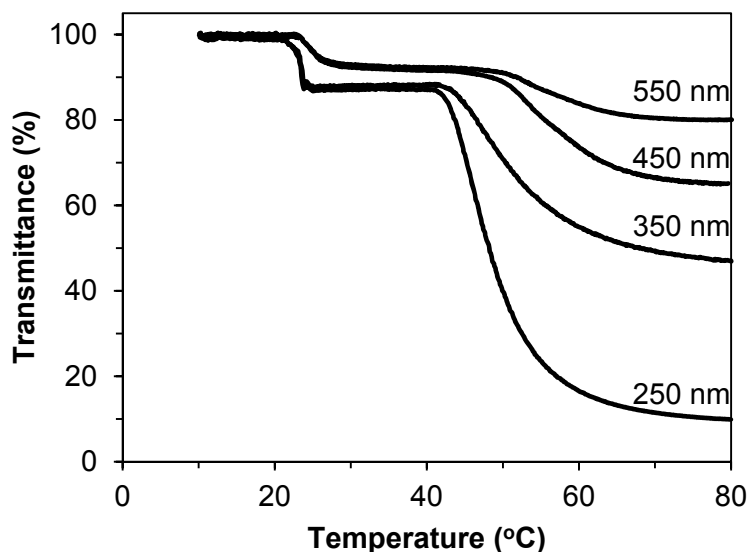
Figure 2.S5 Transmittance of a 1.0 mg/mL aqueous solution of P(nPA$_{0.7}$EA$_{0.3}$)-*b*-P(nPA$_{0.4}$EA$_{0.6}$) as a function of temperature with continuous heating rate of 0.1 °C/min observed at different wavelengths.

2.7 References

1. Li, C.; Madsen, J.; Armes, S. P.; Lewis, A. L. A New Class of Biochemically Degradable, Stimulus-Responsive Triblock Copolymer Gelators. *Angew. Chem. Int. Ed.* **2006,** *45* (21), 3510-3513.

2. Pasparakis, G.; Alexander, C. Sweet Talking Double Hydrophilic Block Copolymer Vesicles. *Angew. Chem. Int. Ed.* **2008,** *47* (26), 4847-4850.

3. Stuart, M. A. C.; Huck, W. T. S.; Genzer, J.; Muller, M.; Ober, C.; Stamm, M.; Sukhorukov, G. B.; Szleifer, I.; Tsukruk, V. V.; Urban, M.; Winnik, F.; Zauscher, S.; Luzinov, I.; Minko, S. Emerging applications of stimuli-responsive polymer materials. *Nat. Mater.* **2010,** *9* (2), 101-113.

4. Jochum, F. D.; Roth, P. J.; Kessler, D.; Theato, P. Double Thermoresponsive Block Copolymers Featuring a Biotin End Group. *Biomacromolecules* **2010,** *11* (9), 2432-2439.

5. Aseyev, V.; Tenhu, H.; Winnik, F. Non-ionic Thermoresponsive Polymers in *Self Organized Nanostructures of Amphiphilic Block Copolymers II.* Müller, A. H. E.; Borisov, O., Eds.; Springer Berlin / Heidelberg, 2011; Vol. 242, pp 29-89.

6. Liu, R.; Fraylich, M.; Saunders, B. Thermoresponsive copolymers: from fundamental studies to applications. *Colloid Polym. Sci.* **2009,** *287* (6), 627-643.

7. Bütün, V.; Liu, S.; Weaver, J. V. M.; Bories-Azeau, X.; Cai, Y.; Armes, S. P. A brief review of 'schizophrenic' block copolymers. *React. Funct. Polym.* **2006,** *66* (1), 157-165.

8. Principi, T.; Goh, C. C. E.; Liu, R. C. W.; Winnik, F. M. Solution Properties of Hydrophobically Modified Copolymers of *N*-Isopropylacrylamide and *N*-Glycine Acrylamide: A Study by Microcalorimetry and Fluorescence Spectroscopy. *Macromolecules* **2000,** *33* (8), 2958-2966.

9. Soga, O.; van Nostrum, C. F.; Hennink, W. E. Poly(*N*-(2-hydroxypropyl) Methacrylamide Mono/Di Lactate): A New Class of Biodegradable Polymers with Tuneable Thermosensitivity. *Biomacromolecules* **2004,** *5* (3), 818-821.

10. Sugihara, S.; Kanaoka, S.; Aoshima, S. Thermosensitive Random Copolymers of Hydrophilic and Hydrophobic Monomers Obtained by Living Cationic Copolymerization1. *Macromolecules* **2004,** *37* (5), 1711-1719.

11. X.X., Z.; D., A.; H.Y., L.; A., B. Copolymers of *N*-alkylacrylamide as thermosensitive hydrogels. *Macromol. Symp.* **2004,** *207*, 187-191.

12. Liu, H. Y.; Zhu, X. X. Lower critical solution temperatures of *N*-substituted acrylamide copolymers in aqueous solutions. *Polymer* **1999,** *40* (25), 6985-6990.

13. Avoce, D.; Liu, H. Y.; Zhu, X. X. *N*-Alkylacrylamide copolymers with (meth)acrylamide derivatives of cholic acid: synthesis and thermosensitivity. *Polymer* **2003,** *44* (4), 1081-1087.

14. Weiss, J.; Böttcher, C.; Laschewsky, A. Self-assembly of double thermoresponsive block copolymers end-capped with complementary trimethylsilyl groups. *Soft Matter* **2011,** *7* (2), 483.

15. Lee, H.-N.; Bai, Z.; Newell, N.; Lodge, T. P. Micelle/Inverse Micelle Self-Assembly of a PEO−PNIPAm Block Copolymer in Ionic Liquids with Double Thermoresponsivity. *Macromolecules* **2010,** *43* (22), 9522-9528.

16. Romão, R. I. S.; Beija, M.; Charreyre, M.-T. r. s.; Farinha, J. P. S.; Gonçalves da Silva, A. l. M. P. S.; Martinho, J. M. G. Schizophrenic Behavior of a Thermoresponsive Double Hydrophilic Diblock Copolymer at the Air−Water Interface. *Langmuir* **2009,** *26* (3), 1807-1815.

17. Maki, Y.; Mori, H.; Endo, T. Synthesis of Amphiphilic and Double-Hydrophilic Block Copolymers Containing Poly(vinyl amine) Segments by RAFT Polymerization of *N*-Vinylphthalimide. *Macromol. Chem. Phys.* **2010,** *211* (1), 45-56.

18. Mertoglu, M.; Garnier, S.; Laschewsky, A.; Skrabania, K.; Storsberg, J. Stimuli responsive amphiphilic block copolymers for aqueous media synthesised via reversible addition fragmentation chain transfer polymerisation (RAFT). *Polymer* **2005,** *46* (18), 7726-7740.

19. Dimitrov, I.; Trzebicka, B.; Müller, A. H. E.; Dworak, A.; Tsvetanov, C. B. Thermosensitive water-soluble copolymers with doubly responsive reversibly interacting entities. *Prog. Polym. Sci.* **2007,** *32* (11), 1275-1343.

20. Cao, Y.; Zhu, X. X.; Luo, J.; Liu, H. Effects of Substitution Groups on the RAFT Polymerization of *N*-Alkylacrylamides in the Preparation of Thermosensitive Block Copolymers. *Macromolecules* **2007,** *40* (18), 6481-6488.

21. Cao, Y.; Zhu, X. X. Preparation of ABC triblock copolymers of *N*-alkyl substituted acrylamides by RAFT polymerization. *Can. J. Chem.* **2007,** *85* (6), 407-411.

22. Cao, Y.; Zhao, N.; Wu, K.; Zhu, X. X. Solution properties of a thermosensitive triblock copolymer of *N*-alkyl substituted acrylamides. *Langmuir* **2009,** *25* (3), 1699-704.

23. Xie, D.; Ye, X.; Ding, Y.; Zhang, G.; Zhao, N.; Wu, K.; Cao, Y.; Zhu, X. X. Multistep Thermosensitivity of Poly(*N*-n-propylacrylamide)-block-poly(*N*-isopropylacrylamide)-block-poly(*N,N*-ethylmethylacrylamide) Triblock Terpolymers in Aqueous Solutions As Studied by Static and Dynamic Light Scattering. *Macromolecules* **2009,** *42* (7), 2715-2720.

24. Braunecker, W. A.; Matyjaszewski, K. Controlled/living radical polymerization: Features, developments, and perspectives. *Prog. Polym. Sci.* **2007,** *32* (1), 93-146.

25. Smith, A. E.; Xu, X.; McCormick, C. L. Stimuli-responsive amphiphilic (co)polymers via RAFT polymerization. *Prog. Polym. Sci.* **2010,** *35* (1-2), 45-93.

26. Shea, K. J.; Stoddard, G. J.; Shavelle, D. M.; Wakui, F.; Choate, R. M. Synthesis and characterization of highly crosslinked poly(acrylamides) and poly(methacrylamides). A new class of macroporous polyamides. *Macromolecules* **1990,** *23* (21), 4497-4507.

27. Lai, J. T.; Filla, D.; Shea, R. Functional Polymers from Novel Carboxyl-Terminated Trithiocarbonates as Highly Efficient RAFT Agents. *Macromolecules* **2002,** *35* (18), 6754-6756.

28. Idziak, I.; Avoce, D.; Lessard, D.; Gravel, D.; Zhu, X. X. Thermosensitivity of Aqueous Solutions of Poly(*N,N*-diethylacrylamide). *Macromolecules* **1999,** *32* (4), 1260-1263.

29. Boutris, C.; Chatzi, E. G.; Kiparissides, C. Characterization of the LCST behaviour of aqueous poly(*N*-isopropylacrylamide) solutions by thermal and cloud point techniques. *Polymer* **1997,** *38* (10), 2567-2570.

30. de Lambert, B.; Charreyre, M.-T.; Chaix, C.; Pichot, C. RAFT polymerization of hydrophobic acrylamide derivatives. *Polymer* **2005,** *46* (3), 623-637.

31. Schilli, C. M.; Zhang, M.; Rizzardo, E.; Thang, S. H.; Chong, Y. K.; Edwards, K.; Karlsson, G.; Müller, A. H. E. A New Double-Responsive Block Copolymer Synthesized via RAFT Polymerization: Poly(*N*-isopropylacrylamide)-block-poly(acrylic acid). *Macromolecules* **2004,** *37* (21), 7861-7866.

32. Convertine, A. J.; Lokitz, B. S.; Lowe, A. B.; Scales, C. W.; Myrick, L. J.; McCormick, C. L. Aqueous RAFT Polymerization of Acrylamide and *N,N*-Dimethylacrylamide at Room Temperature. *Macromol. Rapid Commun.* **2005,** *26* (10), 791-795.

33. Favier, A.; Charreyre, M.-T.; Chaumont, P.; Pichot, C. Study of the RAFT Polymerization of a Water-Soluble Bisubstituted Acrylamide Derivative. 1. Influence of the Dithioester Structure. *Macromolecules* **2002,** *35* (22), 8271-8280.

34. Lowe, A. B.; McCormick, C. L. Reversible addition–fragmentation chain transfer (RAFT) radical polymerization and the synthesis of water-soluble (co)polymers under homogeneous conditions in organic and aqueous media. *Prog. Polym. Sci.* **2007,** *32* (3), 283-351.

35. Sumerlin, B. S.; Donovan, M. S.; Mitsukami, Y.; Lowe, A. B.; McCormick, C. L. Water-Soluble Polymers. 84. Controlled Polymerization in Aqueous Media of Anionic Acrylamido Monomers via RAFT. *Macromolecules* **2001,** *34* (19), 6561-6564.

36. Perrier, S.; Barner-Kowollik, C.; Quinn, J. F.; Vana, P.; Davis, T. P. Origin of Inhibition Effects in the Reversible Addition Fragmentation Chain Transfer (RAFT) Polymerization of Methyl Acrylate. *Macromolecules* **2002,** *35* (22), 8300-8306.

37. Yusa, S.-i.; Shimada, Y.; Mitsukami, Y.; Yamamoto, T.; Morishima, Y. Heat-Induced Association and Dissociation Behavior of Amphiphilic Diblock Copolymers Synthesized via Reversible Addition−Fragmentation Chain Transfer Radical Polymerization. *Macromolecules* **2004,** *37* (20), 7507-7513.

38. Stenzel, M. H. Complex Architecture Design via the RAFT Process: Scope, Strengths and Limitations. In *Handbook of RAFT Polymerization*; Wiley-VCH Verlag GmbH & Co. KGaA, 2008, pp 315-372.

39. Kerker, M. In *The Scattering of Light, and Other ElectromagneticRadiation;* Academic Press: New York, 1969; p 339.

40. Lessard, D. G.; Ousalem, M.; Zhu, X. X.; Eisenberg, A.; Carreau, P. J. Study of the phase transition of poly(*N,N*-diethylacrylamide) in water by rheology and dynamic light scattering. *J. Polym. Sci., Part B: Polym. Phys.* **2003,** *41* (14), 1627-1637.

41. Wu, C.; Wang, X. Globule-to-Coil Transition of a Single Homopolymer Chain in Solution. *Phys. Rev. Lett.* **1998,** *80* (18), 4092-4094.

42. Wang, X.; Qiu, X.; Wu, C. Comparison of the Coil-to-Globule and the Globule-to-Coil Transitions of a Single Poly(*N*-isopropylacrylamide) Homopolymer Chain in Water. *Macromolecules* **1998,** *31* (9), 2972-2976.

43. Weiss, J.; Laschewsky, A. Temperature-Induced Self-Assembly of Triple-Responsive Triblock Copolymers in Aqueous Solutions. *Langmuir* **2011,** *27* (8), 4465-4473.

Chapter 3

Switchable vesicles formed by diblock random copolymers with tunable pH- and thermo-responsiveness*

Abstract

The thermo-responsiveness of polymers in aqueous media can be tuned by the choice of comonomers used in the synthesis of block copolymers made of random sequences of the same co-monomers but of different molar ratios. The same synthetic approach may be applied to other stimuli and we have made diblock random copolymers with both pH- and thermo-responsiveness and studied the formation of vesicles whose membrane core and coronas may be inverted in aqueous media. Sequential reversible addition-fragmentation chain transfer (RAFT) polymerization was used to prepare well-defined block copolymers in the form of A_nB_m-b-A_pC_q, where A, B and C are N-n-propylacrylamide (nPA), 2-(diethylamino)ethyl methacrylate (DEAEMA) and N-ethylacrylamide (EA), respectively. This polymer shows interesting "schizophrenic" behavior in aqueous solutions. Both blocks are thermo-responsive and one block is pH-responsive in which the tertiary amine group of DEAEMA may be protonated at a lower pH. A molecularly dissolved polymer is obtained at neutral pH and ambient temperature. At pH 7 and 37 $^{\circ}$C, the polymer self-assembles into vesicles with the poly($nPA_{0.8}$-co-$EA_{0.2}$) block as the membrane core (mean hydrodynamic diameter of the vesicles D_h = 148 nm). In an alkaline medium (pH 10) at 25 $^{\circ}$C, the membrane core and the coronas of the vesicles are inverted with the poly($nPA_{0.8}$-co-

---

$DEAEMA_{0.2}$) block forming the hydrophobic core of the membrane (D_h = 60 nm). In addition, two-step phase transitions are observed in both alkaline and neutral solutions corresponding to the cloud points of the individual blocks. Here, the random nature of the blocks allows fine-tuning the thermo-responsiveness based solely on lower critical solution temperatures and its combination with pH-sensitivity provides vesicles with switchable membrane core and corona in aqueous solution.

3.1   Introduction

The first examples of so-called "schizophrenic" stimuli-responsive block copolymers were introduced in the late 1990's by Armes and coworkers.[1] These systems form micelles capable of inverting their shell and core in aqueous solutions without adding any organic solvent, in response to an external stimulus that alters the relative hydrophilicity of the blocks. Each block is sensitive to a certain stimulus and can respond individually as it becomes either more hydrophilic or more hydrophobic.[2] They are also sometimes called "confused" block copolymers for their dual behavior.[3] Such stimuli include temperature,[4-7] pH,[8-12] and combinations of ionic strength-pH[1, 13, 14] or temperature-pH.[15-26] All the systems introduced so far benefit from a change in their solution properties under fixed pH or temperature value since tuning such responsiveness may not be easy given the limited choice of the monomers, and they are composed of blocks consisting of a single monomer,[16, 19-25] even though multi-block copolymers may exhibit multiple responses to external stimuli.[27-34] On the other hand, temperature-dependent inversion of core and shell blocks in the micellar aggregates of "schizophrenic" block copolymers has been reported in aqueous solutions based on lower and upper critical solution temperatures (LCST and UCST) of the blocks,[5, 7] but sometimes observing a clear UCST is difficult as the transition may be broad. To the best of our knowledge, there has been no report on such invertible systems with dual thermo-responsiveness exploiting the LCST-like behavior of both blocks. We attempt to address these issues here by preparing an invertible system made in quite a controlled manner, where both tuneable blocks in a diblock copolymer show separate cloud points (CPs) in water.

We have prepared random copolymers that allow the tuning of the cloud point by adjusting the monomer composition in the blocks.[35-38] Block random copolymers showing tunable solution properties for each block have recently been synthesized and studied.[39, 40] Inspired by the natural and synthetic polymers responsive to multiple stimuli, our approach is to make diblock copolymers from random copolymer blocks of pH- and thermo-sensitive comonomers. Here, the pH-sensitive block is also thermo-sensitive, while the second block responds only to temperature changes. Controlling the block length and the composition of the blocks allows the design of systems with tunable responsiveness to a desired pH, a property that may be useful for the rapid release of an encapsulated guest molecule in response to external stimuli. The diblock copolymer consists of two blocks showing separate CPs and a variety of techniques may be used to study their "schizophrenic" self-assembling process into vesicles. The stimuli-responsiveness of individual blocks and the pH-dependent thermo-sensitivity of diblock random copolymers should lead to the inversion of core and corona blocks in the vesicle membranes under suitable conditions and their aggregation at high temperatures.

3.2   Experimental

3.2.1   Materials

2,2'-azobisisobutyronitrile (AIBN, Eastman Kodak) was recrystallized from methanol. Sodium deuteroxide, deuterium chloride, acryloyl chloride, ethylamine (70 % aqueous solution) and n-propylamine were purchased from Aldrich and were used without further purification. 2-(Diethylamino)ethyl methacrylate (DEAEMA) was purchased from Aldrich and vacuum-distilled prior to use. *N*-n-propylacrylamide (nPA) and *N*-ethylacrylamide (EA) were synthesized according to a procedure reported by Shea *et al.*[41] 3-(Benzylsulfanylthiocarbonylsulfanyl)propionic acid (BPA) was prepared according to a procedure described by Stenzel *et al.*[42] and used as a chain transfer agent (CTA). Anhydrous and oxygen-free tetrahydrofuran (THF) was obtained by passage through columns packed with activated alumina and supported copper catalyst (Glass Contour, Irvine, CA). Water was purified using a Millipore Milli-Q system.

3.2.2 Polymer synthesis

A previously reported method was used to synthesize the diblock random copolymer.[39] In this work, THF was used as the solvent and BPA as the RAFT agent. The monomers used for the first copolymerization are nPA and DEAEMA, while nPA and EA are used to prepare the second block. Since DEAEMA is prone to sublimation in the freeze-thaw process, nitrogen bubbling was selected as the degassing method. The reaction mixture of [monomer]:[BPA]:[AIBN] in the molar ratio of 200:1:0.1 and with a total monomer concentration of 0.3 g/mL was purged with N_2 for 30 min prior to immersing it in a preheated oil bath (70 °C). After 90 min reaction time, the polymerization was terminated and the random copolymer was precipitated in petroleum ether, filtered and dried in vacuum at room temperature to yield poly(nPA$_{0.8}$-*co*-DEAEMA$_{0.2}$)-CTA. The resulting random copolymer was then used as the BPA-ended macro-CTA in the second step to prepare a diblock copolymer, poly(nPA$_{0.8}$-*co*-DEAEMA$_{0.2}$)-*block*-poly(nPA$_{0.8}$-*co*-EA$_{0.2}$), using the reactant molar ratio [monomer]:[macro-CTA]:[AIBN] of 200:1:0.1. The procedure for the diblock copolymerization was the same as for the random copolymerization, except that the comonomers were different and BPA was replaced by macro-CTA (Scheme 3.1). Poly(nPA$_{0.8}$-*co*-EA$_{0.2}$) and poly(nPA$_{0.7}$-*co*-DEAEMA$_{0.3}$) were also made separately with the same method to study the LCST of the second block individually and the effect of the DEAEMA content on the thermal behavior, respectively.
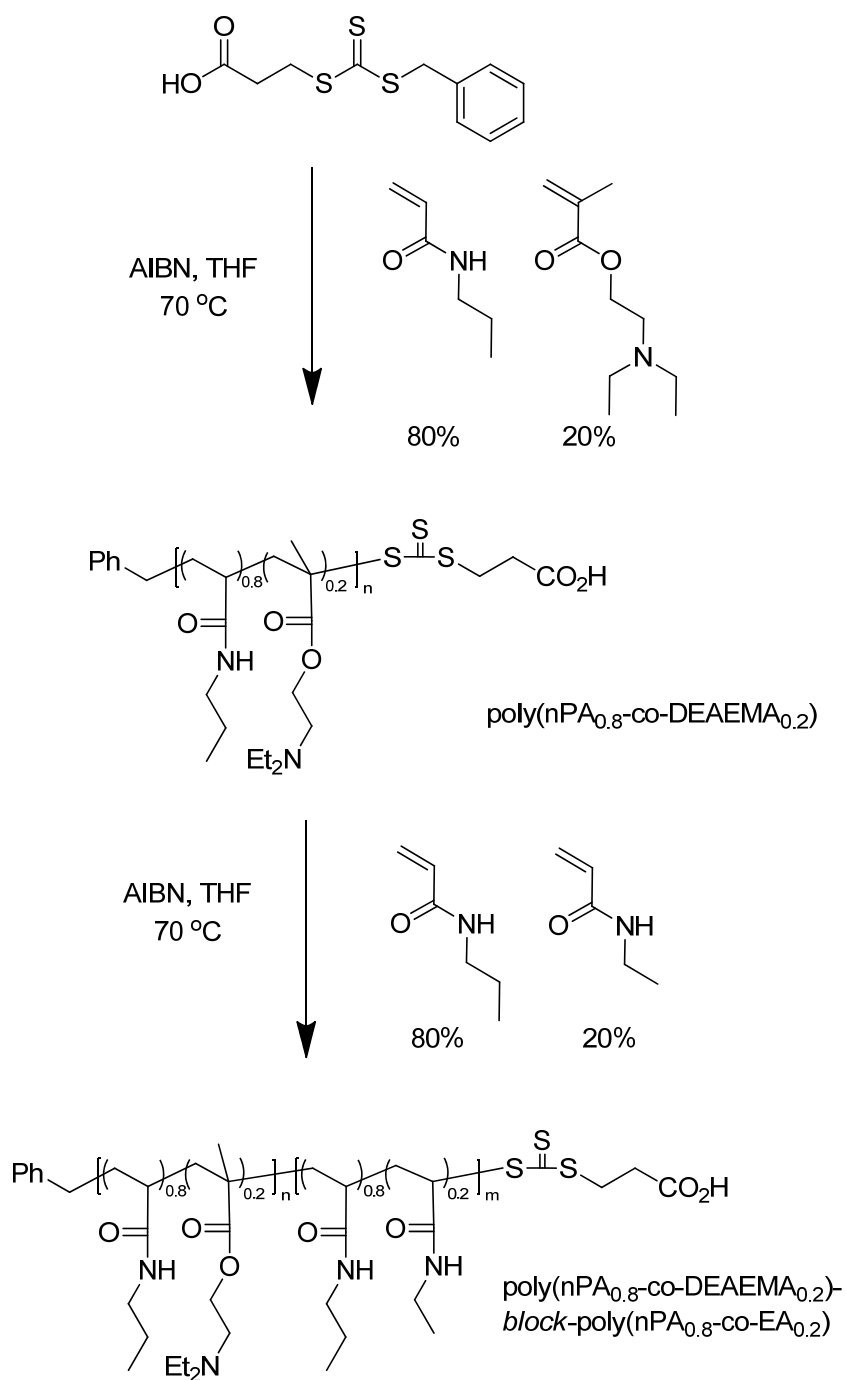
Scheme 3.1 Synthesis of dual responsive diblock random copolymer poly(nPA$_{0.8}$-*co*-DEAEMA$_{0.2}$)-*block*-poly(nPA$_{0.8}$-*co*-EA$_{0.2}$) via RAFT copolymerization of nPA and DEAEMA followed by a chain extension with nPA and EA.

3.2.3 Polymer characterization

Molar masses and polydispersity indices (PDI) of the polymers were determined by SEC on a Waters 1525 system equipped with three Waters Styragel columns and a refractive index detector (Waters 2410) at 35 °C. *N,N*-dimethylformamide (DMF) containing 0.01 M LiBr was used as the mobile phase at a flow rate of 1 mL/min. The system was calibrated by poly(methyl methacrylate) standards.

The NMR spectra of the monomers and polymers in deuterated chloroform (CDCl$_3$) were recorded on a Bruker AV-400 NMR spectrometer operating at 400 MHz for protons, and the temperature-dependent NMR spectra of the diblock random copolymer were recorded on a Bruker AV-500 spectrometer working at 500 MHZ in deuterated water (D$_2$O). The pH of the solutions was adjusted by adding NaOD or DCl solution in D$_2$O. The theoretical molar masses were calculated from the conversions given by ^{1}H NMR according to

$$\bar{M}_{\text{n,th}} = M_{\text{CTA}} + \frac{[\text{monomer}]}{[\text{CTA}]} \times M_{\text{monomer}} \times \text{conversion} \qquad (3.1)$$

where M_{CTA} is the molecular weight of the chain transfer agent and [monomer] and [CTA] are the initial monomer and CTA concentrations, respectively. M_{monomer} is the average molecular weight of the comonomers and calculated from

$$M_{\text{monomer}} = x \times M_1 + (1 - x) \times M_2 \qquad (3.2)$$

where x is the molar fraction of monomer 1 (obtained by ^{1}H NMR) and M$_1$ and M$_2$ are the molecular weights of monomers 1 and 2 in the random copolymer, respectively. For a block copolymer, [CTA] in Equation 1 is replaced by the concentration of macro-CTA.

Atomic force microscopy (AFM) images were acquired in air at room temperature using tapping mode on a (Digital Instruments Dimension 3100 microscope, Santa Barbara, CA) Intermittent contact imaging (i.e., "tapping mode") was performed at a scan rate of 1 Hz using aluminium-coated etched silicon cantilevers (ACTA tips from App Nano Inc.) with a resonance frequency around 300 kHz, a spring constant of ~42 N/m, and tip radius of < 10 nm. All images were acquired with a medium tip oscillation damping (20−30%). The samples were analyzed in the dried state via drop deposition of the 0.05 mg/mL

aqueous solution of the polymer onto a mica surface at desired temperature, following by lyophilization.

Transmission electron microscopy (TEM) images were recorded on lyophilized aqueous samples (0.05 mg/mL) deposited on copper grids (300 mesh, Carbon Type-B, Ted Pella, Inc.) at desired temperature. The images were acquired on FEI Tecnai 12 TEM at 120 kV, equipped with AMT XR80C CCD camera system.

Temperature-dependent zeta potential measurements were conducted in pure Milli-Q water on a Zetasizer instrument (Nano ZS) from Malvern. The zeta potential, Z, is determined through the electrophoretic mobility UE with Henry's equation:

$$UE = \frac{2\varepsilon Z f(\kappa a)}{3\eta} \qquad (3.3)$$

where ε is the dielectric constant, η is the viscosity, and $f(\kappa a)$ is the Henry's function. The value of 1.5 is used for $f(\kappa a)$ in aqueous solutions of moderate electrolyte concentration, which is referred to as the Smoluchowski approximation. The final values were the average of 3 measurements. The cloud points (CPs) of the polymers were determined from the optical transmittance measured on a Cary 300 Bio UV-vis spectrophotometer equipped with a temperature-controlled sample holder. The samples at a concentration range of 0.5 to 0.05 mg/mL were prepared by dissolving the copolymers in deionized water cooled in an ice-water bath, after which the solutions were homogenized by ultrasonication. The pH of the solutions (5 mL) was adjusted by adding microliter quantities of 0.1 N HCl or 0.1 N NaOH. The stability of the pH was checked after 24 h and fine-tuned by further addition of acid or base, if necessary. The absorbance was measured at different wavelengths for the aqueous solution of polymers by continuous heating at a rate of 0.1−0.3 °C/min over various temperature ranges. For individual blocks, the cloud point is given as the temperature at which 50% transmittance was lost upon heating. For block copolymers, the CP is determined from the middle point between the onset and the offset of the transmittance curve as a function of temperature.

Light scattering studies on the pH- and temperature-dependent aggregation behavior were conducted on a CGS-3 compact goniometer (ALV GmbH) equipped with an ALV-5000 multi tau digital real time correlator at selected temperatures using a

Science/Electronics temperature controller. The laser wavelength was 632 nm. In dynamic light scattering (DLS) experiments the scattering angle was fixed at 90°. All solutions were prepared at a concentration of 0.05 mg/mL and dust was removed by filtering through 0.22-μm Millipore filters. The DLS results were analyzed by cumulant method. The decay rate distributions were transformed to a diffusion coefficient and the apparent intensity-weighted hydrodynamic diameters of the polymers were obtained from the Stokes-Einstein equation. In static light scattering (SLS) experiments, apparent weight-average molar masses ($M_{w,app}$) of the diblock copolymer and its aggregates were measured in dilute solutions (0.05 mg/mL) from the angular dependence of the excess absolute time-averaged scattering intensity, known as Rayleigh ratio $R(\theta)$ (typically shown in Figure 3.S1). The angular range was between 30° and 150° with increments of 10°. The values of $M_{w,app}$ were obtained from the extrapolation of partial Zimm plots.[43, 44] The refractive index increments (*dn/dc*) were determined by a Brookhaven (BIC-DNDC) differential refractometer for three temperature ranges in relation to the two cloud points of the block copolymer, CP_1 and CP_2. The values were 0.143 ($T < CP_1$), 0.171 ($CP_1 < T < CP_2$), and 0.174 ($T > CP_2$), respectively.

3.3 Results and discussion

3.3.1 Preparation of the polymers

We demonstrated in an earlier study[39] that the cloud point of the random copolymers made from nPA and EA can be tuned over a wide temperature range of 20−85 °C by adjusting the ratio of comonomers. In addition, the diblock copolymer consisting of such blocks showed two separate phase transition temperatures. As the reactivity of monomers in the RAFT polymerization depends on the chain transfer agent (CTA), a suitable CTA must be chosen to efficiently polymerize both acrylamide- and methacrylate-based monomers. For instance, 2-(dodecylthiocarbonothioylthio)-2-methylpropionic acid (DMP) has been used in our group as a CTA for the polymerization of acrylamides, but DEAEMA was not polymerized with DMP as the RAFT agent. Therefore, 3-(benzylsulfanylthiocarbonylsulfanyl)propionic acid (BPA) was our choice for the (block)

copolymerization of *N*-n-propylacrylamide (nPA) with 2-(diethylamino)ethyl methacrylate (DEAEMA) or *N*-ethylacrylamide (EA). The composition of the blocks obtained was similar to the feed ratio (Table 3.1), and frequent sampling from the reaction mixture showed the statistical nature of the random copolymer of an acrylamide (nPA) and methacrylate (DEAEMA, Table 3.S1). An earlier study on the kinetics of copolymerization of nPA and EA indicated a deviation from linearity at high conversions ($\geq$ 70%), suggesting the presence of dead chains.[39] Therefore, the conversions of the current polymerizations were kept low ($\sim$ 30%) to ensure the livingness of the chains and to achieve similar molar masses for the two blocks, controlled by the [monomer]:[CTA]:[AIBN] ratios. We found that the block containing the methacrylate-based monomer DEAEMA allowed easy addition of the second block, while the block containing only acrylamide monomers is not easily extended to form a diblock copolymer. In addition, DEAEMA is prone to sublimation in a freeze-thaw process, nitrogen bubbling was used for degassing.

Table 3.1 Conversions and compositions of mono- and diblock random copolymers.

Polymer	Monomer ratio in the blocks[1]	Conversion[1] (%)	M_n ($\times 10^3$ g/mol)		PDI[3]
			Theo.[2]	SEC[3]	
P(nPA$_{0.8}$-*co*-DEAEMA$_{0.2}$)	81:19	31	7.9	6.5	1.18
P(nPA$_{0.8}$-*co*-DEAEMA$_{0.2}$)-*b*-P(nPA$_{0.8}$-*co*-EA$_{0.2}$)	78:22	34	13.9	14.6	1.35

[1] Determined by ^{1}H NMR. For the block copolymer, the given composition corresponds to that of the second block. [2] Calculated from Equation 1. [3] Determined by SEC calibrated by poly(methyl methacrylate) standards.

The purification of poly(nPA-*co*-DEAEMA) copolymer by precipitation was necessary prior to its use as a macro-CTA in the subsequent block copolymerization. The properties of the macro-CTA and the resulting block copolymer are listed in Table 3.1. The compositions of the polymers and the molar masses were determined by ^{1}H NMR (Figure 3.S1) and size exclusion chromatography (Figure 3.S2), respectively. An increase in the polydispersity is observed for the diblock copolymer which is frequently reported for the

RAFT polymerization of macro-CTA.[39, 45, 46] As the block symmetry is one of the critical parameters influencing the solubility and the micellization process,[1] block ratio 1:1.25 for poly(nPA-*co*-DEAEMA): poly(nPA-*co*-EA) was selected. The block ratio was calculated from the compositions of the blocks and the molar masses given by SEC. The monomer ratios have been selected to yield two well-separated thermal transitions at neutral pH, one of which is slightly below the body temperature. Based on our earlier study on the effect of nPA:EA molar ratio on the cloud point of the copolymer, the latter transition is obtained at a ratio of 80:20.[39] The solution properties of individual blocks are discussed below. Although it is known that the end groups of thermoresponsive polymers influence the micellization and lower critical solutions temperatures,[47] the end group was not removed to avoid the possible cleavage of the ester bond of DEAEMA. Furthermore, the selected RAFT agent (BPA) is water-soluble, and hence, its effect on the solution properties of the copolymers is expected to be minimal.

3.3.2 Solution properties of the copolymers

The thermal transitions of individual blocks of the diblock random copolymer were measured by UV-vis spectroscopy. Figure 3. 1 shows the transmittance curves of aqueous solutions of poly(nPA$_{0.8}$-*co*-DEAEMA$_{0.2}$) with the properties mentioned in Table 3.1 and poly(nPA$_{0.8}$-*co*-EA$_{0.2}$) with molar masses of 16500 g/mol, and PDI of 1.21.

While the CP of poly(nPA$_{0.8}$-*co*-EA$_{0.2}$) at 33 °C does not change with pH, a strong pH-dependence is observed for poly(nPA$_{0.8}$-*co*-DEAEMA$_{0.2}$), as shown in Figures 3.2 and 3.3. The tertiary amine residues of DEAEMA become protonated and positively charged in acidic medium, making the copolymer more hydrophilic and thus, leading to the complete disappearance of CP at pH 4. While the ester bonds of polyacrylates are subject to hydrolysis in aqueous solutions,[48] those of polymethacrylates show better stability even in acidic and basic solutions.[49] NMR data showed that poly(nPA$_{0.8}$-*co*-DEAEMA$_{0.2}$) was stable against hydrolysis at both pH 7 and 10 used in this study.
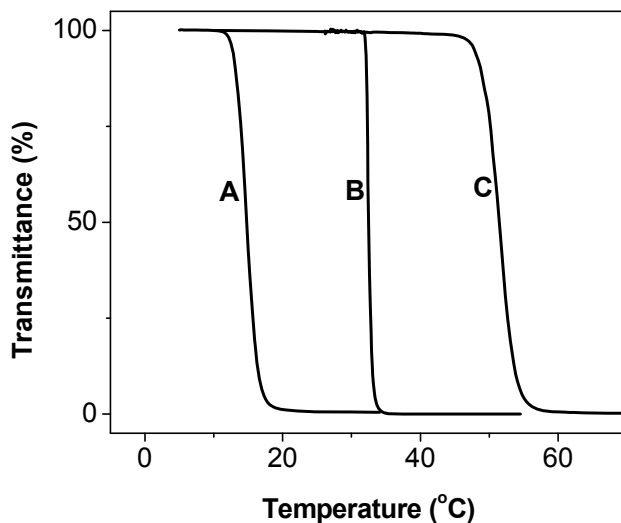
Figure 3. 1 Temperature-dependent transmittance of 0.5 mg/mL aqueous solutions of (A) poly(nPA$_{0.8}$-*co*-DEAEMA$_{0.2}$) at pH 10.0, (B) poly(nPA$_{0.8}$-*co*-EA$_{0.2}$) and (C) poly(nPA$_{0.8}$-*co*-DEAEMA$_{0.2}$) at pH 7.0, observed at a wavelength of 300 nm.

The pK$_a$ of PDEAEMA homopolymer is 7.3,[16] giving an idea of the degree of protonation of DEAEMA moieties in the pH range studied. The solubility of poly(nPA$_{0.8}$-*co*-DEAEMA$_{0.2}$) decreases with increasing pH upon deprotonation and, as a result, the CP decreases gradually from 68 (pH = 6) to 13 $^{\circ}$C (pH > 9, Figure 3.3). The PDEAEMA homopolymer is water-insoluble in its deprotonated form.[11] Therefore, the CP of fully deprotonated poly(nPA$_{0.8}$-*co*-DEAEMA$_{0.2}$) is lower than that of PnPA (20 $^{\circ}$C, M$_n$ = 12800 g/mol).[39]

As shown in Figure 3.1, at both pH 7 and 10, the CP of poly(nPA$_{0.8}$-*co*-DEAEMA$_{0.2}$) is well distinguishable from that of poly(nPA$_{0.8}$-*co*-EA$_{0.2}$) and, hence, two well-separable transitions could be observed also with their block copolymer at these pH values. The composition dependence of the CP for poly(nPA$_x$-*co*-DEAEMA$_{1-x}$) was also observed. For instance, the CP of a copolymer with higher DEAEMA content, poly(nPA$_{0.7}$-*co*-DEAEMA$_{0.3}$) (M$_n$ = 7400 g/mol, PDI = 1.20) at pH 10 lies at 10 $^{\circ}$C, which is lower than that of poly(nPA$_{0.8}$-*co*-DEAEMA$_{0.2}$) (13 $^{\circ}$C, M$_n$ = 6500 g/mol, PDI = 1.18). Thus, the cloud

point of a poly(nPA-*co*-DEAEMA) random copolymer at any desired pH can be adjusted
by tuning its composition.
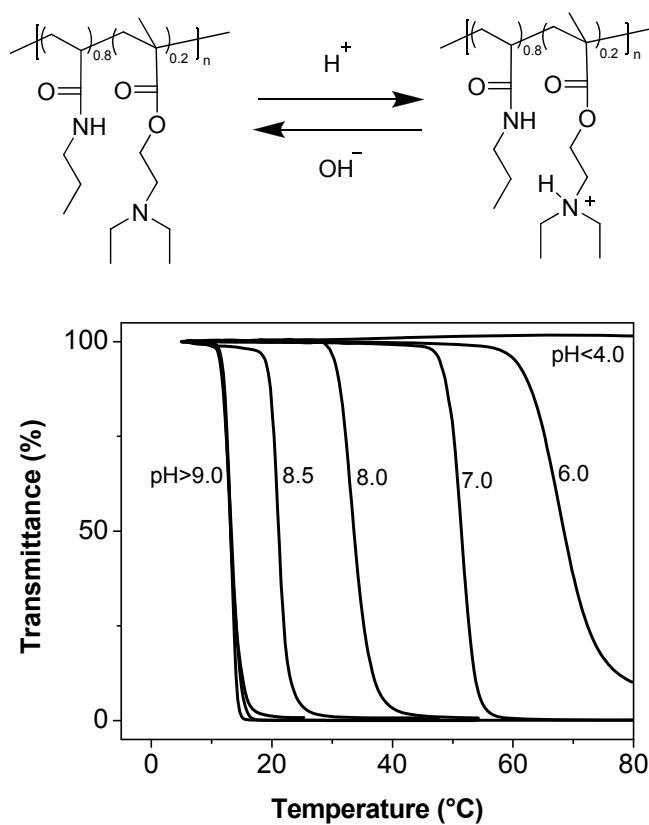
Figure 3.2 Thermosensitivity of 0.5 mg/mL aqueous solution of poly(nPA$_{0.8}$-*co*-
DEAEMA$_{0.2}$) measured by UV-vis spectroscopy at 300 nm and heating rate 0.3
$^{\circ}$C/min at different pH values. The protonation and deprotonation of poly(nPA$_{0.8}$-*co*-
DEAEMA$_{0.2}$) random copolymer depending on the pH is also shown.
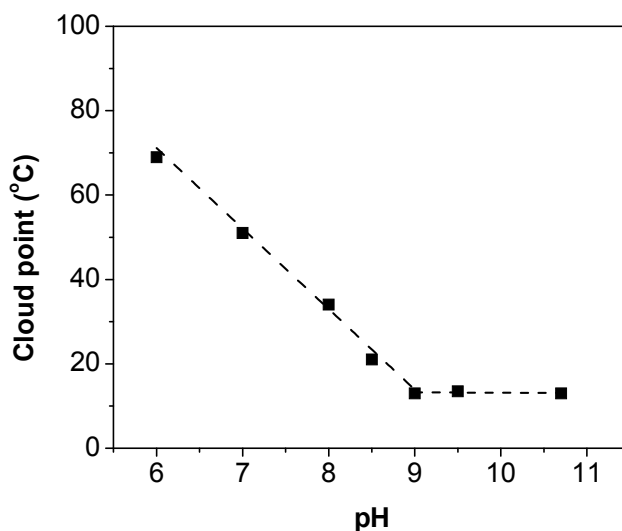
Figure 3.3 The cloud points of the 0.5 mg/mL aqueous solutions of poly(nPA$_{0.8}$-*co*-DEAEMA$_{0.2}$) as a function of pH (extracted from Figure 3.2). The dashed lines are added as visual guides.

3.3.3 Solution properties of diblock random copolymer

The dual thermo-responsive behavior of the diblock random copolymer poly(nPA$_{0.8}$-*co*-DEAEMA$_{0.2}$)-*block*-poly(nPA$_{0.8}$-*co*-EA$_{0.2}$) at pH 7 and 10 was studied by UV-vis, ^{1}H NMR spectroscopy, TEM, AFM imaging, zeta potential measurements, and laser light scattering.

UV-vis spectroscopy. At pH 7 (Figure 3.4A), the more hydrophobic poly(nPA$_{0.8}$-*co*-EA$_{0.2}$) block starts to collapse with increasing temperature at its cloud point of 33 °C, accompanied by a reduction in transmittance. TEM images show that, at this point, vesicles with poly(nPA$_{0.8}$-*co*-EA$_{0.2}$) membrane core are formed (Figure 3.5A). The second aggregation step starts at around 52 °C, corresponding to the cloud point of poly(nPA$_{0.8}$-*co*-DEAEMA$_{0.2}$) at pH 7 (Table 3.2).

The effect of particle size on the apparent turbidity has been discussed previously.[39] The strong wavelength dependence of scattering ($\sim \lambda^{-4}$) means that a radiation of shorter wavelength is scattered more strongly than that of a longer wavelength.[50] Therefore, fewer particles are visible when observed at higher wavelength, leading to a lower apparent

turbidity.[30] Due to the large size of particles formed in the course of the first transition, resulting in a strong shift in transmittance, the second step is not as clear at a low detection wavelength (Figure 3.S4).
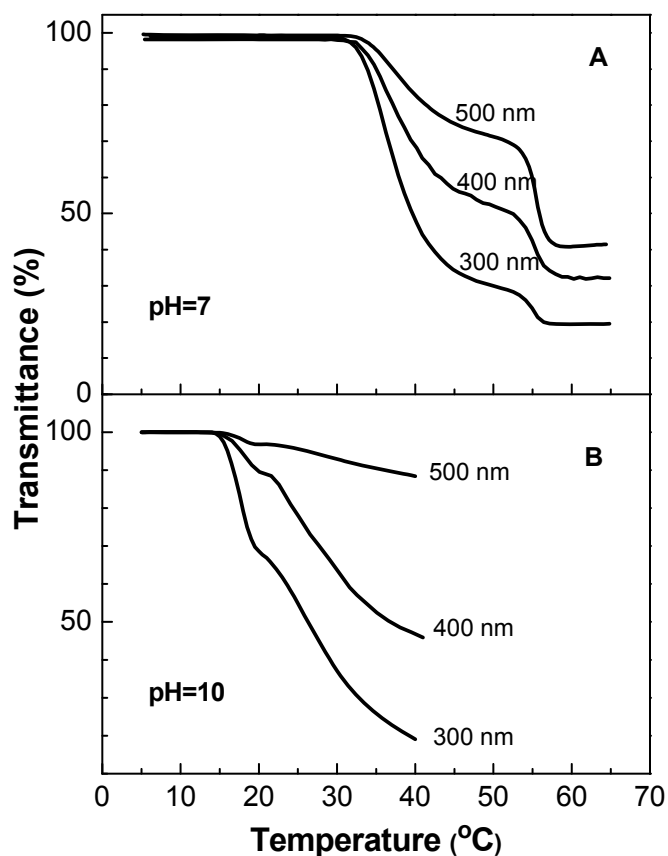
Figure 3.4 Dual stimuli-responsive behavior and the two-step transition observed for aqueous solutions of diblock random copolymer poly(nPA$_{0.8}$-*co*-DEAEMA$_{0.2}$)-*block*-poly(nPA$_{0.8}$-*co*-EA$_{0.2}$) (0.05 mg/mL) at (A) pH 7 and (B) pH 10 measured by UV-vis transmittance at 3 different wavelengths at a heating rate of 0.1 ^{o}C/min.
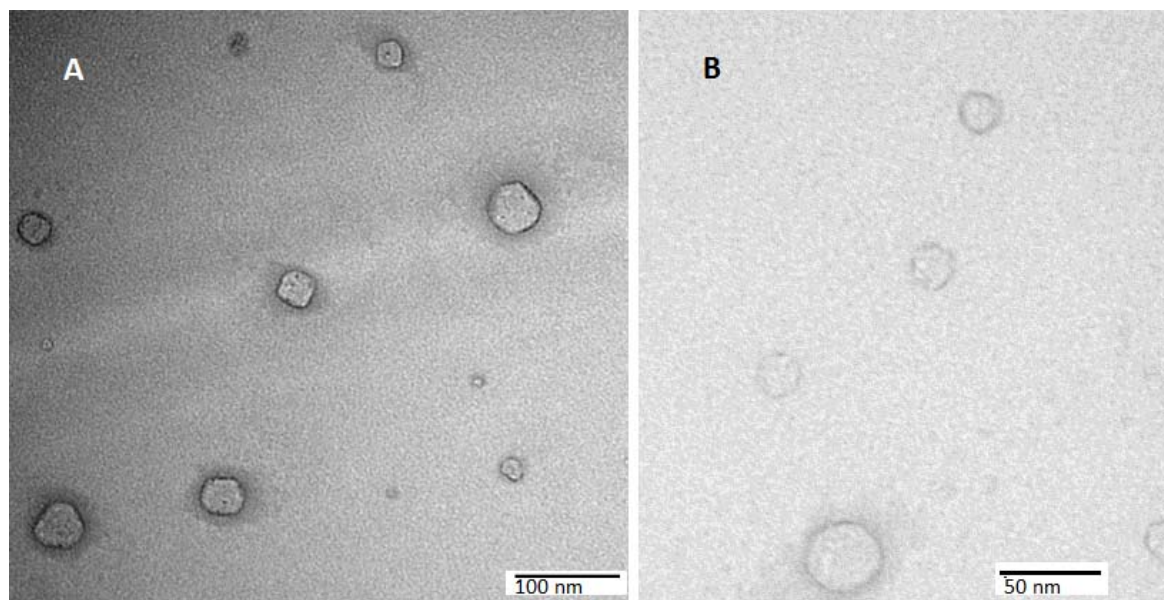
Figure 3.5 Representative TEM images of 0.05 mg/mL aqueous solutions of diblock copolymers deposited on copper grids at (A) pH 7, 37 °C and (B) pH 10, 25 °C, showing vesicles at both conditions. Note that the scale bars are 100 nm and 50 nm, respectively.

At pH 10 (Figure 3.4B), the first cloud point starting at 14 $^{\circ}$C is assigned to the collapse of the poly(nPA$_{0.8}$-*co*-DEAEMA$_{0.2}$) block, where the deprotonated DEAEMA units make this block more hydrophobic. Hence, the poly(nPA$_{0.8}$-*co*-DEAEMA$_{0.2}$) block will form the core of the vesicle membranes upon its collapse (Figure 3.5B). The second step in the transmittance curves starting at 21 $^{\circ}$C is rather broad and the smaller total shift in the transmittance at 500 nm compared to pH 7 reflects the smaller size of the particles at pH 10. This is confirmed by the dynamic light scattering results discussed later. Larger aggregates at pH 7 could be due to the slightly longer poly(nPA$_{0.8}$-*co*-EA$_{0.2}$) block, which collapses first at pH 7.

Table 3.2 Cloud points of individual blocks and the block copolymer at different pH values measured by UV-vis transmittance at 300 nm.*

pH	P(nPA$_{0.8}$-*co*-DEAEMA$_{0.2}$) CP (°C)	nPA0.8-*co*-EA$_{0.2}$ CP (°C)	P(nPA$_{0.8}$-*co*-DEAEMA$_{0.2}$)-*b*-P(nPA$_{0.8}$-*co*-EA$_{0.2}$)	
			CP1 (°C)	CP2 (°C)
7.0	52	33	39	53
10.0	13	33	18	32

* The CPs measured at higher wavelengths are generally 1-3 °C higher.

We have previously observed the interdependence of thermal transitions of a double thermosensitive diblock random copolymer due to a difference in the relative hydrophilicities of the blocks.[39] Thus, the CP of the less hydrophilic block of the diblock copolymer shifts to a higher temperature, while that of the more hydrophilic block moves to a lower temperature, and such a behavior would also be expected for poly(nPA$_{0.8}$-*co*-DEAEMA$_{0.2}$)-*block*-poly(nPA$_{0.8}$-*co*-EA$_{0.2}$). Therefore, at pH 10 the CP of poly(nPA$_{0.8}$-*co*-DEAEMA$_{0.2}$) block is slightly higher and that of poly(nPA$_{0.8}$-*co*-EA$_{0.2}$) block is lower than the corresponding transition temperatures of the individual copolymers. This effect is also seen at pH 7 with the first transition corresponding to the CP of the poly(nPA$_{0.8}$-*co*-EA$_{0.2}$) block, which is slightly higher than the corresponding transition of the individual copolymer. At pH 7, the more hydrophilic and partially protonated poly(nPA$_{0.8}$-*co*-DEAEMA$_{0.2}$) block is much less affected by its neighboring block and the onset of the transition is close to the CP of the individual copolymer.

^{1}H NMR Spectroscopy. ^{1}H NMR was used to study the dual responsive behavior of poly(nPA$_{0.8}$-*co*-DEAEMA$_{0.2}$)-*block*-poly(nPA$_{0.8}$-*co*-EA$_{0.2}$) solutions in D$_2$O. Figure 3.6 shows the temperature-dependent ^{1}H NMR spectra at pH 7 and 10. In Figure 3.6A (pH 10), no difference is observed in the spectra at 10 and 15 °C, but peaks *b* and *c*, both characteristic for poly(nPA$_{0.8}$-*co*-DEAEMA$_{0.2}$), start to show reduced intensity upon heating to 20 and 25 °C, indicating the collapse of poly(nPA$_{0.8}$-*co*-DEAEMA$_{0.2}$), which is now more hydrophobic. Peaks *d* and *f* belong to the poly(nPA$_{0.8}$-*co*-EA$_{0.2}$) block, whereas peak *a* comes from both blocks. Further heating to 30 °C induces no change to peak *f* and a

small change to peaks *a* and *d*, but they show greater attenuation at higher temperatures (35 and 40 °C), where the more hydrophilic block poly($nPA_{0.8}$-*co*-$EA_{0.2}$) is collapsed. In Figure 3.6B (pH 7), the characteristic peaks of poly($nPA_{0.8}$-*co*-$EA_{0.2}$) only start to attenuate at 35 °C, indicating that poly($nPA_{0.8}$-*co*-$EA_{0.2}$) is now the more hydrophobic block and collapses first. Interestingly, the signals of poly($nPA_{0.8}$-*co*-$DEAEMA_{0.2}$) do not disappear even at 65 °C, probably due to the charged nature of this block. Since the pK_a of this block is 7.3,[7] about 67% of amine groups are protonated at pH 7. These charged moieties are still swollen, and peaks *b*, *c*, and *e* even seem to become more visible at higher temperatures, which could suggest high mobility of the protonated domains. While the ^{1}H NMR and UV-vis spectroscopy provide evidence for the "schizophrenic" self-assembling behavior, the aggregate morphologies cannot be deduced. Hence, LLS, TEM and AFM imaging, and zeta potential measurements were undertaken for a better understanding of the aggregation process.
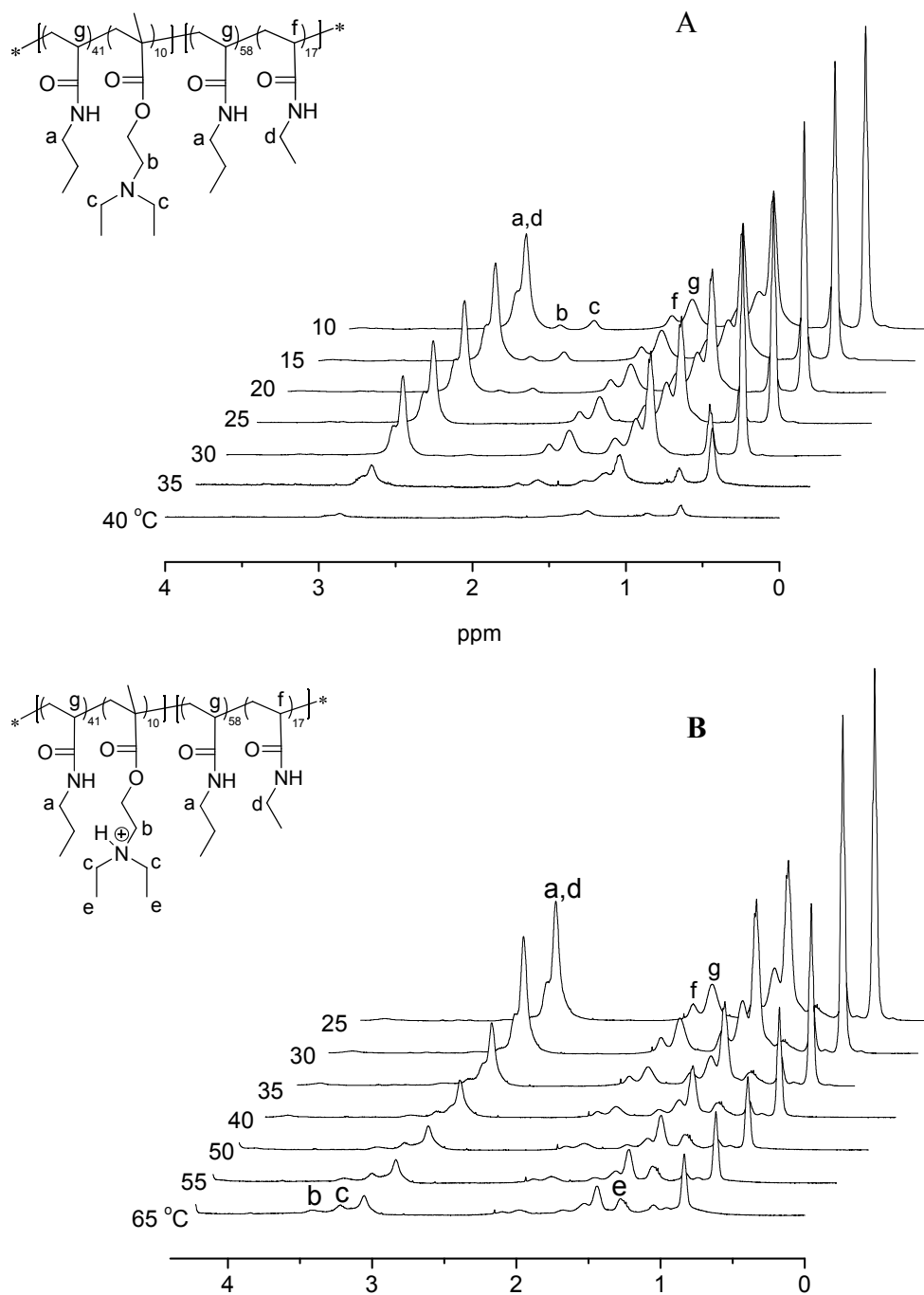
Figure 3.6 ^{1}H NMR spectra of poly(nPA$_{0.8}$-*co*-DEAEMA$_{0.2}$)-*block*-poly(nPA$_{0.8}$-*co*-EA$_{0.2}$) as a function of temperature at (A) pH 10, and (B) pH 7.

Dynamic and static light scattering. According to the light scattering results shown in Table 3.3, the solution of the random block copolymer at pH 7 and 25 $^{\circ}$C mostly contains molecularly dissolved polymer chains with zeta potential lower than 5 mV. Even though we used PMMA as SEC standards, with a structure different from those of the studied polymers, the apparent weight-average molar mass obtained by SLS (1.8×10^4 g/mol) agrees quite well with the one given by SEC in DMF (1.9×10^4 g/mol). A typical example of The samples were heated at 1 $^{\circ}$C intervals within 20-min equilibration time, corresponding to an average heating rate of 0.05 $^{\circ}$C/min. At such slow heating process, the polymer chains have more time for interchain interactions and aggregation before the temperature-induced coil-to-globule transition; therefore, larger aggregates are expected.[51] It must be emphasized that the selected temperatures in Table 3.3, both at pH 7 and 10 (37 and 25 °C, respectively), correspond to conditions where self-assembled nanostructures are formed, namely the temperatures where the transmittance in Figure 3.4 starts to decrease and self-assembling occurs. At temperatures above CP_2, the corona-forming blocks of the vesicles will collapse, leading to aggregation.

Table 3.3 Micellar properties of a diblock random copolymer poly(nPA$_{0.8}$-*co*-DEAEMA$_{0.2}$)-*block*-poly(nPA$_{0.8}$-*co*-EA$_{0.2}$) in 0.05 mg/mL aqueous solutions studied by LLS.

	Temperature (°C)	D_h (nm)[a]	PDI[a]	$M_{w,app}$ (g/mol)[b]	N_{agg}[c]	Zeta potential (mV)
pH 10	37	116	0.029	1.2×10^8	6.7×10^3	-23 ± 2
	25	60	0.184	7.1×10^6	4.0×10^2	-20 ± 1
pH 7	25	7	-	1.8×10^4	~ 1	4 ± 1
	37	148	0.164	1.8×10^8	1.0×10^4	22 ± 1
	55	328	0.266	7.1×10^9	3.9×10^5	25 ± 2

[a] Mean intensity-weighted hydrodynamic diameter and polydispersity index (PDI) determined by DLS. [b] Apparent weight-average molar mass determined by SLS. [c] Aggregation number calculated from $M_{w,app}$.

Based on the cloud points of the individual blocks and the block copolymer, the core of the vesicles membrane is composed of the poly(nPA$_{0.8}$-*co*-EA$_{0.2}$) block at pH 7 and the poly(nPA$_{0.8}$-*co*-DEAEMA$_{0.2}$) block at pH 10. The size distributions obtained during the experiment are depicted in Figure 3.S3.
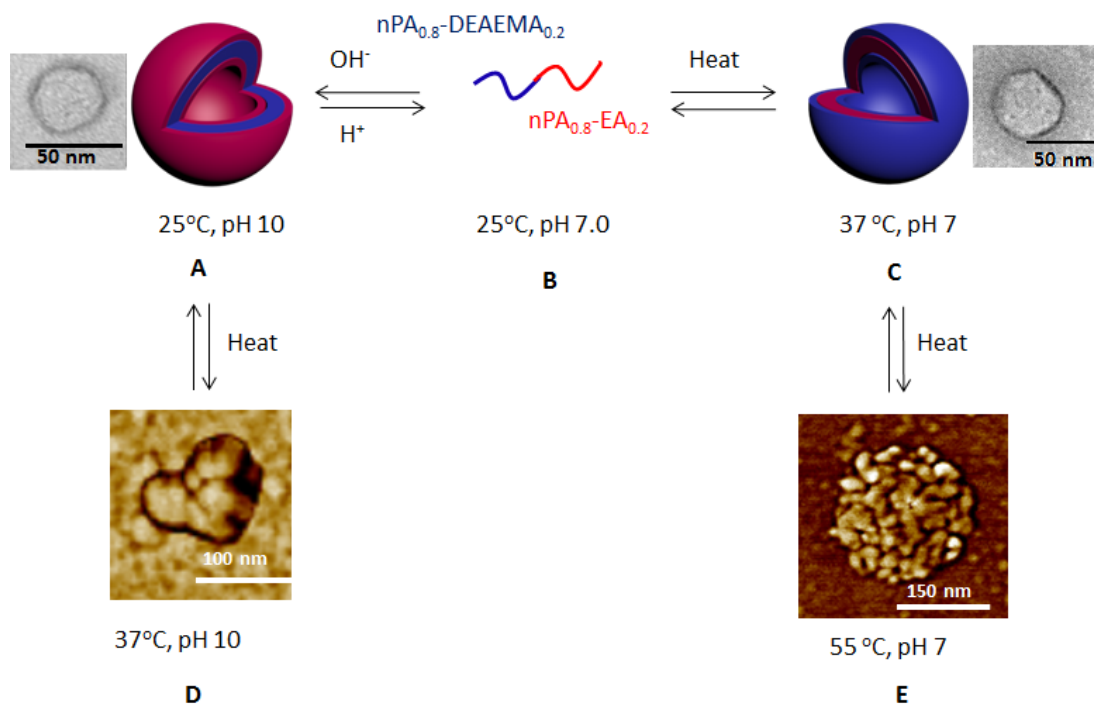
Scheme 3.2 Self-assembling process of poly(nPA$_{0.8}$-*co*-DEAEMA$_{0.2}$)-*block*-poly(nPA$_{0.8}$-*co*-EA$_{0.2}$) into vesicles, and then aggregates upon heating. The images of representative particles are taken from larger TEM and AFM images (Figures 3.5 and 3.7, respectively).

The proposed self-assembling process is depicted in Scheme 3.2. At pH 10, the DEAEMA moieties of poly(nPA$_{0.8}$-*co*-DEAEMA$_{0.2}$) block and also the carboxylic end group of the CTA are deprotonated. Thus, the poly(nPA$_{0.8}$-*co*-DEAEMA$_{0.2}$) block becomes more hydrophobic at 25 °C above its cloud point, while the poly(nPA$_{0.8}$-*co*-EA$_{0.2}$) block is still solvated along with the attached anionic CTA end group. This leads to the formation of vesicles with mean hydrodynamic diameter of 60 nm and N$_{agg}$ ~ 400. The zeta potential of the vesicles is -20 mV due to the anionic chain ends, which are located on the coronas. At

pH 7, the poly(nPA$_{0.8}$-*co*-EA$_{0.2}$) block is dehydrated at 37 $^\circ$C, thus forming the core of the vesicle membrane, while the poly(nPA$_{0.8}$-*co*-DEAEMA$_{0.2}$) block is solvated due to the partial protonation of amine groups. The partially protonated block contributes to the positively charged coronas of inverted vesicles with zeta potential of 22 mV. The hydrodynamic diameter of the vesicles is 148 nm and the aggregation number (N_{agg} ~ 1.0×10^4) is higher than at pH 10. The large hydrodynamic diameter and high aggregation number are typical of vesicular structures. AFM studies at both pH 10 and 7 (Figures 3.7A and 3.7C, respectively) show spherical particles with mean number-average diameters of 60 nm and 67 nm for poly(nPA$_{0.8}$-*co*-DEAEMA$_{0.2}$)-core (pH 10) and poly(nPA$_{0.8}$-*co*-EA$_{0.2}$)-core (pH 7), respectively. The diameters obtained by AFM have been determined in a dried state and are therefore lower than those by DLS in solution. The charged particles at pH 7 are more affected by the removal of water.
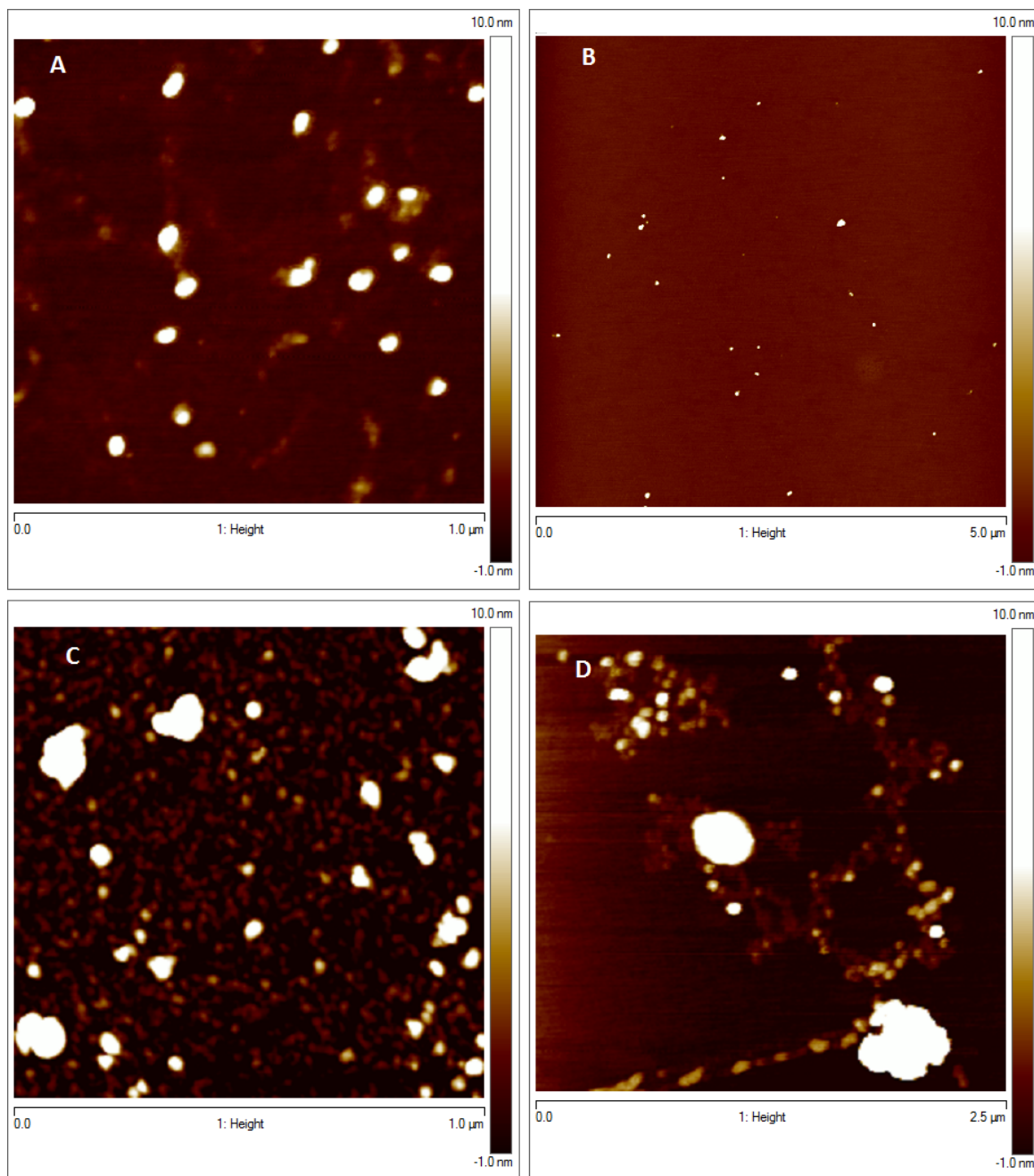
Figure 3.7 AFM images of 0.05 mg/mL aqueous solutions of poly(nPA$_{0.8}$-*co*-DEAEMA$_{0.2}$)-*block*-poly(nPA$_{0.8}$-*co*-EA$_{0.2}$) diblock random copolymer deposited on mica at (A) pH 10 and 25 ^{o}C, (B) pH 7 and 37 ^{o}C, (C) pH 10 and 37 ^{o}C, and (D) pH 7 and 55 ^{o}C. Note that the image width (scale) is 1.0 μm for (A) and (B), 5.0 μm for (C) and 2.5 μm for (D).

The block ratio is known to influence the morphologies of self-assemblies, even when the blocks are stimuli-responsive and capable of changing their relative hydrophilicities in the block copolymer. For example, the pH- and temperature-responsive poly(N,N-diethylaminoethyl methacrylate)-*block*-poly(N-isopropylacrylamide) (PDEAEMA-*b*-PNIPAM) forms spherical micelles in aqueous solution in spite of the core block if the mass fractions of blocks are similar, i.e. 50:50 (wt %). However, if one block is much longer, different self-assembled morphologies can be observed and, for example, the mass ratio of 70:30 (wt %) of PDEAEMA-*b*-PNIPAM leads either to the formation of spherical micelles or vesicles, depending on which block has higher relative hydrophilicity with the selective stimuli.[16] In another example, a double temperature-responsive poly[2-(dimethylamino)ethyl methacrylate-block-di(ethyleneglycol)methyl ether methacrylate] (poly(DMAEMA-*b*-DEGMA)) at 50:50 (wt %). formed multi- or unilamellar vesicles depending on temperature.[52] In our case, the mass ratio of the poly($nPA_{0.8}$-*co*-$DEAEMA_{0.2}$) and poly($nPA_{0.8}$-*co*-$EA_{0.2}$) blocks is 45:55 (wt %) and with this composition, the formation of either micelles or vesicles could be expected. The higher degree of aggregation at pH 7 could stem from the slightly longer poly($nPA_{0.8}$-*co*-$EA_{0.2}$) block collapsing at pH 7 and 37 °C.

If the solution of vesicles at pH 10 is heated from 25 (A in Scheme 3.2) to 37 °C (D), above the cloud point of the corona-forming poly($nPA_{0.8}$-*co*-$EA_{0.2}$) block, the coronas collapse and the vesicles aggregate into larger clusters (D_h = 116 nm, N_{agg} ~ 6.7×10^3). This process corresponds to the second step in the shift in transmittance shown in Figure 3.4B and is accompanied by a decrease in zeta potential to -23 mV. This step is illustrated by AFM imaging in Figure 3.7, and the collapsed particles coexist with the single ones in a polydisperse system with diameters ranging from 25 to 103 nm. On the other hand, the vesicles with both temperature- and pH-sensitive poly($nPA_{0.8}$-*co*-$DEAEMA_{0.2}$) coronas at pH 7 (C in Scheme 3.2) show pH-dependent aggregation upon heating. When the sample (pH 7) is heated to 55 °C, above the cloud point of poly($nPA_{0.8}$-*co*-$DEAEMA_{0.2}$) block, D_h = 328 nm and N_{agg} ~ 3.9×10^5 (E) are obtained with the zeta potential of 25 mV. The molar mass of the aggregates measured by SLS is almost 40 times higher at 55 °C (E) than at 37 °C (C), suggesting that the vesicles at pH 7 show behavior similar to pH 10, aggregating

into larger clusters upon heating. According to the AFM image in Figure 3.7, large aggregates are present in a polydisperse system with diameters between 40-400 nm. According to the phase diagram proposed in Scheme 3.2, the pH-sensitive and thermo-sensitive poly(nPA$_{0.8}$DEAEMA$_{0.2}$) block can either contribute to the core of the vesicle membranes or to stabilizing the coronas, depending on the external stimulus. This feature, in addition to the tunability of the temperatures for switching between vesicles and inverted vesicles, contributes to the versatility of these smart materials.

3.4 Conclusions

The synthetic approach developed in our group for making blocks of random copolymers allows the making of block copolymers responding to a desired condition almost at will within a reasonable range for the external stimuli. This work provides an illustrative example for the design and synthesis of such polymers. Combining pH- and temperature-responsive poly(nPA$_{0.8}$-*co*-DEAEMA$_{0.2}$) and temperature-responsive poly(nPA$_{0.8}$-*co*-EA$_{0.2}$) random copolymers in a diblock copolymer resulted in a system that is responsive to multiple stimuli. The composition-dependent response to the external stimuli allows the design of a wide range of responsive polymers. pH-switchable vesicles exhibiting "schizophrenic" behavior were formed in aqueous solutions and their sizes depend on both pH and temperature. The block copolymer was molecularly dissolved in water at 25 $^{\circ}$C (pH 7), forming vesicles at 37 $^{\circ}$C (pH 7), while the core and corona of the vesicle membranes could be switched at 25 $^{\circ}$C (pH 10). The behavior of the polymers is clearly of fundamental research interest. There may be potential applications where responsiveness to both temperature and pH is desired. For instance, the thermoresponsive "schizophrenic" diblock copolymer PNIPAAm-*b*-PSBMA has recently been studied for its anticoagulant behavior in the human blood in the range of 4−40 $^{\circ}$C.[4] The advantage of the current design is the possibility to tailor such responsiveness to a desired temperature and pH by adjusting the chemical composition of the monomers during the polymerization. The two-step self-assembling process is also an interesting issue that could be the subject of further detailed studies.

3.5 Acknowledgements

3.6 Supporting information

Table 3.S1 Molar ratio of nPA and DEAEMA as a function of reaction time and conversion in RAFT polymerization using BPA as the CTA.

Reaction time (min)	15	30	45	70	90
Conversion (%)	8	13	19	26	32
nPA : DEAEMA molar ratio in the polymer	79 : 21	78 : 22	80 : 20	82 : 18	81 : 19
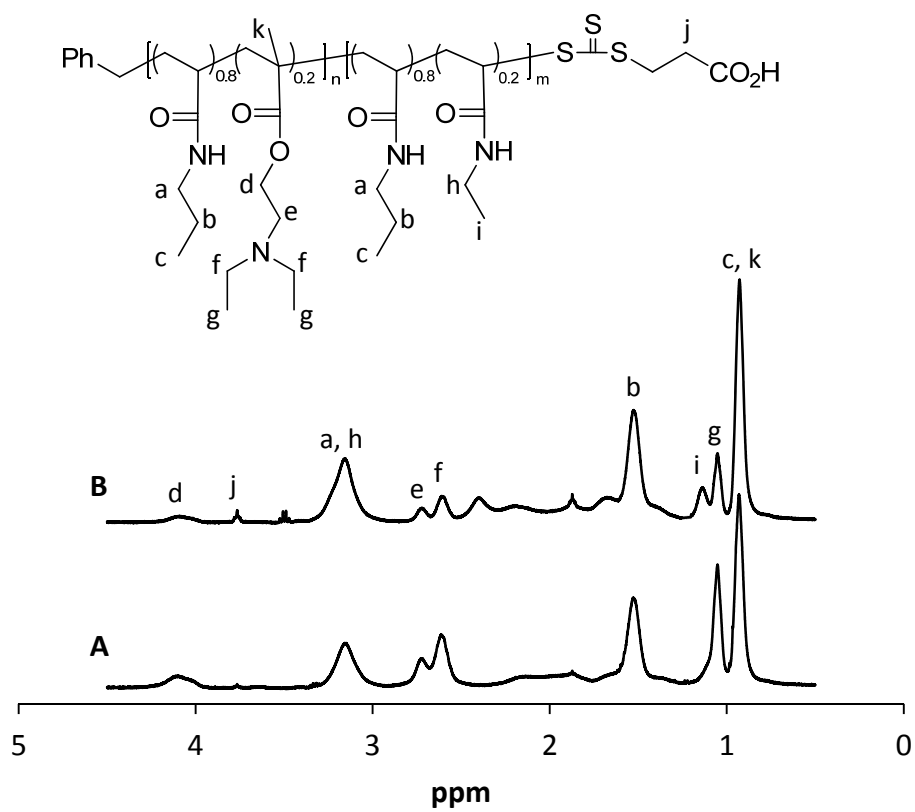
Figure 3.S1 ^{1}H NMR spectra of (A) poly(nPA$_{0.8}$-*co*-DEAEMA$_{0.2}$)-CTA, and (B) the corresponding chain extended diblock random copolymer poly(nPA$_{0.8}$-*co*-DEAEMA$_{0.2}$)-*block*-poly(nPA$_{0.8}$-*co*-EA$_{0.2}$) in CDCl$_3$. The assignments of the signals from the pendant groups of the copolymer are indicated.
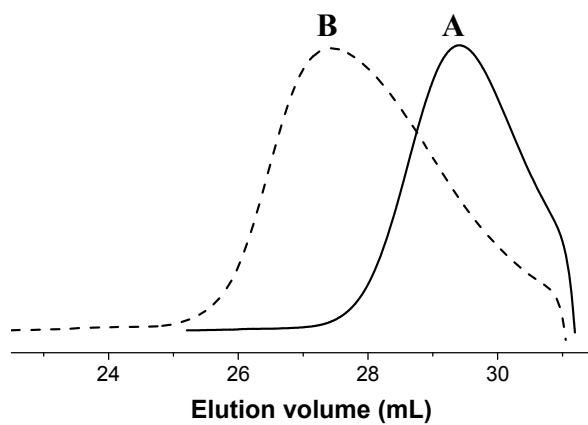
Figure 3.S2 SEC chromatograms of (A) poly(nPA$_{0.8}$-*co*-DEAEMA$_{0.2}$) (macro-CTA) and (B) poly(nPA$_{0.8}$-*co*-DEAEMA$_{0.2}$)-*block*-poly(nPA$_{0.8}$-*co*-EA$_{0.2}$) (the diblock copolymer).
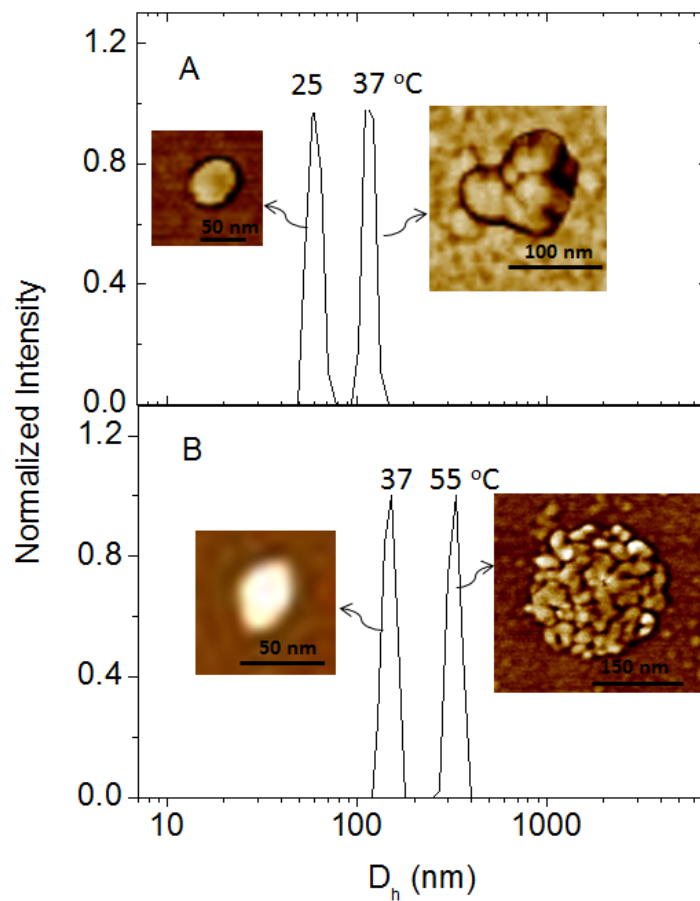
Figure 3.S3 The particle size distributions of the diblock random copolymer poly(nPA$_{0.8}$-*co*-DEAEMA$_{0.2}$)-*block*-poly(nPA$_{0.8}$-*co*-EA$_{0.2}$) in water (0.05 mg/mL) at pH 10 (A) and 7 (B) as observed by DLS at 90°. The corresponding AFM images of vesicles and their aggregates are shown for each distribution.
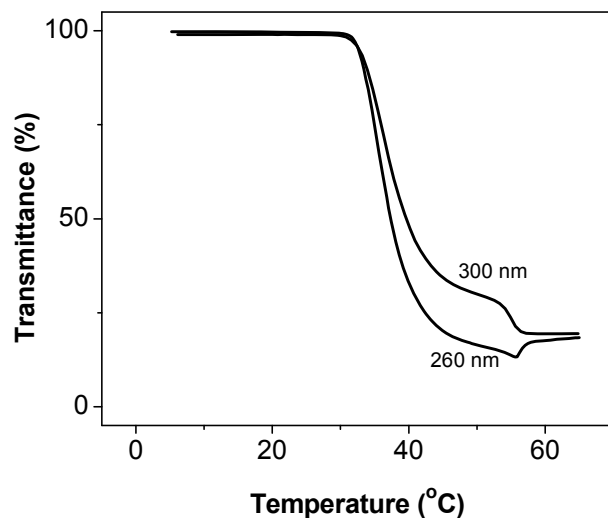
Figure 3.S4 The "abnormal" behavior of 0.05 mg/mL aqueous solution of poly(nPA$_{0.8}$-*co*-DEAEMA$_{0.2}$)-*block*-poly(nPA$_{0.8}$-*co*-EA$_{0.2}$) at pH 7 observed by UV-vis transmittance at 260 nm at a heating rate of 0.1 ^{o}C/min. At around 55 ^{o}C, a small but reproducible increase in transmittance is detected at 260 nm, which is not visible at higher detection wavelengths (300, 400, and 500 nm). No precipitation was visible to the eye in this temperature range and, hence, this shift could arise from the decrease in the number of smaller aggregates upon the collapse of poly(nPA$_{0.8}$-*co*-DEAEMA$_{0.2}$) block at temperatures above its cloud point. As a result, the shape of the temperature-dependent transmittance graph is governed by the number and the size of the aggregates. This is evidenced by the disappearance of this "abnormal" small shift in transmittance at slightly higher detection wavelength (300 nm) and the large aggregate sizes at 55 °C determined by LLS.

3.7 References

1. Bütün, V.; Billingham, N. C.; Armes, S. P., Unusual Aggregation Behavior of a Novel Tertiary Amine Methacrylate-Based Diblock Copolymer: Formation of Micelles and Reverse Micelles in Aqueous Solution. *J. Am. Chem. Soc.* 1998, *120* (45), 11818-11819.

2. Bütün, V.; Liu, S.; Weaver, J. V. M.; Bories-Azeau, X.; Cai, Y.; Armes, S. P., A brief review of 'schizophrenic' block copolymers. *React. Funct. Polym.* 2006, *66* (1), 157-165.

3. Plamper, F. A.; McKee, J. R.; Laukkanen, A.; Nykanen, A.; Walther, A.; Ruokolainen, J.; Aseyev, V.; Tenhu, H., Miktoarm stars of poly(ethylene oxide) and poly(dimethylaminoethyl methacrylate): manipulation of micellization by temperature and light. *Soft Matter* **2009,** *5* (9), 1812-1821.

4. Shih, Y.-J.; Chang, Y.; Deratani, A.; Quemener, D., "Schizophrenic" Hemocompatible Copolymers via Switchable Thermoresponsive Transition of Nonionic/Zwitterionic Block Self-Assembly in Human Blood. *Biomacromolecules* **2012,** *13* (9), 2849-2858.

5. Weaver, J. V. M.; Armes, S. P.; Butun, V., Synthesis and aqueous solution properties of a well-defined thermo-responsive schizophrenic diblock copolymer. *Chem. Commun.* **2002,** No. 18, 2122-2123.

6. Romão, R. I. S.; Beija, M.; Charreyre, M.-T. r. s.; Farinha, J. P. S.; Gonçalves da Silva, A. l. M. P. S.; Martinho, J. M. G., Schizophrenic Behavior of a Thermoresponsive Double Hydrophilic Diblock Copolymer at the Air−Water Interface. *Langmuir* **2010,** *26* (3), 1807-1815.

7. Arotçaréna, M.; Heise, B.; Ishaya, S.; Laschewsky, A., Switching the Inside and the Outside of Aggregates of Water-Soluble Block Copolymers with Double Thermoresponsivity. *J. Am. Chem. Soc.* **2002,** *124* (14), 3787-3793.

8. Cai, Y.; Armes, S. P., A Zwitterionic ABC Triblock Copolymer That Forms a "Trinity" of Micellar Aggregates in Aqueous Solution. *Macromolecules* **2004,** *37* (19), 7116-7122.

9. Dai, S.; Ravi, P.; Tam, K. C.; Mao, B. W.; Gan, L. H., Novel pH-Responsive Amphiphilic Diblock Copolymers with Reversible Micellization Properties. *Langmuir* **2003,** *19* (12), 5175-5177.

10. Rodríguez-Hernández, J.; Lecommandoux, S., Reversible Inside−Out Micellization of pH-responsive and Water-Soluble Vesicles Based on Polypeptide Diblock Copolymers. *J. Am. Chem. Soc.* **2005,** *127* (7), 2026-2027.

11. Liu, S.; Armes, S. P., Polymeric Surfactants for the New Millennium: A pH-Responsive, Zwitterionic, Schizophrenic Diblock Copolymer. *Angew. Chem. Int. Ed.* **2002,** *41* (8), 1413-1416.

12. Du, J.; O'Reilly, R. K., pH-Responsive Vesicles from a Schizophrenic Diblock Copolymer. *Macromol. Chem. Phys.* **2010,** *211* (14), 1530-1537.

13. Liu, S.; Armes, S. P., Synthesis and Aqueous Solution Behavior of a pH-Responsive Schizophrenic Diblock Copolymer. *Langmuir* **2003,** *19* (10), 4432-4438.

14. Bütün, V.; Top, R. B.; Ufuklar, S., Synthesis and Characterization of Novel "Schizophrenic" Water-Soluble Triblock Copolymers and Shell Cross-Linked Micelles. *Macromolecules* **2006,** *39* (3), 1216-1225.

15. Liu, S.; Billingham, N. C.; Armes, S. P., A Schizophrenic Water-Soluble Diblock Copolymer. *Angew. Chem. Int. Ed.* **2001,** *40* (12), 2328-2331.

16. Smith, A. E.; Xu, X.; Kirkland-York, S. E.; Savin, D. A.; McCormick, C. L., "Schizophrenic" Self-Assembly of Block Copolymers SynthesizedviaAqueous RAFT Polymerization: From Micelles to Vesicles†† Paper number 143 in a series on Water-Soluble Polymers. *Macromolecules* **2010,** *43* (3), 1210-1217.

17. Chang, C.; Wei, H.; Feng, J.; Wang, Z.-C.; Wu, X.-J.; Wu, D.-Q.; Cheng, S.-X.; Zhang, X.-Z.; Zhuo, R.-X., Temperature and pH Double Responsive Hybrid Cross-Linked Micelles Based on P(NIPAAm-co-MPMA)-*b*-P(DEA): RAFT Synthesis and "Schizophrenic" Micellization. *Macromolecules* **2009,** *42* (13), 4838-4844.

18. Zhang, Y.; Liu, H.; Hu, J.; Li, C.; Liu, S., Synthesis and Aggregation Behavior of Multi-Responsive Double Hydrophilic ABC Miktoarm Star Terpolymer. *Macromol. Rapid Commun.* **2009,** *30* (11), 941-947.

19. Schilli, C. M.; Zhang, M.; Rizzardo, E.; Thang, S. H.; Chong, Y. K.; Edwards, K.; Karlsson, G.; Müller, A. H. E., A New Double-Responsive Block Copolymer Synthesized via RAFT Polymerization: Poly(*N*-isopropylacrylamide)-block-poly(acrylic acid). *Macromolecules* **2004,** *37* (21), 7861-7866.

20. Ge, Z.; Cai, Y.; Yin, J.; Zhu, Z.; Rao, J.; Liu, S., Synthesis and 'Schizophrenic' Micellization of Double Hydrophilic AB4 Miktoarm Star and AB Diblock Copolymers: Structure and Kinetics of Micellization. *Langmuir* **2006,** *23* (3), 1114-1122.

21. Fournier, D.; Hoogenboom, R.; Thijs, H. M. L.; Paulus, R. M.; Schubert, U. S., Tunable pH- and Temperature-Sensitive Copolymer Libraries by Reversible Addition−Fragmentation Chain Transfer Copolymerizations of Methacrylates. *Macromolecules* **2007,** *40* (4), 915-920.

22. Jiang, X.; Ge, Z.; Xu, J.; Liu, H.; Liu, S., Fabrication of Multiresponsive Shell Cross-Linked Micelles Possessing pH-Controllable Core Swellability and Thermo-Tunable Corona Permeability. *Biomacromolecules* **2007,** *8* (10), 3184-3192.

23. Lowe, A. B.; Torres, M.; Wang, R., A doubly responsive AB diblock copolymer: RAFT synthesis and aqueous solution properties of poly (*N*-isopropylacrylamide-block-4-vinylbenzoic acid). *J. Polym. Sci. Part A: Polym. Chem.* **2007,** *45* (24), 5864-5871.

24. Rao, J.; Luo, Z.; Ge, Z.; Liu, H.; Liu, S., "Schizophrenic" Micellization Associated with Coil-to-Helix Transitions Based on Polypeptide Hybrid Double Hydrophilic Rod–Coil Diblock Copolymer. *Biomacromolecules* **2007,** *8* (12), 3871-3878.

25. Zhang, Y.; Wu, T.; Liu, S., Micellization Kinetics of a Novel Multi-Responsive Double Hydrophilic Diblock Copolymer Studied by Stopped-Flow pH and Temperature Jump. *Macromol. Chem. Phys.* **2007,** *208* (23), 2492-2501.

26. Fei, B.; Yang, Z.; Yang, H.; Hu, Z.; Wang, R.; Xin, J. H., Schizophrenic copolymer from natural biopolymer by facile grafting. *Polymer* **2010,** *51* (4), 890-896.

27. Weiss, J.; Laschewsky, A., Temperature-Induced Self-Assembly of Triple-Responsive Triblock Copolymers in Aqueous Solutions. *Langmuir* **2011,** *27* (8), 4465-4473.

28. Maki, Y.; Mori, H.; Endo, T., Synthesis of Amphiphilic and Double-Hydrophilic Block Copolymers Containing Poly(vinyl amine) Segments by RAFT Polymerization of *N*-Vinylphthalimide. *Macromol. Chem. Phys.* **2010,** *211* (1), 45-56.

29. Mertoglu, M.; Garnier, S.; Laschewsky, A.; Skrabania, K.; Storsberg, J., Stimuli responsive amphiphilic block copolymers for aqueous media synthesised via reversible addition fragmentation chain transfer polymerisation (RAFT). *Polymer* **2005,** *46* (18), 7726-7740.

30. Cao, Y.; Zhao, N.; Wu, K.; Zhu, X. X., Solution properties of a thermosensitive triblock copolymer of *N*-alkyl substituted acrylamides. *Langmuir* **2009,** *25* (3), 1699-704.

31. Cao, Y.; Zhu, X. X.; Luo, J.; Liu, H., Effects of Substitution Groups on the RAFT Polymerization of *N*-Alkylacrylamides in the Preparation of Thermosensitive Block Copolymers. *Macromolecules* **2007,** *40* (18), 6481-6488.

32. Cristiano, C. M. Z.; Soldi, V.; Li, C.; Armes, S. P.; Rochas, C.; Pignot-Paintrand, I.; Borsali, R., Thermo-Responsive Copolymers Based on Poly(*N*-isopropylacrylamide) and Poly[2-(methacryloyloxy)ethyl phosphorylcholine]: Light Scattering and Microscopy Experiments. *Macromol. Chem. Phys.* **2009,** *210* (20), 1726-1733.

33. Jochum, F. D.; Roth, P. J.; Kessler, D.; Theato, P., Double Thermoresponsive Block Copolymers Featuring a Biotin End Group. *Biomacromolecules* **2010,** *11* (9), 2432-2439.

34. Weiss, J.; Böttcher, C.; Laschewsky, A., Self-assembly of double thermoresponsive block copolymers end-capped with complementary trimethylsilyl groups. *Soft Matter* **2011,** *7* (2), 483.

35. Liu, H. Y.; Zhu, X. X., Lower critical solution temperatures of *N*-substituted acrylamide copolymers in aqueous solutions. *Polymer* **1999,** *40* (25), 6985-6990.

36. Avoce, D.; Liu, H. Y.; Zhu, X. X., *N*-Alkylacrylamide copolymers with (meth)acrylamide derivatives of cholic acid: synthesis and thermosensitivity. *Polymer* **2003,** *44* (4), 1081-1087.

37. Liu, H.; Avoce, D.; Song, Z.; Zhu, X. X., *N*-Isopropylacrylamide Copolymers with Acrylamide and Methacrylamide Derivatives of Cholic Acid: Synthesis and Characterization. *Macromol. Rapid Commun.* **2001,** *22* (9), 675-680.

38. Plamper, F. A.; Steinschulte, A. A.; Hofmann, C. H.; Drude, N.; Mergel, O.; Herbert, C.; Erberich, M.; Schulte, B.; Winter, R.; Richtering, W., Toward Copolymers with Ideal Thermosensitivity: Solution Properties of Linear, Well-Defined Polymers of *N*-Isopropyl Acrylamide and *N,N*-Diethyl Acrylamide. *Macromolecules* **2012,** *45* (19), 8021-8026.

39. Savoji, M. T.; Strandman, S.; Zhu, X. X., Block Random Copolymers of *N*-Alkyl-Substituted Acrylamides with Double Thermosensitivity. *Macromolecules* **2012,** *45* (4), 2001-2006.

40. Kotsuchibashi, Y.; Ebara, M.; Idota, N.; Narain, R.; Aoyagi, T., A 'smart' approach towards the formation of multifunctional nano-assemblies by simple mixing of block copolymers having a common temperature sensitive segment. *Polym. Chem.* **2012,** *3* (5), 1150.

41. Shea, K. J.; Stoddard, G. J.; Shavelle, D. M.; Wakui, F.; Choate, R. M., Synthesis and characterization of highly crosslinked poly(acrylamides) and poly(methacrylamides). A new class of macroporous polyamides. *Macromolecules* **1990,** *23* (21), 4497-4507.

42. Stenzel, M. H.; Davis, T. P.; Fane, A. G., Honeycomb structured porous films prepared from carbohydrate based polymers synthesized via the RAFT process. *J. Mater. Chem.* **2003,** *13* (9), 2090-2097.

43. Wang, X.; Qiu, X.; Wu, C., Comparison of the Coil-to-Globule and the Globule-to-Coil Transitions of a Single Poly(*N*-isopropylacrylamide) Homopolymer Chain in Water. *Macromolecules* **1998,** *31* (9), 2972-2976.

44. Xu, J.; Luo, S.; Shi, W.; Liu, S., Two-Stage Collapse of Unimolecular Micelles with Double Thermoresponsive Coronas. *Langmuir* **2005,** *22* (3), 989-997.

45. Smith, A. E.; Xu, X.; Abell, T. U.; Kirkland, S. E.; Hensarling, R. M.; McCormick, C. L., Tuning Nanostructure Morphology and Gold Nanoparticle "Locking" of Multi-Responsive Amphiphilic Diblock Copolymers† † Paper No. 138 in a series on Water Soluble Polymers. *Macromolecules* **2009,** *42* (8), 2958-2964.

46. Zhang, J.; Jiang, X.; Zhang, Y.; Li, Y.; Liu, S., Facile Fabrication of Reversible Core Cross-Linked Micelles Possessing Thermosensitive Swellability. *Macromolecules* **2007,** *40* (25), 9125-9132.

47. Nakayama, M.; Okano, T., Polymer Terminal Group Effects on Properties of Thermoresponsive Polymeric Micelles with Controlled Outer-Shell Chain Lengths. *Biomacromolecules* **2005,** *6* (4), 2320-2327.

48. McCool, M. B.; Senogles, E., The self-catalysed hydrolysis of poly(*N,N*-dimethylaminoethyl acrylate). *Eur. Polym. J.* **1989,** *25* (7-8), 857-860.

49. van de Wetering, P.; Zuidam, N. J.; van Steenbergen, M. J.; van der Houwen, O. A. G. J.; Underberg, W. J. M.; Hennink, W. E., A Mechanistic Study of the Hydrolytic Stability of Poly(2-(dimethylamino)ethyl methacrylate). *Macromolecules* **1998,** *31* (23), 8063-8068.

50. Kerker, M., *The scattering of light, and other electromagnetic radiation*. Academic Press: New York, 1969.

51. Qiu, X.; Wu, C., Study of the Core−Shell Nanoparticle Formed through the "Coil-to-Globule" Transition of Poly(*N*-isopropylacrylamide) Grafted with Poly(ethylene oxide). *Macromolecules* **1997,** *30* (25), 7921-7926.

52. Pietsch, C.; Mansfeld, U.; Guerrero-Sanchez, C.; Hoeppener, S.; Vollrath, A.; Wagner, M.; Hoogenboom, R.; Saubern, S.; Thang, S. H.; Becer, C. R.; Chiefari, J.; Schubert, U. S., Thermo-Induced Self-Assembly of Responsive Poly(DMAEMA-*b*-DEGMA) Block Copolymers into Multi- and Unilamellar Vesicles. *Macromolecules* **2012,** *45* (23), 9292-9302.

Chapter 4

Invertible vesicles and micelles formed by dually-responsive diblock random copolymers in aqueous solutions*

Abstract

Dually-responsive diblock random copolymers poly(nPA$_{0.8}$-*co*-DEAEMA$_{0.2}$)-*block*-poly(nPA$_{0.8}$-*co*-EA$_{0.2}$) were made from *N*-n-propylacrylamide (nPA), 2-(diethylamino)ethyl methacrylate (DEAEMA) and *N*-ethylacrylamide (EA) via reversible addition-fragmentation chain transfer (RAFT) polymerization. Copolymers of different block length ratios, poly(nPA$_{28}$-*co*-DEAEMA$_7$)-*block*-poly(nPA$_{29}$-*co*-EA$_7$) (P1) and poly(nPA$_{28}$-*co*-DEAEMA$_7$)-*block*-poly(nPA$_{70}$-*co*-EA$_{18}$) (P2), self-assembl into vesicles and micelle-like aggregates, respectively, in aqueous solutions and both show "schizophrenic" inversion behavior when the pH and temperature are varied. The relative lengths of the two blocks are shown to affect the self-assembly of amphiphilic diblock copolymers. P1 has a similar length for both blocks and forms spherical vesicles (hydrodynamic diameter D_h = 167 nm) with the first block poly(nPA$_{29}$-*co*-EA$_7$) as the membrane inner layer at pH 7 and 37 ^{o}C (above the cloud point of the more hydrophobic block, CP1), while spherical micelle-like aggregates (D_h = 76 nm) are obtained at pH 10 and 25 ^{o}C (above CP1) with the second block poly(nPA$_{28}$-*co*-DEAEMA$_7$) as the core. In comparison, P2 has a different block length ratio (1:3, thus a much longer second block) and forms spherical micelle-like aggregates above CP1 at both pH 7 (the second block as the core, D_h = 241 nm) and pH 10 (the first block as the core, D_h = 107), respectively. Further aggregation was observed by heating the polymer solution above the cloud point of the more hydrophilic block (CP2). The variation of the length and chemical composition of the blocks allows the tuning of the

---

responsiveness of the block copolymers toward both pH and temperature and determines the formation of either micelles or vesicles during the aggregation.

4.1 Introduction

Amphiphilic block copolymers have attracted much research interest because of their capability of forming various self-assembled structures, particularly in aqueous solutions. Several reviews have been published on such amphiphilic systems and their self-assemblies.[1-8] The spontaneous self-assembly is the result of a balance between attractive and repulsive forces, such as hydrophobic interaction, hydrogen bonding, coordination to metals, and steric or electrostatic repulsion.[9] Some parameters affecting this balance include the block ratio and the selectivity of the solvent. By introducing blocks responsive to different external stimuli, such as pH or temperature, it is possible to make systems that exhibit so-called "schizophrenic" behavior, forming invertible structures in aqueous solutions without the addition of organic solvents.[10-13] The diblock copolymer based on 2-(*N*-morpholino)ethyl methacrylate (MEMA) and 2-(diethylamino)ethyl methacrylate (DEAEMA) was the first reported copolymer capable of switching between micelles and inverted micelles by the change in ionic strength or pH of the solution.[10]

The relative length of hydrophobic and hydrophilic segments is also expected to affect the self-assembly behavior of stimuli-responsive systems. We have earlier described the effect of adjusting the length of a single block on the aggregation mechanism of a thermo-responsive triblock terpolymer poly(*N-n*-propylacrylamide)-*block*-poly(*N*-isopropylacrylamide)-*block*-poly(*N,N*-ethylmethylacrylamide) (PnPA-*b*-PiPA-*b*-PEMA) in aqueous solutions.[14] Homopolymers have been used as the consisting blocks in most reported block copolymers to obtain spherical micelles,[15-17] disc-[18-20] and stacked disc-like micelles,[19] rods,[21] and various types of vesicles[16, 22-25] in solution. More recently, thermoresponsive diblock copolymers consisting of random copolymers have been reported,[26, 27] which self-assemble in aqueous solution at desired temperatures. The transition temperatures of individual blocks can be varied by adjusting their monomer compositions. In our previous work, we used this approach to prepare a symmetrical diblock random copolymer with tunable pH- and thermo-responsiveness, capable of

forming invertible structures responding to changing stimuli.[28] This polymer was composed of two random copolymer blocks, one block responsive to temperature, poly(N-n-propylacrylamide-co-N-ethylacrylamide) (poly(nPA$_{0.8}$-co-EA$_{0.2}$)), and another responsive to both pH and temperature changes, poly[N-n-propylacrylamide-co-2-(diethylamino)ethyl methacrylate] (poly(nPA$_{0.8}$-co-DEAEMA$_{0.2}$)). The pH-sensitive block became positively-charged below its pK$_a$ and thus more hydrophilic with a lower cloud point. As a result, switchable vesicles were obtained where the membrane inner and outer layers were inverted by changing the pH or the temperature. Due to the complexity of the obtained invertible systems, the aggregation mechanism of such diblock random copolymers remains to be better understood, especially the effect of the relative lengths of hydrophilic and hydrophobic segments on the aggregate morphology and the inversion process. In this work, we address this problem by changing the ratio of block lengths while keeping the block composition constant to explore the possibility of tuning the self-assembly behavior of dually stimuli-responsive diblock random copolymers, since the stimuli-induced inversion of the aggregates may be interesting for controlled loading and release applications.[29]

4.2 Experimental

4.2.1 Materials

2,2'-Azobisisobutyronitrile (AIBN, from Eastman Kodak) was recrystallized from methanol. Acryloyl chloride, ethylamine (70 % aqueous solution) and n-propylamine were purchased from Aldrich, and were used without further purification. 2-(Diethylamino)ethyl methacrylate (DEAEMA, from Aldrich) was vacuum-distilled prior to use. Previously reported procedures were followed in the preparation of the monomers N-n-propylacrylamide (nPA) and N-ethylacrylamide (EA)[30] and the chain transfer agent (CTA)3-(benzylsulfanylthiocarbonylsulfanyl)propionic acid (BPA).[31] Anhydrous and oxygen-free tetrahydrofuran (THF) was obtained by passing the solvent through columns packed with activated alumina and supported copper catalyst (Glass Contour, Irvine, CA). Water was purified using a Millipore Milli-Q system.

4.2.2 Polymer synthesis

A previously reported method[28] was used to prepare diblock random copolymers with the same monomer ratios but different chain lengths. The first block, poly(nPA_{28}-*co*-$DEAEMA_7$), with a molar ratio of nPA:DEAEMA = 4:1 was synthesized with a molar ratio of 200:1:0.1 for the reaction mixture of [monomer]:[BPA]:[AIBN] during 60 min reaction time. The resulting random copolymer poly($nPA_{0.8}$-*co*-$DEAEMA_{0.2}$)-CTA was then chain-extended by RAFT copolymerization to provide another block with the same composition nPA : EA = 8:2 but different chain lengths. The first (P1) has nearly the same block length, poly(nPA_{28}-*co*-$DEAEMA_7$)-*block*-poly(nPA_{29}-*co*-EA_7), obtained from a reaction mixture of [monomer]:[macro-CTA]:[AIBN] with molar ratio of 200:1:0.1 during 90 min, and the second (P2) has a longer second block, poly(nPA_{28}-*co*-$DEAEMA_7$)-*block*-poly(nPA_{70}-*co*-EA_{18}), with a reactant molar ratio [monomer]:[macro-CTA]:[AIBN] of 400:1:0.1 after 4 h.

4.2.3 Polymer characterization

Molar masses and polydispersity indices (PDI) of the polymers were determined by size exclusion chromatography (SEC) on a Waters 1525 system working with two Waters Styragel columns and a refractive index detector (Waters 2410). *N,N*-dimethylformamide (DMF) containing 0.01 M LiBr was used as the mobile phase at 50 °C with a flow rate of 1 mL/min. Poly(methyl methacrylate) standards were used for the molar mass calibration. The NMR spectra of the polymers were recorded on a Bruker AV-400 NMR spectrometer operating at 400 MHz for protons in deuterated chloroform ($CDCl_3$).

The formation of the polymer aggregates was studied by dynamic light scattering (DLS) conducted on a Malvern Zetasizer instrument (Nano ZS) equipped with a 4 mW He-Ne 633 nm laser. All solutions were prepared at a concentration of 0.05 mg/mL in pure Milli-Q water and dust was removed by filtering through 0.22-μm Millipore filters. Measurements were conducted in a backscattering (173°) mode. Intensity-weighted hydrodynamic diameter (D_h) values were obtained as a function of temperature with a heating rate of ca. 0.1 °C/min.

The cloud points (CPs) of the polymers in aqueous solutions were determined from optical transmittance measured on a Cary 300 Bio UV-vis spectrophotometer with a Cary

temperature controller in the wavelength range of 260-500 nm. Polymer solutions in deionized water (0.05 mg/mL) were continuously heated at a rate of 0.3 °C/min over different temperature ranges. The cloud point (CP) was taken as the middle point between the onset and the offset of abrupt change in the transmittance curve as a function of temperature.

Transmission electron microscopy (TEM) was performed on a FEI Tecnai 12 TEM at 120 kV, equipped with AMT XR80C CCD camera system. Aqueous solutions of the copolymers (0.05 mg/mL) were heated with a Cary temperature controller. The solution was deposited on copper grids (300 mesh, Carbon Type-B, Ted Pella, Inc.) at a desired temperature and rapidly frozen in liquid nitrogen. The samples were lyophilized and kept under vacuum until use.

Atomic force microscopy (AFM) images were acquired in air at room temperature using tapping mode at a scan rate of 1 Hz (Digital Instruments Dimension 3100 microscope, Santa Barbara, CA). All images were acquired with a medium tip oscillation damping (20−30%). The samples were analyzed in the dried state via drop deposition of the 0.05 mg/mL aqueous solution of the polymer onto a mica surface at a desired temperature followed by lyophilization.

4.3 Results and discussion

4.3.1 Preparation of diblock random copolymers

The SEC chromatograms of the macro-CTA of the first block and the two final block copolymers are shown in Figure 4.1, demonstrating the livingness of the block copolymerization. The conversions of the polymerizations were kept low (25%) to avoid the presence of dead chains, assuring the living character of macro-CTA and relatively low polydispersity of final block copolymers. The monomer compositions of mono- and diblock copolymers were calculated from ^{1}H NMR results, as described earlier.[28] The final compositions of the blocks were close to the initial monomer ratio in the feed, and the statistical nature of the macro-CTA random copolymer composed of acrylamide (nPA) and methacrylate (DEAEMA) monomers, despite their different reactivities, was assumed on

the basis of frequent sampling of the reaction mixture and high reproducibility of the polymerizations,[28] even though the possible formation of comonomer gradient[32, 33] cannot be ruled out. The results of the block copolymerizations are summarized in Table 4.1.
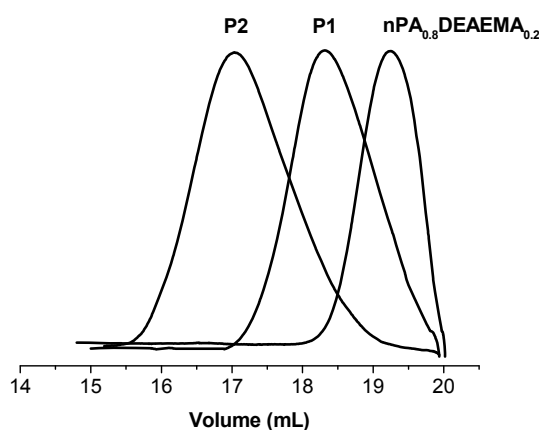
Figure 4.1 SEC chromatograms of P(nPA$_{0.8}$DEAEMA$_{0.2}$) (macro-CTA), P1 and P2 in DMF. Solvent signals appearing at elution volume ~20 mL are excluded.

Table 4.1. Structural properties of mono- and diblock random copolymers.

Entry	P(nPA$_{0.8}$-co-DEAEMA$_{0.2}$)		P(nPA$_{0.8}$-co-DEAEMA$_{0.2}$)-b-P(nPA$_{0.8}$-co-EA$_{0.2}$)			
	M$_n$, 1st block^a	PDI^a	M$_n$, 2nd block^b	M$_n$, total^a	PDI^a	L (nm)^c
P1	4,800	1.15	4,000	8,800	1.21	13.3
P2	4,800	1.15	12,100	16,900	1.30	20.4

^{a}Determined by SEC in DMF against poly(methyl methacrylate) standards. ^{b}Calculated from SEC results. ^{c}Contour length (L): the theoretical maximum length of the extended block copolymer polymer chain.

4.3.2 Thermo-responsiveness in aqueous solutions

We have previously shown that the thermo- and pH-responsiveness of the blocks can be adjusted according to their composition.[26, 28] It was shown that the CPs of P(nPA$_{0.8}$-co-DEAEMA$_{0.2}$) copolymer at pH 7 and 10 are 52 and 13 °C, respectively,[28] although the CP slightly changes after addition of the second block. The pH-independent CP of P(nPA$_{0.8}$-co-

EA$_{0.2}$) was found to be 33 °C.[26] In general, a higher fraction of the more hydrophobic comonomer (nPA) leads to a lower cloud point, while the protonation of DEAEMA moieties upon decreasing pH makes the dually stimuli-responsive block more hydrophilic, thus raising its cloud point. The relative block length is known to influence the morphologies of self-assembled structures, and the phase transition temperatures of the individual blocks in a dually-responsive block copolymer are interdependent.[16, 22, 26, 28] In this work, the length of the dually responsive P(nPA$_{0.8}$-*co*-DEAEMA$_{0.2}$) block is constant while the length of the thermo-responsive P(nPA$_{0.8}$-*co*-EA$_{0.2}$) block is varied. Therefore, the degree of protonation for the P(nPA$_{0.8}$-*co*-DEAEMA$_{0.2}$) block is expected to be the same for both P1 and P2 in the solutions.

Figure 4.2 shows the transmittance curves of dilute (0.05 mg/mL) aqueous solutions of P1 and P2 upon heating at pH 7 and 10. When observed at 500 nm, a reduction in transmittance starting at 29 °C is observed for the solutions of both P1 and P2 at pH 7 (Figures 4.2A and 4.2B). This transition corresponds to the cloud point of the more hydrophobic second block (CP1) at pH 7, poly(nPA$_{29}$-*co*-EA$_7$) for P1 and poly(nPA$_{70}$-*co*-EA$_{18}$) for P2; the longer block has a slightly lower CP1 (Table 4.2), obviously an effect of the molar mass of the block. At pH 7, the poly(nPA$_{28}$-*co*-DEAEMA$_7$) block is partially protonated and thus more hydrophilic, but a clear transition in transmittance (CP2) can be observed corresponding to its collapse which results in the aggregation of the particles. This transition starts at 51 °C for P1 (Figure 4.2A) and 49 °C for P2 (Figure 4.2B), showing that the longer hydrophobic block of P2 has a somewhat stronger effect on the collapse of the partially protonated first block at pH 7. The second transition of P1 with block ratio of 1 : 0.83 (Table 4.1) is close to the value reported earlier for the diblock random copolymer with the same monomer composition and similar block ratio, 1:1.25 (52 °C, P3 in Table 4.2).
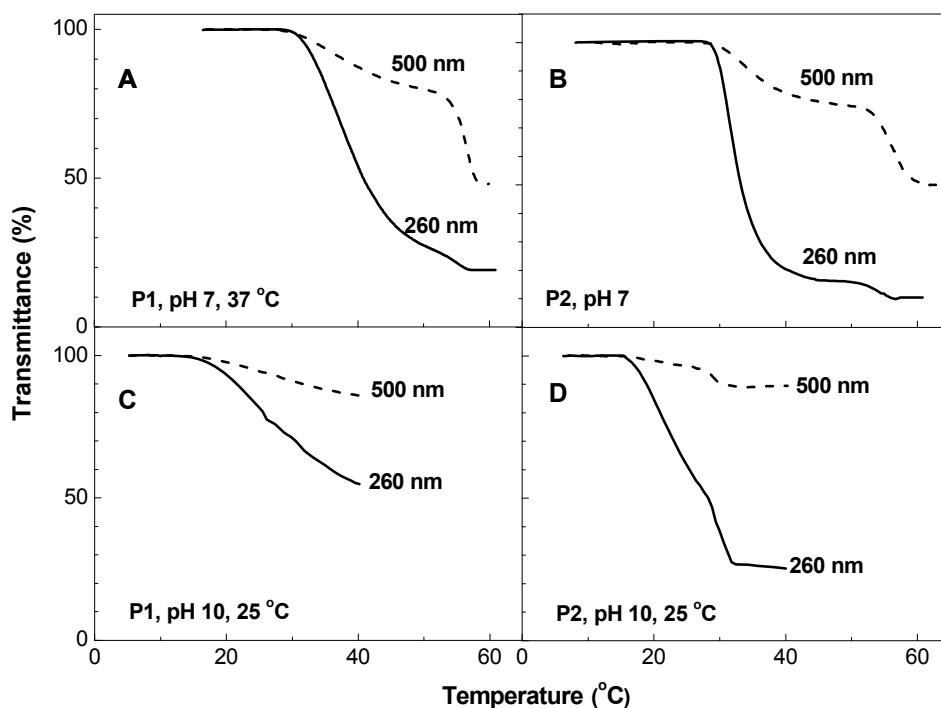
Figure 4.2 Dual stimuli-responsive behavior observed for 0.05 mg/mL aqueous solutions of (A) P1 at pH 7, (B) P2 at pH 7, (C) P1 at pH 10, and (D) P2 at pH 10 measured by UV-vis transmittance at 2 different wavelengths at a heating rate of 0.3 °C/min. A two-step transition is observed in most of the curves.

At pH 10, the onset of the first transition (CP1) is observed at 14 °C, as shown in Figure 4.2C and 2D for both P1 and P2. The poly(nPA$_{28}$-*co*-DEAEMA$_7$) block is now in its deprotonated form, making it the more hydrophobic block with a lower cloud point. The shifts in transmittance at pH 10 are less pronounced than at pH 7, making the determination of the exact middle points of the transitions and the onset temperature of CP2 for P2 more difficult. The relatively short poly(nPA$_{29}$-*co*-EA$_7$) block in P1 does not show a clear change in the transmittance to yield a CP2 (Figure 4.2C), while the transition for longer poly(nPA$_{70}$-*co*-EA$_{18}$) in P2 with a block ratio 1:2.25 starts at 28 °C (Figure 4.2D). However, a marked increase of the D$_h$ for both P1 and P2 was observed at CP1 and CP2 in the DLS measurements at pH 10 (Figure 4.3B) similar to the observation by Weiss *et al.*[15]

The strong wavelength dependence of scattering ($\sim \lambda^{-4}$) is responsible for the larger change in transmittance at a shorter wavelength (260 nm) in all the graphs of Figure 4.2. All these thermally-induced transitions are reversible, and clear aggregate-free solutions were obtained by cooling the solutions below the first cloud points.

Table 4.2. The cloud points of the diblock random copolymers. Values measured by UV-vis transmittance at 500 nm.

		CP1 (^{o}C)[a]		CP2 (^{o}C)[a]		M_n (g/mol)[b]	
		Onset	Middle	Onset	Middle	1st block	2nd block
	P1	29	38	51	56	4,000	4,800
pH 7	P2	28	32	49	55	12,100	4,800
	P3[c]	33	40	53	55	8,100	6,500
	P1	14	25	-	-	4,800	4,000
pH 10	P2	14	21	28	30	4,800	12,100
	P3[c]	16	18	23	31	6,500	8,100

[a]The two values correspond to the 50% decrease in transmittance between the onset and the offset of the transmittance curves observed at 500 nm. [b]Here, the 1st and 2nd blocks under the M_n column correspond to the 1st and 2nd blocks to aggregate, showing CP1 and CP2 at each pH, respectively. For example, the 1st block at pH 7 and 10 refers to P(nPA$_{0.8}$-co-EA$_{0.2}$) and P(nPA$_{0.8}$-co-DEAEMA$_{0.2}$), respectively. [c]P3; poly(nPA$_{48}$-co-DEAEMA$_{12}$)-$block$-(nPA$_{43}$-co-EA$_{11}$) prepared in our previous work.[28]

4.3.3 Self-assembly of diblock random copolymers.

The evolution of the mean hydrodynamic diameter (D_h) of the polymers in water at a concentration of 0.05 mg/mL was followed as a function of temperature at pH 7 and 10, and the results are shown in Figure 4.3. The pH- and temperature-dependent self-assembly of block random copolymers was also visualized by TEM and AFM of freeze-dried solutions. At pH 7 and below 27 ^{o}C, the solutions consist mostly of molecularly dissolved polymer chains (Figure 4.3A). However, the size distributions for both P1 and P2 were bimodal (Figures 4.S2A and 4.S2B) due to the presence of a small fraction of loose aggregates arising from the interaction between the hydrophobic moieties,[34] which are in a

fast exchange equilibrium with single chains.[35] The polymer chains start to self-assemble with rising temperature, and the more hydrophobic poly(nPA$_{29}$-*co*-EA$_7$) block in P1 and poly(nPA$_{70}$-*co*-EA$_{18}$) in P2 undergo a phase transition. Observed by DLS, above the first cloud point of P1, the size of the aggregates remains at ~170 nm up to 54 $^{\circ}$C (range I in Figure 4.3A). This size is larger than the contour length of the polymer would suggest for a normal radius of simple micelles or star-like aggregates (13.3 nm, Table 4.1). TEM (Figure 4.4A) and AFM (Figure 4.5A) images of a freeze-dried sample of P1 at pH 7 and 37 °C (Table 4.3) reveal the vesicular morphology and spherical shape of the aggregates, where the membrane inner layer should consist of the more hydrophobic P(nPA$_{0.8}$-*co*-EA$_{0.2}$) block. Raising the temperature above 52 $^{\circ}$C induces an increase in D$_h$ to ~230 nm (stage II) corresponding to another step of thermoresponsive aggregates.
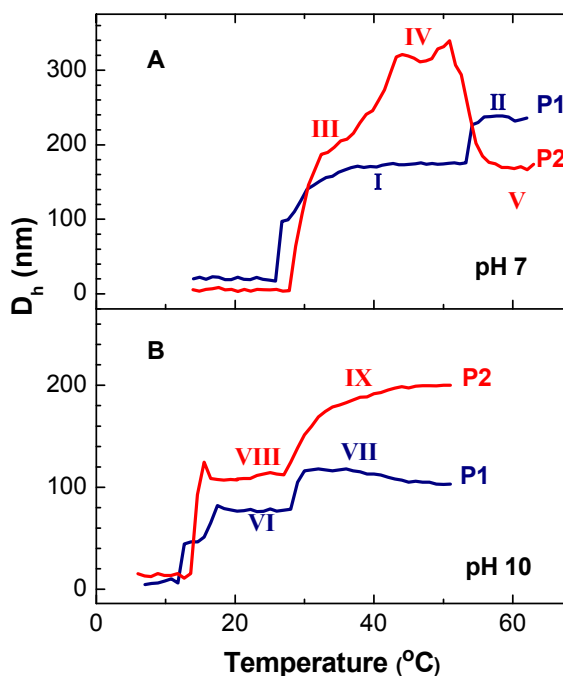
Figure 4.3. Temperature dependence of the mean hydrodynamic diameter (D$_h$) obtained by dynamic light scattering for 0.05 mg/mL aqueous solution of P1 and P2 at (A) pH 7 and (B) pH 10.
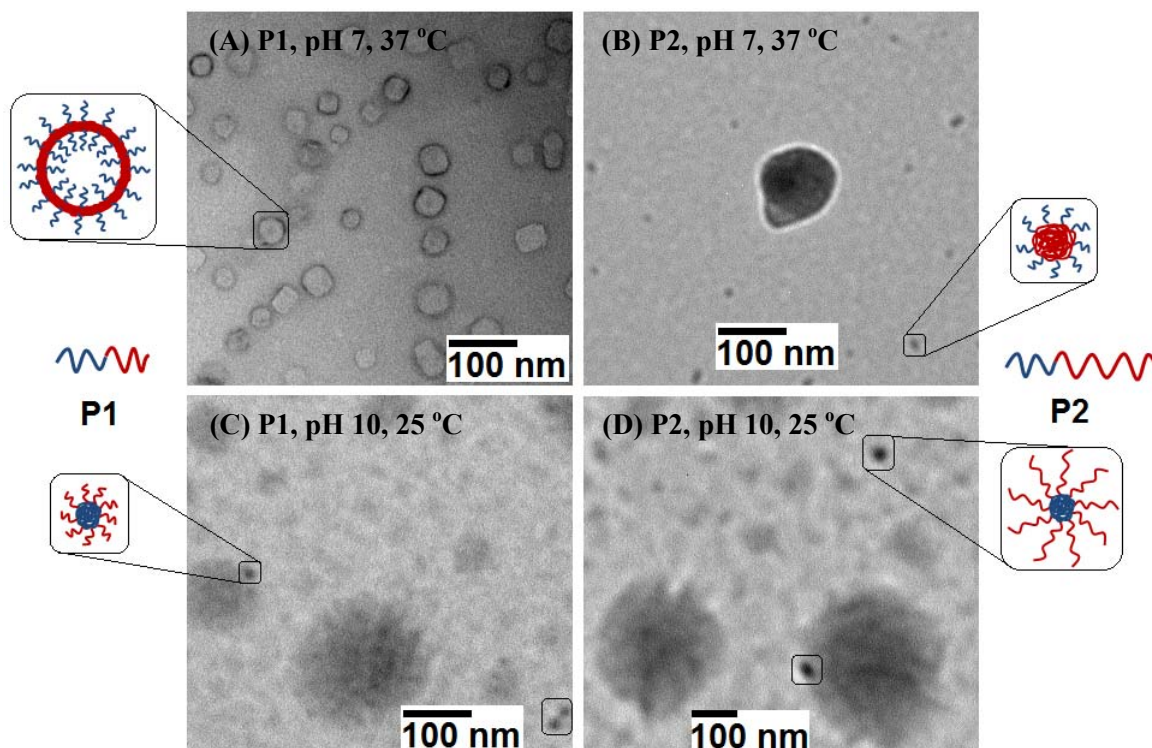
Figure 4.4. TEM images of 0.05 mg/mL aqueous solutions deposited on copper grids for (A) P1 at pH 7 and 37 °C, (B) P2 at pH 7 and 37 °C, (C) P1 at pH 10 and 25 °C, and (D) P2 at pH 10 and 25 °C. The blue and red segments in the insets correspond to poly(nPA$_{0.8}$-*co*-DEAEMA$_{0.2}$) and poly(nPA$_{0.8}$-*co*-EA$_{0.2}$), respectively.

Table 4.3. Mean diameters of self-assemblies (in nm) measured by different methods for the aqueous solutions of P1 and P2 at pH 7 and 10.

condition				CP1 < T1 < CP2			CP2 < T2	
pH	T1 (°C)	T2 (°C)		DLS[a]	AFM[b]	TEM[b]	DLS[a]	AFM[b]
7	37	55	P1	167	75	48 (33-67)	230	138
			P2	241	65	26 (18-168)	170	125
10	25	37	P1	76	88	77 (21-212)	118	104
			P2	107	70	65 (21-442)	186	73

[a]Intensity-weighted mean hydrodynamic diameter (D$_h$) in 0.05 mg/mL aqueous solution. [b]Number-averaged mean diameter of dried aggregates (the size range is given in the brackets). Larger-sized aggregates are clusters of several micelles.

The behavior of P2 at pH 7 above the CP1 is quite different from that of P1. Increasing the temperature above 28 $^{\circ}$C results in a mean hydrodynamic diameter of ~190 nm, measured by DLS (point III in Figure 4.3A). Again, the size of the aggregates is larger than the contour length of P2 (20.4 nm) corresponding to the size of simple micelles (Table 4.1). Unlike P1, there is no evidence for vesicle formation in the TEM images of P2 (Figure 4.4B). However, single micelles with collapsed poly(nPA$_{70}$-co-EA$_{18}$) core were observed by TEM (Figure 4.4B) and AFM (Figure 4.5B) at 37 $^{\circ}$C. Large aggregates (up to 168 nm, Table 4.3) were also observed by TEM for P1 which seem to be clusters of micelles. The aggregates grow to 315 nm (point IV in Figure 4.3A, AFM images in Figure 4.S1) at higher temperatures. The large poly(nPA$_{70}$-co-EA$_{18}$) core may not be sufficiently stabilized by the relatively short hydrophilic poly(nPA$_{28}$-co-DEAEMA$_7$) blocks, similar to the observation by Weiss et $al.$[15] for amphiphilic diblock copolymers. Further heating to 55 °C (Table 4.3) leads to the dehydration of the more hydrophilic block and the collapse of the aggregates, as indicated by a decrease in D$_h$ (stage V in Figure 4.3A). The mean sizes of the aggregates estimated by the different methods for P1 and P2 below and above CP2 at pH 7 are listed in Table 4.3. The mean diameters obtained by AFM and TEM are the average of at least 50 particles. The corona of the particles are charged and highly hydrated at pH 7, resulting in large hydrodynamic diameters obtained by DLS comparing to those by TEM in the dried state.

Both P1 and P2 show bimodal size distributions in the DLS measurements (Figures 4.S2C and D) at pH 10 below the CP1 of the more hydrophobic block, which is now the deprotonated poly(nPA$_{28}$-co-DEAEMA$_7$). P1 shows an increase in particle size at 12 $^{\circ}$C, while P2 shows the same increase starting at a slightly higher temperature (14 $^{\circ}$C). This small difference may be attributed to the presence of a longer neighboring P(nPA$_{0.8}$-co-EA$_{0.2}$) block in P2 (poly(nPA$_{70}$-co-EA$_{18}$)). Both polymers show two transitions in Figure 4.3B with a plateau between CP1 and CP2 (30 $^{\circ}$C). The shorter hydrophilic block in P1 results in a smaller mean hydrodynamic diameter of the aggregates at 25 $^{\circ}$C (76 nm, point VI in Figure 4.3B) than in the case of P2 (107 nm, point VIII in Figure 4.3B). On the basis of TEM (Figures 4.4C and D) and AFM (Figures 4.5C and D) images, small micelles with collapsed poly(nPA$_{28}$-co-DEAEMA$_7$) core were observed together with large aggregates of the micelles for both P1 and P2 at 25 $^{\circ}$C (Table 4.3). In TEM images also the large

aggregates of P1 have smaller diameters than P2. On the other hand, the longer hydrophilic block in P2 at pH 10 results in more stable micelles. Therefore, P2 solution has a larger population of small micelles than P2, which results in lower number-averaged mean diameter obtained by TEM (Table 4.3). Increasing the temperature to 37 °C (Table 4.3), above CP2 of both P1 and P2, leads to the dehydration and collapse of poly(nPA$_{0.8}$-co-EA$_{0.2}$) block accompanied by further aggregation resulting in an increase in particle size corresponding to stages VII and IX in Figure 4.3B for P1 and P2, respectively. This is also observed in the AFM images of the aggregates at 37 °C (Figure 4.S3). The mean sizes of aggregates estimated by the different methods for P1 and P2 below and above the CP2 at pH 10 are listed in Table 4.3. As expected, larger and less regular aggregates are obtained above the CP2 for P2 with a longer corona block, similar to the results of Laschewsky and coworkers.[15] While P2 continued to aggregate with increasing temperature, P1 shows a slight decrease in D$_h$ upon further heating. This difference may arise from the different lengths of the corona blocks.
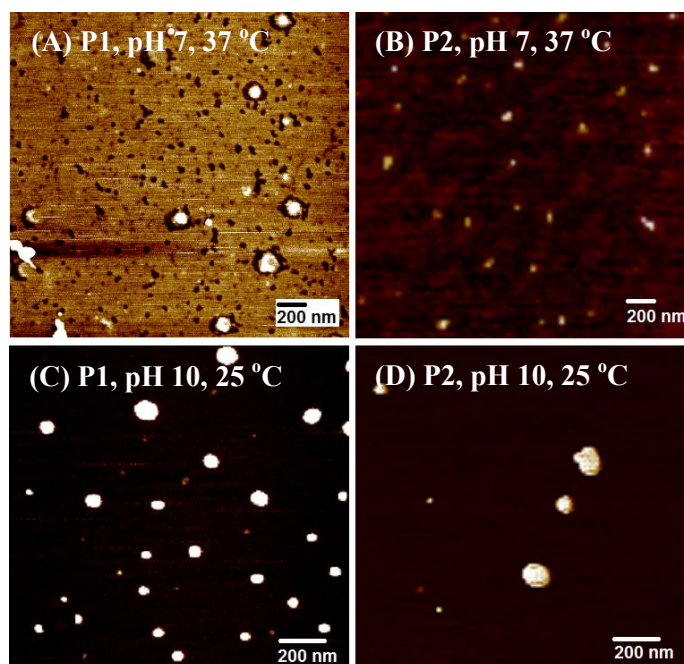
Figure 4.5. AFM images of aqueous solutions (0.05 mg/mL) of P1 and P2 above their CP1, deposited on mica. (A) P1 at pH 7 and 37 °C, (B) P2 at pH 7 and 37 °C, (C) P1 at pH 10 and 25 °C, and (D) P2 at pH 10 and 25 °C.

P1 is a nearly symmetric block copolymer, where the ratio of poly(nPA$_{28}$-*co*-DEAEMA$_7$) and poly(nPA$_{29}$-*co*-EA$_7$) blocks is 53:47 wt%, and with this composition, either vesicles or micelles may be formed as reported in the literature on stimuli-responsive block copolymers.[16, 22, 26, 28] When the temperature of its solution at pH 7 is raised to 37 ^{o}C, the polymer chains self-assemble to form vesicles with poly(nPA$_{29}$-*co*-EA$_7$) and poly(nPA$_{28}$-*co*-DEAEMA$_7$) blocks as the inner and outer layers of the membrane, respectively, as depicted in Scheme 4.1A. Heating above the CP of the poly(nPA$_{28}$-*co*-DEAEMA$_7$) block leads to aggregation, and large clusters of spherical aggregates can be observed by AFM (Figures 4.S3A and B). On the other hand, increasing the pH of the solution of P1 up to 10 at a constant temperature of 25 ^{o}C results in the formation of spherical micelles with a poly(nPA$_{28}$-*co*-DEAEMA$_7$) core and a poly(nPA$_{29}$-*co*-EA$_7$) corona, which aggregate further when the temperature rises above the CP of the poly(nPA$_{29}$-*co*-EA$_7$) block. Interestingly, vesicles were obtained in our previous study[28] under the same conditions for P(nPA$_{0.8}$-*co*-DEAEMA$_{0.2}$)-*b*-P(nPA$_{0.8}$-*co*-EA$_{0.2}$) with a slightly different block ratio, 45:55 wt%, and longer blocks (6500 and 8100 g/mol vs. 4800 and 4000 g/mol of the current work). This suggests that the composition of the block random copolymer may be quite critical for the self-assembly process, and the compositions close to 50:50 wt% could be on the threshold of different aggregate morphologies for such a polymer system.

The ratio of poly(nPA$_{28}$-*co*-DEAEMA$_7$) and poly(nPA$_{70}$-*co*-EA$_{18}$) blocks in P2 is 31.5:68.5 wt%. This polymer forms invertible micelles at pH 7 and 10 above the CP of the more hydrophobic block (CP1), where the core and the shell blocks may be switched according to the pH of the solution. Micelles at pH 7 with a partially protonated poly(nPA$_{28}$-*co*-DEAEMA$_7$) shell are more stable than their inverted counterparts at pH 10. Therefore, single micelles contribute to the majority of the particles formed by P2 at pH 7 (Figure 4.4B), while the solution at pH 10 mostly contains bigger aggregates of the micelles (Figure 4.4D). However, because of the much longer poly(nPA$_{70}$-*co*-EA$_{18}$) block in the core, further aggregation was observed for the micelles with poly(nPA$_{28}$-*co*-DEAEMA$_7$) shell, and large clusters of the aggregates are observed for P2 at pH 7 and 45 °C (Scheme 4.1B), which collapse when heated above the CP of the poly(nPA$_{28}$-*co*-DEAEMA$_7$) block (55 °C in Scheme 4.1B). The morphological changes of P1 and P2 are

different from those observed for pH- and temperature-responsive poly(*N,N*-diethylaminoethyl methacrylate)-*block*-poly(*N*-isopropylacrylamide) (PDEAEMA-*b*-PNIPAM), which forms spherical micelles at a block ratio of 47:53 wt% at high pH or high temperature, but shows a micelle-to-vesicle transition at the composition of 29:71 wt%.[16] In that case, each of the blocks responds to a different stimulus, while introducing a dually-responsive block into a thermo-responsive block brings about double thermo-sensitivity and, at the same time, makes the aggregation behavior of our system more complex, as indicated by the visually observable polydispersity and large sizes of the aggregates. Therefore, Scheme 4.1 represents only a simplified picture of the self-assembly of the real system.
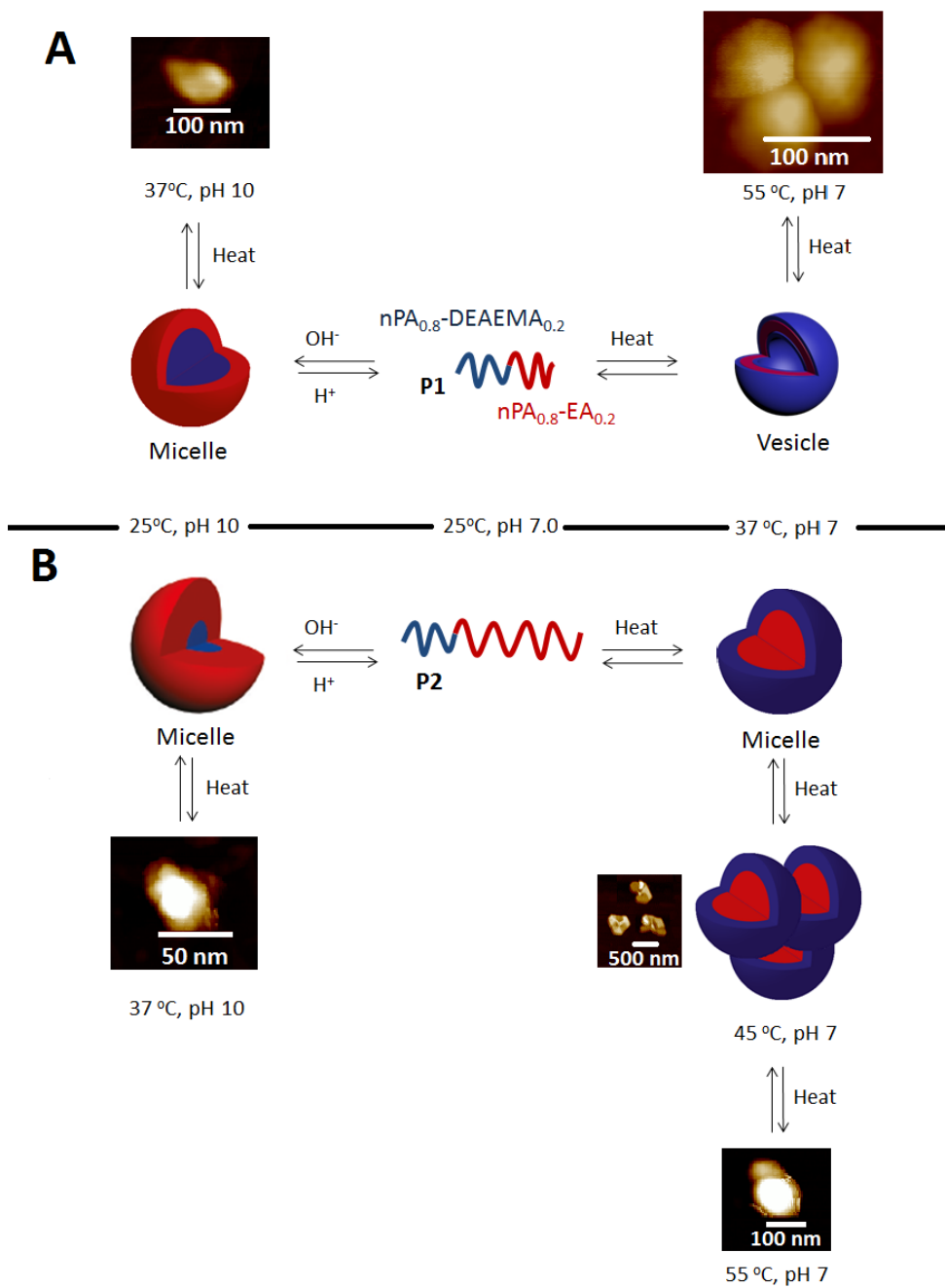
Scheme 4.1. Invertible micellization behavior of (A) P1, above, and (B) P2, below, in water by changing the temperature and pH. The representative images were taken from larger AFM images.

4.4 Conclusion

Dually-responsive diblock random copolymers are capable of forming either micells or vesicles in aqueous solutions. The change in the relative hydrophilicity of the blocks results in inverted structures, and may switch the self-assembled morphology between vesicles and micelles. In general, molecularly dissolved polymer chains together with loose aggregates co-exist at a lower temperature, but larger aggregates form above the cloud point of the copolymer. In the case of the symmetric diblock copolymer P1 of similar block lengths, vesicles may form during heating, while micelles are obtained together with micellar aggregates by raising the pH. The process is accompanied by a switch of the more hydrophobic block of the copolymer. Upon changing the relative lengths of the blocks as in the case of P2 with a much longer second block, micelles with a small fraction of micellar aggregates form under identical conditions while the core and shell of the micelles switch when the stimuli (temperature or pH changes) are applied. The ease in the adjustment of the composition and block length in the preparation of such copolymers provides the possibility of making a variety of copolymers which may form different types of aggregates in aqueous solutions and may switch or change their assembled structures under controllable conditions. Switching between vesicles and micelles may provide a convenient way for fast release of encapsulated reagents. The positively-charged surface of the vesicles in the case of the protonated form of the polymer may interact with biological membranes via electrostatic interactions destined for biochemical applications.

4.5 Acknowledgments

4.5 Supporting information
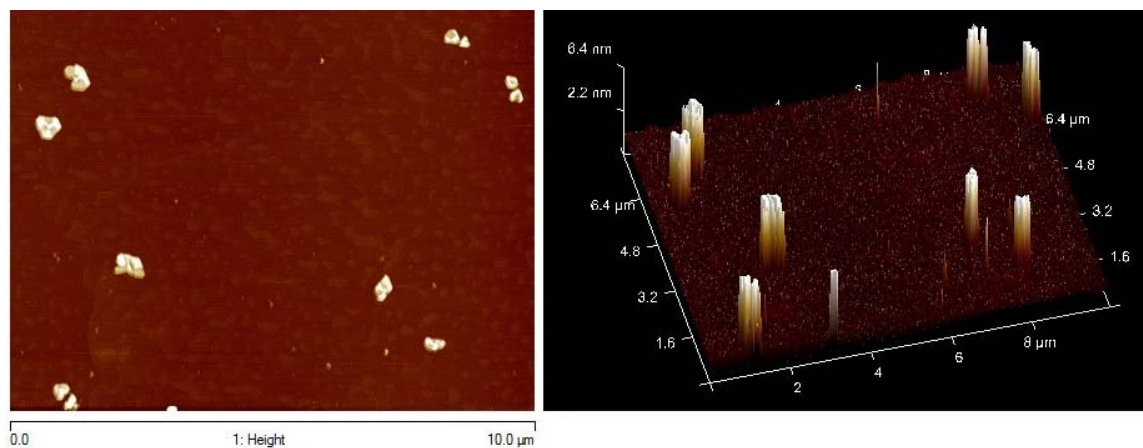
Figure 4.S1 AFM image of P2 on mica at pH 7 and 47 °C corresponding to point IV in Figure 4.3A.
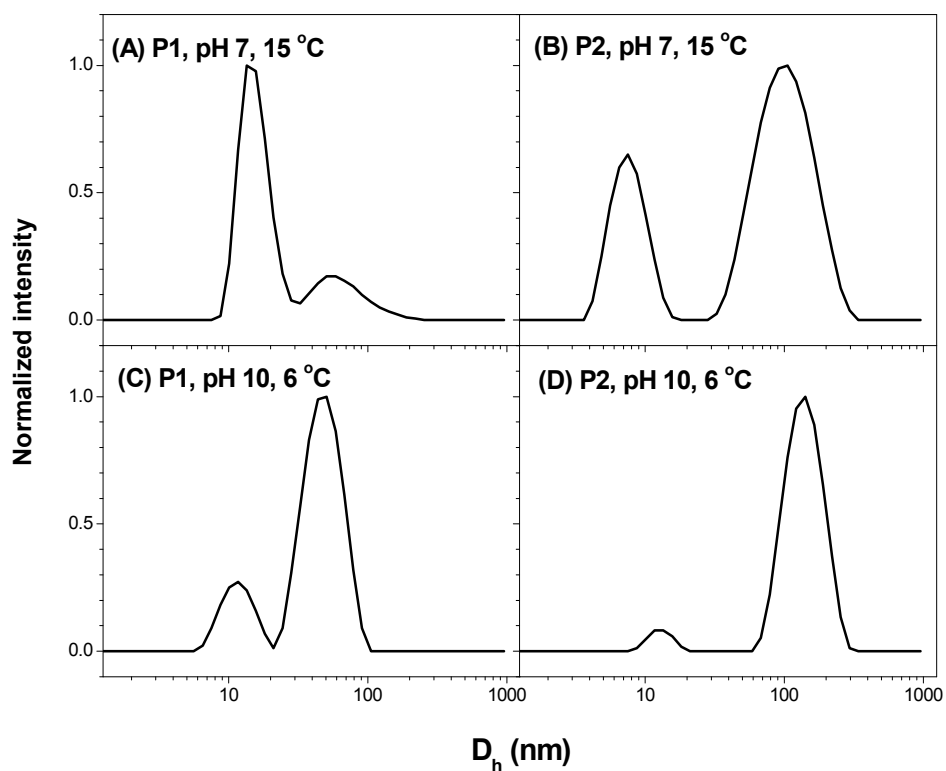
Figure 4.S2. The particle size distributions for 0.05 mg/mL aqueous solutions of (A) P1 at pH 7 and 15 °C, (B) P2 at pH 7 and 15 °C, (C) P1 at pH 10 and 6 °C, and (D) P2 at pH 10 and 6 °C as observed by DLS. The temperature is below the CP1 for both P1 and P2.
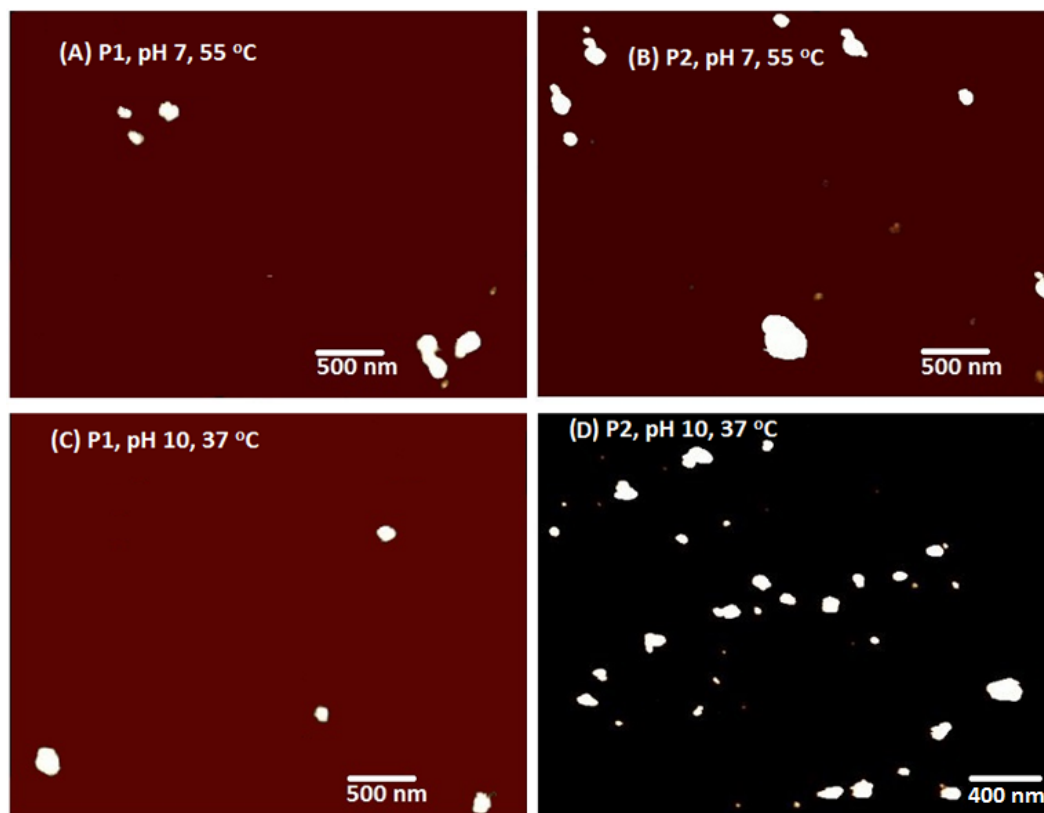
Figure 4.S3. AFM images of 0.05 mg/mL aqueous solutions of P1 and P2 above their CP2, deposited on mica. (A) P1 at pH 7 and 55 °C, (B) P2 at pH 7 and 55 °C, (C) P1 at pH 10 and 37 °C, and (D) P2 at pH 10 and 37 °C.

4.6 References

1.   Cui, H.; Chen, Z.; Zhong, S.; Wooley, K. L.; Pochan, D. J. Block Copolymer Assembly via Kinetic Control. *Science* **2007,** *317* (5838), 647-650.

2.   Riess, G. Micellization of block copolymers. *Prog. Polym. Sci.* **2003,** *28* (7), 1107-1170.

3.   Opsteen, J. A.; Cornelissen, J. J. L. M.; Hest, J. C. M. v. Block copolymer vesicles. *Pure Appl. Chem.* **2004,** *76* (7-8), 1309-1319.

4.   Gohy, J.-F. Block Copolymer Micelles. In *Block Copolymers II*, Abetz, V., Ed.; Springer Berlin Heidelberg, 2005; Vol. 190, pp 65-136.

5.   Holder, S. J.; Sommerdijk, N. A. J. M. New micellar morphologies from amphiphilic block copolymers: disks, toroids and bicontinuous micelles. *Polym. Chem.* **2011,** *2* (5), 1018-1028.

6.   Du, J.; O'Reilly, R. K. Advances and challenges in smart and functional polymer vesicles. *Soft Matter* **2009,** *5* (19), 3544-3561.

7.   Förster, S.; Abetz, V.; Müller, A. E. Polyelectrolyte Block Copolymer Micelles. In *Polyelectrolytes with Defined Molecular Architecture II*, Schmidt, M., Ed.; Springer Berlin Heidelberg, 2004; Vol. 166, pp 173-210.

8.   Discher, D. E.; Eisenberg, A. Polymer Vesicles. *Science* **2002,** *297* (5583), 967-973.

9.   Borisov, O.; Zhulina, E.; Leermakers, F. M.; Müller, A. E. Self-Assembled Structures of Amphiphilic Ionic Block Copolymers: Theory, Self-Consistent Field Modeling and Experiment. In *Self Organized Nanostructures of Amphiphilic Block Copolymers I*, Müller, A. H. E.; Borisov, O., Eds.; Springer Berlin Heidelberg, 2011; Vol. 241, pp 57-129.

10.   Bütün, V.; Billingham, N. C.; Armes, S. P. Unusual Aggregation Behavior of a Novel Tertiary Amine Methacrylate-Based Diblock Copolymer: Formation of Micelles and Reverse Micelles in Aqueous Solution. *J. Am. Chem. Soc.* **1998,** *120* (45), 11818-11819.

11.   Plamper, F. A.; McKee, J. R.; Laukkanen, A.; Nykanen, A.; Walther, A.; Ruokolainen, J.; Aseyev, V.; Tenhu, H. Miktoarm stars of poly(ethylene oxide) and poly(dimethylaminoethyl methacrylate): manipulation of micellization by temperature and light. *Soft Matter* **2009,** *5* (9), 1812-1821.

12.   Liu, S.; Billingham, N. C.; Armes, S. P. A Schizophrenic Water-Soluble Diblock Copolymer. *Angew. Chem. Int. Ed.* **2001,** *40* (12), 2328-2331.

13.   Shih, Y.-J.; Chang, Y.; Deratani, A.; Quemener, D. "Schizophrenic" Hemocompatible Copolymers via Switchable Thermoresponsive Transition of Nonionic/Zwitterionic Block Self-Assembly in Human Blood. *Biomacromolecules* **2012,** *13* (9), 2849-2858.

14.   Xie, D.; Ye, X.; Ding, Y.; Zhang, G.; Zhao, N.; Wu, K.; Cao, Y.; Zhu, X. X. Multistep Thermosensitivity of Poly(*N*-n-propylacrylamide)-block-poly(*N*-isopropylacrylamide)-block-poly(*N,N*-ethylmethylacrylamide) Triblock Terpolymers in Aqueous Solutions As Studied by Static and Dynamic Light Scattering. *Macromolecules* **2009,** *42* (7), 2715-2720.

15.   Weiss, J.; Böttcher, C.; Laschewsky, A. Self-assembly of double thermoresponsive block copolymers end-capped with complementary trimethylsilyl groups. *Soft Matter* **2011,** *7* (2), 483.

16.   Smith, A. E.; Xu, X.; Kirkland-York, S. E.; Savin, D. A.; McCormick, C. L. "Schizophrenic" Self-Assembly of Block Copolymers SynthesizedviaAqueous RAFT Polymerization: From Micelles to Vesicles†† Paper number 143 in a series on Water-Soluble Polymers. *Macromolecules* **2010,** *43* (3), 1210-1217.

17.   Read, E. S.; Armes, S. P. Recent advances in shell cross-linked micelles. *Chem. Commun.* **2007,** (29), 3021-3035.

18.   Voets, I. K.; de Keizer, A.; de Waard, P.; Frederik, P. M.; Bomans, P. H. H.; Schmalz, H.; Walther, A.; King, S. M.; Leermakers, F. A. M.; Cohen Stuart, M. A. Double-Faced Micelles from Water-Soluble Polymers. *Angew. Chem. Int. Ed.* **2006,** *45* (40), 6673-6676.

19.   Venkataraman, S.; Lee, A. L.; Maune, H. T.; Hedrick, J. L.; Prabhu, V. M.; Yang, Y. Y. Formation of Disk- and Stacked-Disk-like Self-Assembled Morphologies from Cholesterol-Functionalized Amphiphilic Polycarbonate Diblock Copolymers. *Macromolecules* **2013,** *46* (12), 4839-4846.

20.   Edmonds, W. F.; Li, Z.; Hillmyer, M. A.; Lodge, T. P. Disk Micelles from Nonionic Coil−Coil Diblock Copolymers. *Macromolecules* **2006,** *39* (13), 4526-4530.

21.   Wang, X.; Guerin, G.; Wang, H.; Wang, Y.; Manners, I.; Winnik, M. A. Cylindrical Block Copolymer Micelles and Co-Micelles of Controlled Length and Architecture. *Science* **2007,** *317* (5838), 644-647.

22.   Pietsch, C.; Mansfeld, U.; Guerrero-Sanchez, C.; Hoeppener, S.; Vollrath, A.; Wagner, M.; Hoogenboom, R.; Saubern, S.; Thang, S. H.; Becer, C. R.; Chiefari, J.;

Schubert, U. S. Thermo-Induced Self-Assembly of Responsive Poly(DMAEMA-*b*-DEGMA) Block Copolymers into Multi- and Unilamellar Vesicles. *Macromolecules* **2012,** *45* (23), 9292-9302.

23.   Luo, L.; Eisenberg, A. Thermodynamic Stabilization Mechanism of Block Copolymer Vesicles. *J. Am. Chem. Soc.* **2001,** *123* (5), 1012-1013.

24.   Yu, K.; Eisenberg, A. Bilayer Morphologies of Self-Assembled Crew-Cut Aggregates of Amphiphilic PS-*b*-PEO Diblock Copolymers in Solution. *Macromolecules* **1998,** *31* (11), 3509-3518.

25.   Chen, Y.; Du, J.; Xiong, M.; Guo, H.; Jinnai, H.; Kaneko, T. Perforated Block Copolymer Vesicles with a Highly Folded Membrane. *Macromolecules* **2007,** *40* (13), 4389-4392.

26.   Savoji, M. T.; Strandman, S.; Zhu, X. X. Block Random Copolymers of *N*-Alkyl-Substituted Acrylamides with Double Thermosensitivity. *Macromolecules* **2012,** *45* (4), 2001-2006.

27.   Kotsuchibashi, Y.; Ebara, M.; Idota, N.; Narain, R.; Aoyagi, T. A 'smart' approach towards the formation of multifunctional nano-assemblies by simple mixing of block copolymers having a common temperature sensitive segment. *Polym. Chem.* **2012,** *3* (5), 1150.

28.   Savoji, M. T.; Strandman, S.; Zhu, X. X. Switchable Vesicles Formed by Diblock Random Copolymers with Tunable pH- and Thermo-Responsiveness. *Langmuir* **2013,** *29* (23), 6823-6832.

29.   Vriezema, D. M.; Comellas Aragonès, M.; Elemans, J. A. A. W.; Cornelissen, J. J. L. M.; Rowan, A. E.; Nolte, R. J. M. Self-Assembled Nanoreactors. *Chem. Rev.* **2005,** *105* (4), 1445-1490.

30.   Shea, K. J.; Stoddard, G. J.; Shavelle, D. M.; Wakui, F.; Choate, R. M. Synthesis and characterization of highly crosslinked poly(acrylamides) and poly(methacrylamides). A new class of macroporous polyamides. *Macromolecules* **1990,** *23* (21), 4497-4507.

31.   Stenzel, M. H.; Davis, T. P.; Fane, A. G. Honeycomb structured porous films prepared from carbohydrate based polymers synthesized via the RAFT process. *J. Mater. Chem.* **2003,** *13* (9).

32.   Park, J.-S.; Kataoka, K. Comprehensive and Accurate Control of Thermosensitivity of Poly(2-alkyl-2-oxazoline)s via Well-Defined Gradient or Random Copolymerization. *Macromolecules* **2007,** *40* (10), 3599-3609.

33.   Xiang, P.; Ye, Z. Alternating, gradient, block, and block–gradient copolymers of ethylene and norbornene by Pd–Diimine-Catalyzed "living" copolymerization. *Journal of Polymer Science Part A: Polym. Chem.* **2013,** *51* (3), 672-686.

34.   Nichifor, M.; Lopes, A.; Carpov, A.; Melo, E. Aggregation in Water of Dextran Hydrophobically Modified with Bile Acids. *Macromolecules* **1999,** *32* (21), 7078-7085.

35.   Yan, J.; Ji, W.; Chen, E.; Li, Z.; Liang, D. Association and Aggregation Behavior of Poly(ethylene oxide)-*b*-Poly (*N*-isopropylacrylamide) in Aqueous Solution. *Macromolecules* **2008,** *41* (13), 4908-4913.

Chapter 5

Conclusions and future work

5.1 General conclusions

Diblock copolymers play an important role in many fields of science and technology. However, there were no publications describing block copolymers that can respond to the external stimuli in a controlled manner when the present research began. All reported materials respond under a fixed condition (temperature and/or pH). The main idea of the present work was to develop a novel diblock polymer in which both blocks can be tuned separately to respond to the external stimuli in a controlled fashion. For the first time, diblock random copolymers for this purpose are introduced in this work. Those polymers benefit from two major modification methods to provide tunable stimuli–responsive polymeric materials with double step responsiveness. Block copolymerization is the first modification method to obtain multi-responsive copolymers.[1] The second method is using random copolymers as the constituent block, which allows for the tuning of the cloud point by adjustment of the comonomer ratio.[2] Here, both modification methods were combined.

5.1.1 Polymer synthesis

Sequential RAFT polymerization was successfully used to make random copolymers and chain extended diblock random copolymers.

To obtain double thermoresponsive diblock random copolymers, poly(nPA$_x$-co-EA$_{1-x}$)-$block$-poly(nPA$_y$-co-EA$_{1-y}$) copolymers were made. They were successfully made by RAFT polymerization with a proper selection of CTA. DMP can serve as a good RAFT agent for nearly statistical polymerization of monosubstituted N-alkylacrylamides, nPA and EA due to their similar activities in RAFT polymerization. Kinetics of the copolymerization and the

composition of the polymers have been investigated to obtain block copolymers with desired properties. The conditions for obtaining copolymers with well-defined structures and narrow molecular weight distributions were developed and optimized.

The same synthetic approach was applied to make diblock random copolymers with both pH- and thermo-responsiveness. Well-defined diblock random copolymers in the form of A_nB_m-b-A_pC_q were prepared using sequential RAFT polymerization, where A, B and C are nPA, DEAEMA, and EA, respectively. Copolymerization of DEAEMA with nPA can induce pH-responsiveness to the "smart" polymer. In this work, it was observed that not only can we make random copolymers with well-defined structure using monosubstituted N-alkylacrylamides (nPA and EA) comonomers, but by choosing an appropriate RAFT polymerization condition we can also prepare random copolymers with desired compositions from methacrylate-based (DEAEMA) and acrylamide-based (nPA) comonomers, despite their different reactivities in free radical polymerization. Combining pH- and temperature-responsive poly(nPA$_{0.8}$-co-DEAEMA$_{0.2}$) and temperature-responsive poly(nPA$_{0.8}$-co-EA$_{0.2}$) random copolymers in a diblock resulted in a system that is responsive to multiple stimuli. It was also found that methacrylate-based DEAEMA must be part of the first synthesized block, because it cannot add to poly(nPA-co-EA)-CTA for chain extension to a diblock.

5.1.2 Solution behavior of the polymers

Tunable cloud points could be obtained by adjusting the comonomer ratio for random copolymers within the temperature range of 20-85 °C. Greater hydrophilic monomer content results in higher temperature at which the random copolymers respond. On the other hand, an appropriate design of both blocks could result in a clear stepwise aggregation of the block copolymer. It was shown in this thesis that by applying two modification methods on the same polymer we were able to tailor the response of each block in a double step responsive system. If the difference in the cloud points of two blocks is at least 15 $^{\circ}$C, it is possible to observe two distinct transition temperatures for the aqueous solution of double thermo-responsive diblock random copolymer made from N-alkyl-substituted acrylamides. In this regard, poly(nPA$_{0.7}$-co-EA$_{0.3}$) with the CP of 37°C (near the physiological temperatures) and poly(nPA$_{0.4}$-co-EA$_{0.6}$) with the CP of 52°C were

selected. Therefore, the diblock copolymer exhibited a two-step phase transition upon heating. Increasing the temperature up to 41 $^{\circ}$C resulted in the collapse of the first block and aggregation of the polymer chains, while further heating to 53 °C induced further clustering and contraction of the shell through the dehydration of the outer block.

Introducing pH-responsiveness to the diblock random copolymer resulted in tunable thermo- and pH-responsive diblock random copolymers that show interesting "schizophrenic" behavior. Combining pH- and thermo-responsive poly(nPA$_{0.8}$-*co*-DEAEMA$_{0.2}$) and temperature-responsive poly(nPA$_{0.8}$-*co*-EA$_{0.2}$) random copolymers in a diblock copolymer results in a switchable system that is responsive to double stimuli. The block copolymers were molecularly dissolved in water at 25 $^{\circ}$C (pH 7), self-assembling to vesicles or micelles with poly(nPA$_{0.8}$-*co*-EA$_{0.2}$) as the hydrophobic core at 37 $^{\circ}$C (pH 7), while the core and corona could be switched at 25 $^{\circ}$C (pH 10). It was observed that block symmetry influences the solubility and the micellization process. In fact, the architecture of the self-assemblies in aqueous solution depends on the chain length of the blocks, resulting in switchable vesicles and micelles. The block copolymer self-assembles to vesicles at 37 $^{\circ}$C (pH 7) and vesicles with the inverted membrane core and the corona at 25 $^{\circ}$C (pH 10) for the block ratio 44:56 wt% for poly(nPA$_{0.8}$-*co*-DEAEMA$_{0.2}$): poly(nPA$_{0.8}$-*co*-EA$_{0.2}$). For the block ratio of 53:47 wt%, vesicles with poly(nPA$_{0.8}$-*co*-EA$_{0.2}$) as the membrane core form at elevated temperature while spherical micelles with poly(nPA$_{0.8}$-*co*-DEAEMA$_{0.2}$) as the hydrophobic core are obtained by increasing the pH. When the block ratio is 31.5:68.5 wt%, by increasing the temperature, spherical micelles are formed with poly(nPA$_{0.8}$-*co*-EA$_{0.2}$) as the core, and by increasing the pH, poly(nPA$_{0.8}$-*co*-DEAEMA$_{0.2}$) is the core of the micelles. In addition, two-step phase transitions, corresponding to the cloud points of the individual blocks, were observed in both alkaline and neutral solutions. The results suggest that even relatively minor changes in block ratios can alter the morphologies of aggregates and the thermo-responsive behavior of the polymers, which emphasizes the importance of controlled syntheses.

5.1.3 Characterization

Several analytical techniques were optimized in this study to determine the solution behavior of diblock random copolymers. Best results were obtained for heating rates

between 0.1 and 0.3 ^{o}C/min and solution concentrations between 0.05 and 1 mg/mL for UV-vis spectroscopy, DLS, and SLS studies. In addition to heating rate and concentration, sample preparation is of importance for AFM and TEM imaging. Lyophilization of a drop of solution at the desired temperature on the preheated substrate allowed for successful AFM and TEM imaging. A variety of techniques, particularly GPC, ^{1}H-NMR, DLS, SLS, zeta potential measurements, as well as the imaging techniques, AFM and TEM, demonstrated successful controlled radical polymerization, tunable thermo- and pH-responsiveness, "schizophrenic" behavior, various morphologies by applying different combinations of stimuli, and the effect of polymer structure on the solution behavior.

5.2 Perspectives of the project

These block random copolymers expand the scope of smart polymers and give the promise of novel materials with tailored stimuli-responsive properties. There may be possible opportunities for fundamental studies on their solution behavior, in addition to potential applications where tuned multi-responsiveness to temperature and/or pH is needed.

5.2.1 Fundamental studies on the aggregation mechanism

Double thermo-responsive diblock random copolymers of pre-determined compositions have been made in this work. In Chapter 2, the same monomers are used for both blocks but of different molar ratios, i.e., nPA:EA ratios of 70:30 and 40:60 for the first and second blocks, respectively. In chapters 3 and 4, the same monomer molar ratio, 80:20, was chosen, but one of the monomers was different in each block, namely, 80:20 nPA:DEAEMA and nPA:EA in the first and second blocks, respectively. In addition, the length of the second block varied from 1 to 2.5 times the molecular weight of the first block. The variation of the polymers afforded a collection of stimuli-responsive copolymers that help to elucidate the mechanisms of the formation of different morphologies of the self-assemblies and provide a better physico-chemical understanding of these complex systems.

The first block in the double stimuli-responsive copolymer consists of both thermo- and pH-responsive monomers (nPA and DEAEMA), while the second block consists of only thermo-responsive monomers (nPA and EA). Incorporation of the pH-responsive monomer in the second block of thermo- and pH-responsive polymer increases further the complexity of this kind of diblock random copolymers. This could be interesting in the context of advanced dual behavior materials.

The copolymers in this thesis consist of mono-substituted *N*-alkylacrylamides, nPA and EA. We had also prepared random copolymers with well-defined structure from a combination of mono- and di-substituted *N*-alkylacrylamides. RAFT copolymerization of *N*-tert-butylacrylamide (tBA) and *N,N*-dimethylacrylamide (DMA) resulted in thermo-responsive copolymers, while PDMA and PtBA homopolymers are soluble and insoluble in water, respectively. Although the random copolymers showed a variable cloud point that depended on the monomer composition, the diblock copolymer obtained from the two random blocks did not show the expected stepwise thermo-responsiveness. Therefore, these results are not discussed in this thesis. Future experiments on the properties of self-assemblies in solution of copolymers with greater differences in structure and composition would be useful in this context.

5.2.2 Potential applications

Application for CO_2 sensor. Thermo- and CO_2-responsive random copolymers made from NIPAM and DMAEMA (or DEAEMA) were reported by Han *et al.*[3] CO_2 bubbling in these polymer solutions has the same effect as decreasing the pH and results in protonation of the pendant tertiary amine in DMAEMA (or DEAEMA). Therefore, CO_2 bubbling makes the polymer chains more hydrophilic and shifts the LCST of the polymer to a higher temperature. Inversely, purging an inert gas such as N_2 or Ar in the polymer solution removes CO_2 and results in deprotonation of the amine groups which shifts the LCST of the polymer solution to a lower temperature. Figure 5.1 shows the effect of CO_2 bubbling for one minute in the 0.5 mg/mL aqueous solution of poly(nPA$_{28}$-*co*-DEAEMA$_7$) at room temperature. The opaque solution in Figure 5.1A shows that poly(nPA$_{28}$-*co*-DEAEMA$_7$) is insoluble in water at room temperature (cloud point of 14 ^{o}C). However, protonation of the

DEAEMA amine groups caused by CO_2 bubbling forms a transparent solution of dissolved polymer (Figure 5.1B).
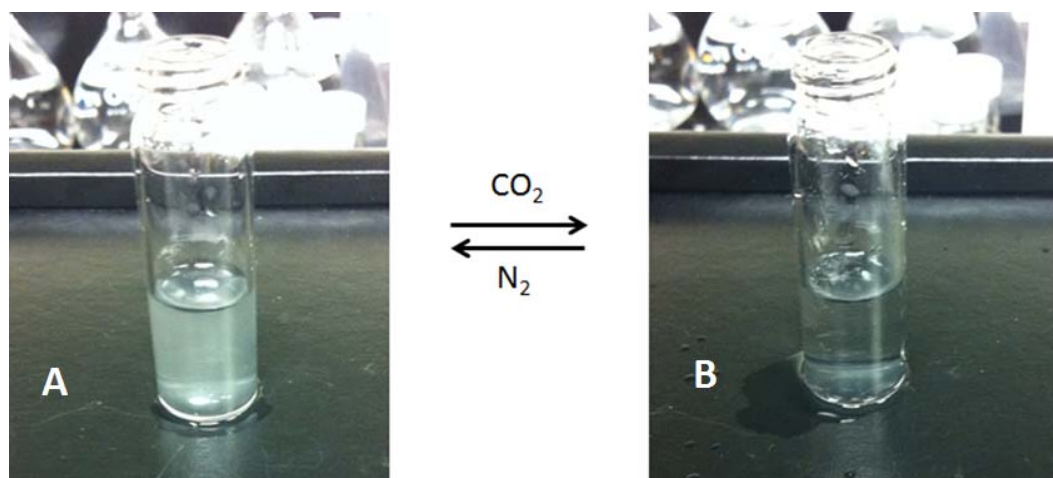
Figure 5.1 Photographs of the 0.5 mg/mL aqueous solution of poly(nPA$_{28}$-*co*-DEAEMA$_7$) at room temperature after passing CO_2 or N_2 through the solution.

Application for separation. Self-assembly properties of block copolymers provide a good opportunity for good separation performances. Liu *et al.*[4] separated basic proteins via physical coating of poly(ethylene oxide)-*block*-poly(4-vinylpyridine) in capillary zone electrophoresis. By using diblock random copolymers, we can design desired compositions of random copolymers that enable the polymer to be in the collapsed or swollen state in solution at desired temperatures and pH. Moreover, double step responsiveness can be used in microphase separation techniques. Hydrophobic agents can be encapsulated in the hydrophobic core of core-shell micelles stabilized by a hydrophilic corona formed above the first transition temperature (T1). Separation will be completed by insoluble aggregates formed by heating the solution to the second transition temperature (T2). The proposed mechanism for separation is shown in Figure 5.2.
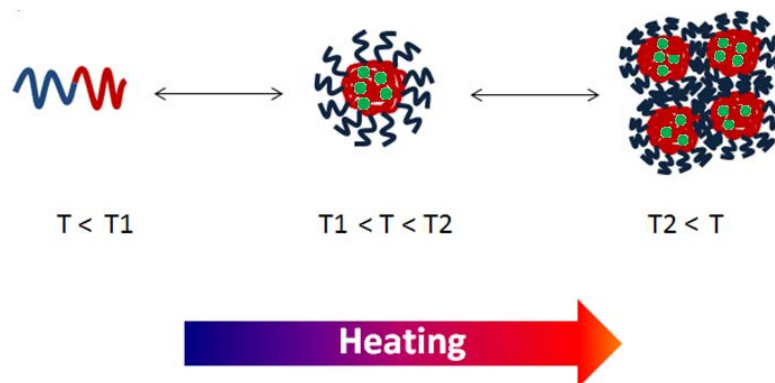
Figure 5.2 The proposed mechanism for separation of the hydrophobic agent (green circles) by two step transition of the double thermoresponsive polymer.

Surface modification. The properties of the thin films or nanoparticles can be altered by stimuli-responsive polymers grafted on their surface. For example, Zhang *et al.*[5] reported an "on-off" catalytic behavior for gold nanoparticles coated by poly(2-diethylaminoethyl methacrylate) (PDEAEMA-AuNPs). CO_2 purging in the solution resulted in the dissolved and extended polymer chains on the AuNPs surface and promoted the catalytic properties of the AuNPs for the reduction of 4-nitrophenol into 4-aminophenol. On the other hand, the removal of CO_2 by N_2 bubbling could put the AuNPs in the catalysis "off" state.

The surface properties can switch from the property of one polymer to the property of the second polymer in a dually responsive block copolymer. Diblock random copolymers can be considered as interesting candidates to modify the solid surfaces in this regard. An ultimate suggested application could be the selective catalyst for certain reactions. If each block is functionalized with a certain active agent (catalytic site), the corresponding reaction could be promoted or quenched due to the expansion or collapse of the block, respectively. Thermo- and pH-dependent swelling and shrinking of the shell could be used for alternately exposing and hiding functional groups in diblock random copolymers, which modulates the catalytic activity of the system.

As shown in Figure 5.3A, each block can collapse while the other is still swollen. Hence, the active sites on each block can be selectively exposed to the reactants in the solution. Another possible architecture for surface modification is the individual grafting of the random copolymers on the surface (Figure 5.3B). As mentioned earlier, we can control

the pH and temperature at which the polymer can collapse and swell by designing an appropriate composition for the random blocks. Therefore, a wide range of reaction conditions can be applied for this system.
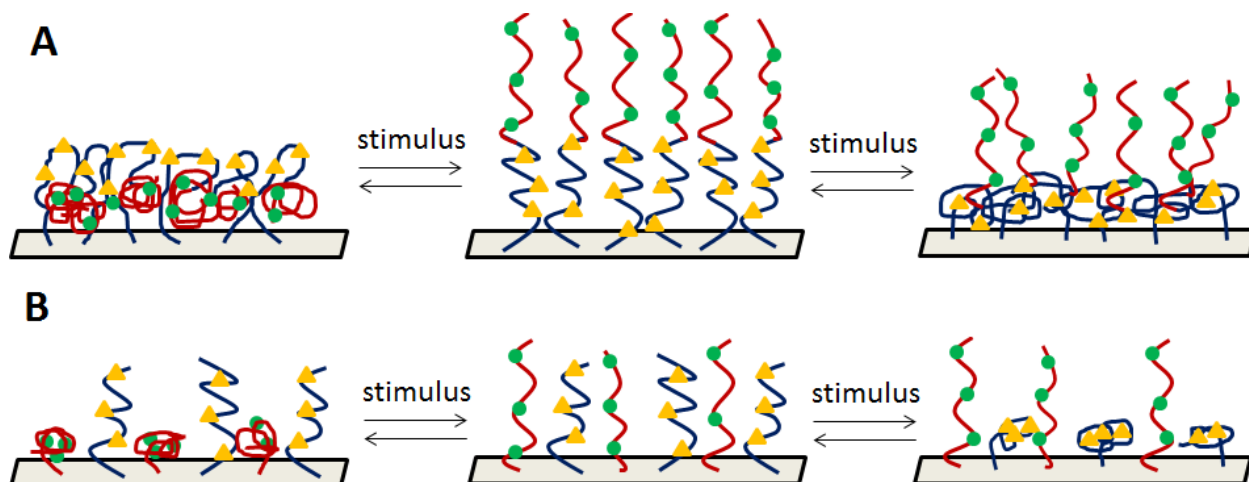
Figure 5.3 Proposed dual behavior of surface-grafted (A) diblock random copolymer, and (B) individual random copolymers bearing active sites (spheres and triangles)

Biocompatibility of diblock random copolymers. Although there are numerous examples of polymeric stimuli-responsive systems, their *in vivo* biomedical applications remain to be explored. Most of the pH-responsive polymers contain amine or carboxyl groups, and they have serious limitation in biological application, because they are not biodegradable.[6] On the other hand, thermoresponsive poly(*N*-alkylacrylamide)s are also generally nondegradable. Future studies will be required to benefit from unique properties of diblock random copolymers *in vivo* applications by using biocompatible polymers such as elastin-like polymers (ELPs) and poly(L-glutamic acid) (PGA) as thermo- and pH-responsive blocks, respectively. ELPs are repetitive polypeptides similar to the elastin structure which consists of a pentapeptide repeat, VPGXG, where V stands for L-valine, P for L-proline, G for glycine, and X represents any natural amino acid except proline. The design of ELPs with a desired LSCT between 0 to 100 °C has recently been reviewed.[7]

Biomedical applications. Although the described system in this work is not proven yet to be biocompatible, it shows interesting properties that would be promising for certain biomedical applications such as drug release.

Release study of the encapsulated agent. It would be interesting to investigate the controlled release of encapsulated agents from both micelles and vesicles formed by our polymers (Figure 5.2). As mentioned earlier, our system has a unique block copolymer structure where each block consists of a random copolymer. The random nature of the blocks allows for fine tuning of the pH and temperature at which micelles or vesicles can form. The dual behavior which stems from the diblock nature of the copolymer can induce reversibility of the micelles and vesicles. For example, we can design a polymeric system with the ability of making micelles (or vesicles) at pH~4 and 37 $^{\circ}$C (stomach condition), which is also capable of inversion at pH~8.5 and 37 $^{\circ}$C (duodenum condition). Formation of the micelles (or vesicles) with the inverted core and shell is quite interesting in two ways: (1) rapid release of the encapsulated agent can take place, and (2) no individual polymer chains remain in the gastrointestinal tract, and unnecessary carrier can be removed after release in the form of aggregates.

Polymer vesicles (polymersomes) are of particular interest due to their hydrophobic membrane and hydrophilic corona, as well as their central hollow cavity, which has been proposed to facilitate their use as delivery vehicles in biomedical applications.[8] The rearrangement of self-assemblies from vesicles to micelles, observed in thermo- and pH-responsive diblock random copolymers, could be used for controlled and fast release of encapsulated agents similar to the observation by Doncom *et al*.[9]

5.3 References

1.   Xie, D.; Ye, X.; Ding, Y.; Zhang, G.; Zhao, N.; Wu, K.; Cao, Y.; Zhu, X. X., Multistep Thermosensitivity of Poly(*N*-n-propylacrylamide)-block-poly(*N*-isopropylacrylamide)-block-poly(*N,N*-ethylmethylacrylamide) Triblock Terpolymers in Aqueous Solutions As Studied by Static and Dynamic Light Scattering. *Macromolecules* **2009,** *42* (7), 2715-2720.

2.   Liu, H. Y.; Zhu, X. X., Lower critical solution temperatures of *N*-substituted acrylamide copolymers in aqueous solutions. *Polymer* **1999,** *40* (25), 6985-6990.

3.   Han, D.; Tong, X.; Boissière, O.; Zhao, Y., General Strategy for Making CO2-Switchable Polymers. *ACS Macro Lett.* **2011,** *1* (1), 57-61.

4.   Liu, H.; Shi, R.; Wan, W.; Yang, R.; Wang, Y., A well-defined diblock copolymer of poly-(ethylene oxide)-block-poly (4-vinylpyridine) for separation of basic proteins by capillary zone electrophoresis. *Electrophoresis* **2008,** *29* (13), 2812-2819.

5.   Zhang, J.; Han, D.; Zhang, H.; Chaker, M.; Zhao, Y.; Ma, D., In situ recyclable gold nanoparticles using CO2-switchable polymers for catalytic reduction of 4-nitrophenol. *Chem. Commun.* **2012,** *48* (94), 11510-11512.

6.   Zhao, C.; He, P.; Xiao, C.; Gao, X.; Zhuang, X.; Chen, X., Synthesis of temperature and pH-responsive crosslinked micelles from polypeptide-based graft copolymer. *J. Colloid Interface Sci.* **2011,** *359* (2), 436-442.

7.   Aseyev, V.; Tenhu, H.; Winnik, F., Non-ionic Thermoresponsive Polymers in Water. In *Self Organized Nanostructures of Amphiphilic Block Copolymers II*, Müller, A. H. E.; Borisov, O., Eds. Springer Berlin Heidelberg: **2011**; Vol. 242, pp 29-89.

8.   Damien, A.; Wilms, E. B.; Zhu, X. X., *N*-Alkylacrylamide copolymers with (meth)acrylamide derivatives of cholic acid: Solution properties and aggregation. *e-polymers* **2004**.

9.   Doncom, K. E. B.; Hansell, C. F.; Theato, P.; O'Reilly, R. K., pH-switchable polymer nanostructures for controlled release. *Polym. Chem.* **2012,** *3* (10), 3007-3015.